2009

SPATIO-TEMPORAL DYNAMICS OF BIOMES IN THE NORTHWESTERN UNITED STATES (9000 YBP TO THE PRESENT)

Christopher Caleb Stump
The University of Montana

SPATIO-TEMPORAL DYNAMICS OF BIOMES IN THE NORTHWESTERN UNITED STATES (9000 YBP TO THE PRESENT)

By

Christopher Stump

B.S., Montana State University, Bozeman, Montana, 2003

Thesis

presented in partial fulfillment of the requirements
for the degree of

Master of Science
in Geography

The University of Montana
Missoula, MT

December 2009

Approved by:

Perry Brown, Associate Provost for Graduate Education
Graduate School

Dr. Anna E. Klene, Chair
Geography

Dr. Ulrich Kamp,
Geography

Dr. Samuel A. Cushman,
USDA Forest Service

Susan Rinehart,
USDA Forest Service

Dr. Eric G. Edlund
University of California, Berkeley

Christopher Stump, M.S., Fall 2009 Geography

Spatio-temporal dynamics of biomes in the northwestern United States (9000 YBP to the present)

Chairperson: Anna E. Klene

The goal of this study was to quantitatively analyze and map the vegetation composition of forest, grassland, and steppe ecosystems in the northwestern United States in the present and through the last 9,000 years. The modern analysis used canonical correspondence analysis (CCA) on pollen percentages from recent sediment cores reflecting modern vegetation assemblages and climates to evaluate the amount of influence of selected environmental variables on present species distributions. The fossil analysis used non-metric multi-dimensional scaling (NMDS) on a merged database containing relative pollen percentages from the last 9000 years. A predefined list of environmental parameters and floristically and ecologically important pollen percentages were used to measure the dissimilarity between modern and fossil pollen regimes over the region at specific time periods. The numeric values obtained from both statistical analyses were interpolated and mapped via Geographic Information Systems (GIS) to display major vegetation types throughout the northwestern United States through time, allowing visual assessment of changing environmental gradients.

ACKNOWLEDGEMENTS

The inspiration, conceptual shaping, funding, and finished product would not have been possible without the patience, expertise, and commitment accommodated by my committee. Susan Rinehart and Anna Klene procured project funding through a challenge cost share agreement between the US Forest Service Region One and the Geography Department of The University of Montana (Agreement #03-CS-11015600-052). Susan was also instrumental in determining how information obtained from paleolithic sources is utilized within the Forest Service. Anna consistently helped with statistical validation, GIS techniques, and technical writing. Sam Cushman inspired me to learn and master the use of various statistical ordination methods combined with GIS mapping methodologies, and ensured interpretations obtained from those methods were sound. Eric Edlund served as the pollen analysis and data preparation expert, while Ulrich Kamp made certain dating chronologies were accurate within the text. An extremely helpful example script was provided by Nick Crookston of the USFS Rocky Mountain Research Station in Moscow, Idaho, allowing imputation of missing pollen taxon variables. Jack Williams of the University of Wisconsin supplied the paleopollen dataset and provided guidance on data preparation. Also, many friends and family members provided emotional support while working around my hectic schedule, enabling me to continue to actively pursue skiing, hunting, fishing, and countless other outdoor activities with little interruption. Finally, my girlfriend Marie Taylor's unrelenting patience was instrumental in the successful completion of this project.

TABLE OF CONTENTS

LIST OF FIGURES

LIST OF TABLES

1. INTRODUCTION

Fire-behavior scientists, ecologists, forest planners, and range managers require a comprehensive understanding of historical ecosystem processes and drivers to set management goals and help dictate the direction of management activities. During the past few decades, the importance of management tools to effectively guide overall land management, conservation, and restoration practices has emerged, based on past climate, disturbance regimes, and changing vegetation mosaics as affected by a host of local and regional environmental factors (Christensen et al., 1996; Bakker, 2005).

A relatively new concept is historic range of variation (HRV). The basic premise of HRV is that knowledge of past and current climate, vegetation, and physical interactions can serve as a reference for organizations trying to restore, conserve, or manage present day landscapes (Landres et al., 1999). HRV in ecological applications typically include the study of environmental parameters such as broad-scale change in vegetation composition, alterations of the disturbance regime interval, as well as climatic parameters and their influences on past ecosystems and processes. However, these studies typically focus on relatively recent times (hundreds of years) and additional knowledge is gained by examining a longer time scale.

Studies of fossil pollen data and comparisons of paleoclimate model simulations compared with detailed paleoenvironmental maps constructed from paleovegetation records clearly show the influence of changing climate on vegetation composition and species range distribution (Wright Jr., 1993; Whitlock and Bartlein, 1997). By comparing paleoclimate model results and pollen vegetation data from the eastern Cascade Range for the last 21,000 years, Whitlock and Bartlein (1997) were able to

determine vegetation expansion and retreat for a suite of species over millennia. This information provides land managers and conservationists a measure with which to compare modern day climate and vegetation patterns, and tie these measures to regional or local stages of community composition.

Similarly, regional fire-return intervals (or disturbance regimes), are closely correlated with phases of ecological succession. Disturbance regime is also tied to broad-scale changes in climate and vegetation scenarios over long time periods (Swetnam et al., 1999). Fire disturbance has long been recognized as a catalyst of vegetation change during periods of shifting temperature and precipitation regimes, and contribute to a broader understanding of natural or ecologic systems (Whitlock and Bartlein, 1997; Swetnam and Betancourt, 1998; Swetnam et al., 1999). Identifying specific temporal phases where climate, vegetation, and disturbance regime changes have taken place is paramount to those seeking to understand forest ecosystems and apply best management practices over large landscapes. Comparing similar climatic and vegetation mosaics in the present day to those that have occurred in the past supplies managers with a tool to infer historic climate and vegetation patterns and measure the departure from historic conditions, and drive land management practices and objectives for future management applications and scenarios (Swetnam et al., 1999).

HRV information also assists in promoting future sustainability and restoration goals of broad scale landscape ecosystems, plus supports management decisions in lawsuits and other legal mitigation situations (Johnson et al., 1999). Unfortunately, little natural range of variation information exists for much of the western United States, especially in the northern Rocky Mountains. Most of the HRV records in the northern

Rockies are based upon tree-ring studies, which infer climate and disturbance regimes over relatively short time periods. Sediment cores with detailed pollen records can reveal fire-return intervals and changes in vegetative community composition over longer time scales, however, relatively few are available within the study area. Thus, it is difficult to compile vegetation composition and climate baselines spanning several millennia to provide context for effective land and forest management (Whitlock et al., 2003).

The goal of this research was to quantitatively analyze and map the post-Pleistocene dynamics of vegetation and climate within forest, grassland, and steppe ecosystems in the Northern Rocky Mountain Region (NRM) over the last 9,000 years. This was accomplished by incorporating a combination of direct and indirect gradient statistical techniques with GIS mapping procedures to display the broad-scale dynamics of vegetation composition in the greater NRM. A predefined list of environmental parameters and floristically and ecologically important species or Genus pollen percentages (obtained from sediment cores and modern surface samples) were utilized to measure the dissimilarity between fossil pollen assemblages and modern pollen assemblages over the region at specific time periods. Finally, a map series was constructed to display the temporal change in vegetation composition and the departure from modern day conditions by interpolating from a collection of fossil pollen sites and modern surface sample locations.

2. BACKGROUND

2.1 Historic Range of Variation

Historic range of ecological variation (HRV; also referred to as the "range of natural variation") is defined by Landres et al. (1999) as "the spatial and temporal variation in ecological conditions that have been relatively unaffected by people within a given period of time and geographical area, appropriate to an expressed goal or outcome". The notion of HRV has been utilized by natural resource managers since the 1960's, and stems from two closely intertwined concepts: 1) past historical conditions and processes offer a context or reference to compare to present day conditions, and 2) disturbance-driven spatial and temporal variability is a fundamental attribute of all ecological systems (Landres et al., 1999).

Today, ecological studies based on HRV use a variety of historic records and techniques to reconstruct and compare past climate, vegetation, and disturbance regimes. Geologic processes like sedimentation in bogs and small lakes chronicle the rate and amount of pollen, charcoal, and plant macrofossils in depositional environments. Additional sources include tree-rings, journals, historic maps, weather observations, photographs, and more recently, satellite imagery, to supply a baseline for reference and to add conceptual support to data findings from older, less abundant sources (Landres et al., 1999; Swetnam et al., 1999). This information is used to reconstruct vegetative communities of forests and grasslands, determine the long-term fire return interval of a site, and discern the changes in these parameters over long time periods, sometimes exceeding twenty thousand years.

In the United States, departures from historical fire regimes and return intervals have been used to target large-scale restoration projects and management direction (Caprio and Graber, 1999), and are becoming more commonly used as the basis for national, regional, and local fire planning (Hann and Bunnell, 2001). Using natural variation in management is grounded in ecological premises. However, recent reviews of the literature suggest that HRV has potentially greater value in understanding and evaluating change in ecosystems, and in inferring the type and degree of change to be expected in large ecosystems, than it does in determining and directing management goals (Holling and Meffe, 1996; Landres et al., 1999). Therefore, management goals and direction should be informed by past variation of ecosystem parameters, including management goals focused on restoring natural processes and conditions, with more focus applied to ecological integrity, sustainability, and resilience for current and future conditions (White and Walker 1997).

This study takes a different approach than most HRV-based research in that this analysis has a very different spatial and temporal scale. Unlike studies which focused on disturbance regimes and their effect on vegetation composition in physiographic regions at decadal time scales (Swetnam et al., 1999) or centurial chronologies (Nonaka and Spies, 2005), this study provides managers with summation of vegetation composition change affected by changing climate at a subcontinental scale over many millennium.

2.2 Climate and Vegetation Interactions in the northwestern United States

Climate in western North America has undergone considerable change as a result of the Earth's orbital patterns which caused glacial and interglacial ages over the last several million years (Bonnickson, 2000). Over the last 20,000 years, North America emerged from the last ice age as the climate warmed, marking the transition from the Pleistocene to Holocene epoch (Figure 1; (Pielou, 1992; Bonnickson, 2000). This study focused on vegetation and climate variation from 9000 ybp to the present day.

The retreat of the Laurentide ice sheet and the smaller mountain glaciers deposited soil, and exposed bare, young soils suitable for 'pioneer' species which favor freshly disturbed soils (Bonnickson, 2000). In most locales of the northwestern U.S. and southern Canada, sagebrush steppe dominated the landscape immediately following the retreat of the major Cordilleran ice sheets. Lodgepole pine colonized small, isolated bands in mountain foothills, in young and disturbed soils immediately after deglaciation (Baker, 1983; Barnosky et al., 1987; Thompson and Anderson, 2000; Thompson et al., 2004). In most sites throughout Idaho and Montana, lodgepole pine, western white pine, and certain fir species colonized deglaciated landscapes by approximately 15,000 ybp, dependent on elevation, and continued expanding northward following the receding glaciers (Baker, 1983). High elevation locations surrounding the Yellowstone Plateau and adjacent areas contain a multitude of studies documenting the appearance of *Picea*, *Abies*, and *Pinus* between 14,000 and 11,000 ybp, as a result of the decline of species characteristic of alpine tundra (Baker and Richmond, 1978; Lynch, 1998; Millspaugh et

al., 2000). White and black spruce migrated northward from the Midwest and Great Plains into Canada. Ponderosa pine first colonized the American Southwest, and followed the glaciers as they retreated northward. Other coastal and interior mountain pine species such as western white pine, Douglas fir, cedar, spruce, and hemlock followed closely behind successional advances of grass, sagebrush, and other ground cover composites after glacial retreat (Figure 2).

Thus, the premise that climatic variation drove paleoenvironmental change from the Quaternary to present day is now widely accepted. Individual species migrated at different rates and at different times dependent on locational and ecologic succession (Pielou, 1992), while major shifts in vegetation assemblage distributions occurred on elevational, climatic, and latitudinal gradients throughout the West (Jackson and Overpeck, 2000; Brunelle et al., 2005).

Changing land use patterns, European agricultural practices (Bakker, 2005), and the dispersal and elimination of Native peoples throughout western North America have also greatly affected vegetation patterns and altered fire return intervals in both mountain and prairie environments (Bonnicksen, 2000). Every Native American tribe in the Northern Rockies used fire to clear lands for agriculture and enhance growing conditions for certain plants such as camas (Bonnickson, 2000; Hessburg and Agee, 2003), improve game foraging habitat to attract animals for improved hunting and herding grounds (Chittenden and Richardson, 1969; Bonnickson, 2000), and for defense and attack purposes against enemies (Fiedel, 1987).

Over the last 100 years, total fire suppression, led predominantly by the US Forest Service, greatly reduced fire occurrence throughout North America. Forests and

rangelands were once conceptualized and utilized primarily as an economic commodity, thus intense efforts were applied to ensure their productivity utilizing natural resource extraction practices with limited knowledge of the detrimental ecological effects of fire removal from the landscape (Barker, 2005). Mountain environments experienced dramatic reforestation, reducing patchwork mosaics of pine-sagebrush parkland in high elevation areas, while trees encroached upon grassland ecosystems including the Centennial Valley of southwestern Montana over the last 60 years (Sankey et al., 2006).

2.3 Paleoenvironmental Reconstruction Methods

An early Norwegian paleoecological study performed by Blytt (1876)), and summarized by Woodward (1987), found remnants of aspen, pine, and oak deposited in a Danish bog that possessed markedly different geographical distributions from the modern day. Some of these tree species, such as oak, are currently found only in the southern extent of Denmark, and their presence inferred a warmer and wetter climate than currently observed. From this simple observation, Blytt (1876) hypothesized that climate, and hence landcover, had changed considerably in the past. Today, similar hypotheses are supported because plant species have exhibited very little evolutionary change (especially in terms of their individual response to environmental limiting factors) since 50,000 ybp (Jackson and Williams, 2004).

Very similar methods and conclusions now form the basis of paleoecology and palynology. Lennart Von Post was the first recorded researcher to construct and effectively use pollen diagrams to show the historic variation of community vegetation

abundances using counted fossil pollen and plant remains from 1916 (Fries, 1967). At the time of publication of von Post's early works, radiocarbon dating methods were not available but von Post could use a readily apparent and identifiable stratigraphic layer that occurred at his peat and bog sites to confidently identify the same temporal time at different depths at multiple sample sites.

The advent of carbon-14 radiocarbon dating (^{14}C dating methods) has allowed the dating and comparison of temporal changes of plant macrofossils, fossil pollen, and sediment or charcoal from sediment varves between multiple sample sites without distinctly recognizable sedimentary layers. It has allowed for cross comparison of pollen sites at multiple temporal and spatial scales, including local or catchment basin-sized analyses (Mehringer et al., 1977; Mack, 1983; Power et al., 2006), spatially larger regional assessments of vegetation, climate and charcoal (Brunelle and Whitlock, 2003; Brunelle et al., 2005) and even continental-scale comparisons of vegetation and climate change (Bartlein, 1998; Peyron et al., 1998; 2000; Williams et al., 2004; Whitmore et al., 2005). Reliable dating results can be obtained 30,000 to 40,000 years before present, making it well suited for establishing chronologies in the late Quaternary (Bartlein, 1995).

Paleoecological-statistical analyses are usually performed using two main categories of pollen data: binary and relative abundance. Typical binary pollen data in paleoecology is presence/absence data, usually with the number "0" inferring absence and "1" indicating presence. Binary data are most often utilized in conjunction with cluster analysis which force pollen assemblages or compositions into representative groups for further data analysis, processing, and interpretation. Abundance data can be in

the form of relative abundance (pollen percentages), absolute pollen counts per study site from respective researchers, or estimates of pollen percentages from slices of sediment core (Shi, 1993).

Accurate pollen abundance data are usually more informative than binary presence-absence data, but only if the sample data is obtained with few biases or sampling errors. Cumulative inaccuracies of sampling errors can cause misleading and erroneous interpretations of the results (Hirst and Jackson, 2007). The data used in this study are relative abundances, and the dataset is stored in the form of pollen percentages ranging from 0 to 100 percent of the total pollen sum counted at each site.

2.4 Quantitative Data Analysis Methods of Paleoecological Data

Although extensive literature exists for the theory and various applications of multivariate methods in an ecological framework (Kenkel and Orloci, 1986; ter Braak and Prentice, 1988; Kovach, 1989; Legendre and Legendre, 1998), little has been written that comprehensively and systematically relates these methods to paleoecology and paleobiogeography (Shi, 1993). Methods incorporating cluster analysis and ordination approaches are more often being used to describe individual species and vegetative community composition response and interactions to environmental gradients, as well as to establish correlations between vegetation composition and environmental site characteristics (Shi, 1993; Austin, 2005). Different quantitative methods have been utilized with varying degrees of success. These range from the calibration of fossil pollen assemblages to modern pollen assemblages in an attempt to infer ground cover and species composition, known as extended range value models (ERV's), to biomization

procedures coupled with modern analog techniques (MAT), and to statistical multivariate approaches aimed at describing individual species and community-level interactions such as principal components analysis (PCA), canonical correspondence analysis (CCA), and non-metric multidimensional scaling (NMDS).

2.4.1 Extended Range Value Models (ERV's)

Quaternary paleoecologists have consistently struggled with identifying strictly quantitative techniques to reconstruct and map past vegetation communities and migration of individual plant species or groups. Early attempts at calibrating fossil pollen assemblages to observed species abundance in a given study area involved the use of extended range value (ERV) models. ERV models attempt to correct for problems associated with the "Fagerlind Effect," the misrepresentation of vegetative community composition because of species which over- or under-produce pollen relative to other species (Jackson and Wong, 1994; Jackson and Kearsley, 1998) . For example, *Pinus* is considered an over-producer of pollen, and may appear as though it is the dominant vegetation entity in the vicinity of the study site, when in reality *Pinus* may actually account for a small percentage of land cover and vegetation composition in the study area. *Pinus* pollen is often so prolific in sediment cores and moss polsters because it possesses excellent dispersal capabilities, produces large amounts of pollen, and usually produces over many months, leading to large pollen deposits at many sites, even those outside the normal historic range of certain *Pinus* species (Birks and Gordon, 1985).

However, ERV models are no longer utilized as a means to measure historic vegetation variation since they cannot take into account the effect of environmental variables and because detailed knowledge of many species' pollen dispersal capabilities are still largely unknown, rendering results that were often inconsistent, unpredictable, and misleading (Jackson and Kearsley, 1998; Jackson, 2006). Dissimilarity analysis methods such as squared chord-distance (SCD) and maximum likelihood techniques have often been implemented to measure the amount of similarity (or dissimilarity) between different fossil pollen assemblages and known modern pollen assemblages, biomes, or plant life-form types. Dissimilarity coefficients also measure the difference between multi-variant samples which provide a quantitative aid for the identification of modern analogs to fossil pollen assemblages (Overpeck et al., 1985; Gavin et al., 2003).

2.4.2 The Modern Analog Technique (MAT) and Biomization Procedures

Overpeck et al. (1985) compared several dissimilarity techniques and found SCD sensitive enough to discern fossil pollen assemblages that occurred in various vegetation compositions including mixed, deciduous, and boreal forest types in the Upper Peninsula of Michigan. SCD values from fossil pollen assemblages were then compared to known modern pollen assemblages and grouped into broad categories of forest cover. The SCD values were precise enough that they could be mapped via isopols to visually show the forest composition of southern Michigan based upon the corresponding pollen spectra (modern pollen surface samples). This reasoning by analogy has been adopted recently by researchers and termed the "modern analog technique" (or MAT) initially by

Overpeck et al. (1985) and refined in later research (Overpeck et al., 1992; Williams, 2002; Jackson and Williams, 2004; Whitmore et al., 2005).

The central supposition of MAT is if two samples contain a similar mixture of pollen, then the communities that produced these assemblages were also similar. A fundamental limiting factor of the modern analog technique is that it cannot make accurate or meaningful assignments of past biomes for fossil pollen samples which have no close analog available, or no-analog assignments for future predictions (Jackson and Williams, 2004; Fox, 2007). Changing environmental conditions during the Quaternary have clearly resulted in past plant associations with no modern equivalent. For example, *Picea critchfieldii* was once a dominant tree species in the Lower Mississippi Valley during the Last Glacial Maximum (LGM), but was probably extinct by 10,000 ybp, along with its associated groundcover species (Overpeck et al., 1992; Jackson and Overpeck, 2000) greatly altering the vegetation composition in middle America with the removal of the species, thus disallowing any analog to be applied. A relatively new variant of MAT is the "Hierarchical Analog Technique" (HAT) which provides a formalized method for generalizing pollen data according to plant/climate functional similarities. This enables fossil pollen assemblages with no modern counterparts to be linked to the closest match in the modern day through a series of hierarchical procedures (Williams, 2002; Williams et al., 2004).

Williams (2002) regrouped fossil and modern pollen data into plant functional types (PFTs) based on life form, phrenology, leaf shape, and climate tolerance. SCD calculations were first conducted to determine whether there were any close matches to the modern pollen data. If a match did exist, then that pollen assemblage was assigned to

its corresponding class. If no match existed, the pollen assemblage was aggregated by PFT or biome designation and the SCD dissimilarity calculation repeated. This process was repeated until a modern analog was identified, or at least the sample was forced into the closest modern analog (Williams, 2002).

PFTs are important within this study because the concept behind PFTs is the same idea as any gradient or ordination analysis approach: to relate plant function, morphology, and distributions to environmental gradients. PFTs have undoubtedly played an important role in plant geography and have been used in studies of climate, climate change, and disturbance over time, (Woodward and Cramer, 1996; Lavorel and Cramer, 1999; Austin, 2005). This process is similar to the biomization technique presented by Peyron et al. (1996) and Peyron (1998; 2000), which generalizes both the pollen and land-cover data into broader classes to allow each pollen assemblage to be linked to a modern analog, thus allowing the creation of animated maps at defined time periods.

Other recent paleoenvironmental reconstructions have incorporated remotely sensed imagery to aid in determining vegetation classifications, strengthen modeling techniques, and enhance mapping scenarios. Williams (2002) employed 1 × 1 km gridded Advanced Very High Resolution Radiometer (AVHRR) satellite imagery linked to modern pollen surface samples to effectively map the density of needle-leaved, broadleaved, and herbaceous groundcover for eastern North America from the LGM to the year 2000. A collection of modern surface pollen samples and fossil pollen sites were identified, mapped, and the pixel characteristics in which modern pollen surface samples were located were used to represent these modern sites. Next, the HAT was performed

on the fossil pollen assemblages to assign them to modern vegetation and climate schemas. Finally, Williams produced a temporal map series showing each biome's change in climate, vegetation composition, and distribution through time.

Significant limitations to the MAT approaches are the requirements of a large number of sample sites and an informative and accurate biome (or other land classification system) to determine the deviation from modern conditions. This premise is seldom met in studies utilizing fossil pollen as a means to analyze HRV. The MAT approach also does not measure the interaction of environmental variables on fossil or modern pollen assemblages. The only quantitative means to analyze these measures is the use of statistical gradient methods.

2.4.3 Ordination and Gradient Analysis Methods

Ordination analyses and gradients come in many different forms, applicable to a variety of objectives, data types, and methodologies. Ordination simply means to arrange items along one or more axes in 'number', or 'species' space. This is performed graphically to summarize complex relationships in the hope of extracting one or several dominant axes from the possible number of axes or solutions. Ecological ordination orders taxon variables in an ecological space in relation to predefined environmental and/or species (and in this study, historical) gradients. On a broad level, this approach is also commonly referred to as 'gradient analysis'. Gradient methods are particularly useful in community ecology, allowing one to investigate complex relationships between combinations of individual species, as well as species abundances combined with environmental variables, while avoiding the pitfalls of modern analog and community-

based approaches. Gradient methods reveal trends and relationships within the community data itself, and depending on the method used, allow researchers to predict species distribution and abundance as inferred from environmental variables, and vice versa (Prentice, 1977; Hill and Gauch, 1980; Palmer, 1993).

Of particular importance to landscape managers is the concept of 'resource' or 'environmental' gradients (Hannah et al., 2002; Whitlock et al., 2003; Brunelle et al., 2005). These usually involve the computation and analysis of dissimilarity matrices computed from raw data consisting of species and environmental measurements (such as soil type, ground cover, elevation, and soil moisture content) stemming from a number of plots or study sites (ter Braak and Prentice, 1988). One common example is that species composition is expected to change with elevation on a mountain. Likewise, species composition would shift through time given changing environmental factors and conditions (McCune et al., 2002).

Different forms of gradient analysis have been utilized in paleoecology to infer both past climates and vegetation compositions from modern pollen surface samples and fossil pollen sediment cores. MacDonald and Ritchie (1986) used principal components biplots and discriminant analysis to explore the relationship between modern pollen surface assemblages and major vegetation zones (or biomes) in the interior of Canada. Likewise Bartlein et al. (1986), used multiple regression models to study the correlation between fossil pollen assemblages and known modern vegetation interactions to interpret ancient climate regimes in the American Midwest and eastern North America.

2.4.4 Principal Components and Canonical Correspondence Analysis

Gradient methods often utilized in analyzing community structure in paleobiogeography include principal components analysis (PCA), canonical correspondence analysis (CCA), and non-metric multi-dimensional scaling (NMDS). PCA is an indirect gradient technique that ordinates species among plots based on species composition, and does not utilize environmental variables to constrain the ordination axes. PCA techniques are linear ordination methods, since they assume linear relationships between species abundance and environmental factors (Kovach, 1989; Shi, 1993). . Conceptually, PCA is similar to performing a series of multiple regression analyses in an attempt to define a series of 'hypothetic environmental variables' that best describes the variation in species or variable abundance. CCA is a direct ordination technique that depicts the influence of selected environmental variables on species' distribution, occurrence, and abundance within an area of interest. CCA attempts to quantify the underlying pattern of community variation, as well as important or influential species' distributions along selected environmental gradients. To do this, CCA constrains variables to be linear combinations of provided environmental variables, thereby enabling the identification of possible spatial or environmental gradients in the vegetation data via data matrices comprised of species abundance and biophysical factors. The biophysical matrix is often used to predict species abundance (ter Braak, 1986; 1987; ter Braak and Prentice, 1988).

PCA has been used extensively to study the effects of indicator species, changes in species composition, and the predictability of various biophysical factors over time

(MacDonald and Ritchie, 1986; MacDonald, 1987; Williams, 2002). In a geometric model, PCA projects sample points onto a plane that minimizes the sum of squared distances from the points (Prentice, 1986a). The axes coordinates of the samples on each principal component are called principal component scores. Sample scores and individual taxon loadings can be graphed on biplot diagrams to portray the effects of pollen percentages or taxon loadings at the study sites. PCA can be sampled to contemporaneous samples at specific time intervals to show changes in geographic patterns over time (Huntley and Birks, 1983).

An improvement to this method would be to perform PCA on a 'time-space' data matrix (such as pollen spectra at study points compared at 500 or 1000-year time intervals) throughout a given study area or geographic region in conjunction with a combination of multivariate methods including PCA, CCA, and NMDS, to provide vegetation composition and climate trajectories. Examination of only one time period yields a static snapshot of ecological conditions, composition, and reference to study plots. However, by examining these trends over multiple intervals, one can detect ecological change throughout large, diverse areas over long time periods. In PCA, the axes act as variables (or taxa), while the samples located on these axes are distributed according to each taxons' abundance. The distance between points in ordination space are measured by dissimilarity coefficients including Euclidean, Manhattan, Sorensen, and Mahalonobis distance matrices, to name a few (Prentice, 1986b).

2.4.5 Non-Metric Multi-Dimensional Scaling

Unlike PCA and CCA, non-metric multi-dimensional scaling (aka NMDS, MDS, or NMS) has no underlying assumptions regarding normality or linearity within the dataset. Rather, NMDS uses the rank order information in a dissimilarity matrix, as opposed to its pure metric information, and is considered a "nonparametric" family of curves, since it measures the departure in monotonicity in a configuration. NMDS is, at the statistical level, very similar to least-squares regression analysis and is commonly viewed as a form of statistical fitting. Solutions with the best fit are measured by performing a monotone regression on the dissimilarity of the normalized residual variance, termed stress. Stress in an NMDS run is actually the residual sum of squares and is often reported as a percentage. Smaller values of stress indicate a better fit or solution to the problem. Stress, ranging from 0 to 1, indicates how well a configuration or ordination solution matches the dissimilarity matrix (Kruskal, 1964b; Kenkel and Orloci, 1986; Shi, 1993; Legendre and Legendre, 1998). Typically, one hundred iterations (stress calculated using the "method of gradients" or "method of steepest descent") are necessary to reach the best solution or configuration which are revealed on a 'scree diagram' or 'scree plot' (Kruskal, 1964a; McCune et al., 2002). Kruskal (1964a) and Clarke (1993) provide guidance in the form of a stress value table to evaluate an NMDS solution goodness of fit (Table 1).

NMDS permits the study of relationships between dissimilarity matrices and the associated output distance by constructing an ordination diagram where the distances between plots have maximum rank order agreement with the similarity measures between

plots, with the capability of capturing two-dimensional gradients (Austin, 2005). NMDS comes in two forms: metric and non-metric. MDS (the metric version) assumes that the dissimilarities are proportional to a distance measure, while nonmetric NMDS is related to a "monotonicity assumption" (van Wezel and Kosters, 2004), or that the dissimilarities are monotonically related to Euclidean distance or other distance method chosen to represent the data structure. Essentially, NMDS algorithms and equations estimate a spatial representation for a given dissimilarity matrix where the rank order of the distances between the original data objects agrees with the rank order of the dissimilarities as closely as possible (van Wezel and Kosters, 2004).

With the advent of more advanced and efficient computing capabilities, NMDS has gained recognition as a superior data analysis and graphical method for displaying large, complex datasets, often finding better relationships and correlations between environmental and species abundance data than variations of PCA. This is especially true for datasets encompassing wide ranges of variation, usually due to large study areas, as is the case in this study (Kenkel and Orloci, 1986; Prentice, 1986a).

2.5 Study Area

The study area stretches from the southwest Canadian coast, southward through Washington and Oregon, east into Idaho, Wyoming, and Montana, and finally terminating in the western Dakotas (Figure 3). The western portion of USDA Forest Service Region One formed the core area of interest, but a larger area was chosen to maximize the number of fossil and modern day surface pollen sites, which are few, especially in the mountains. The low number of surface and sediment core sites in these

areas is due to the complex terrain causing difficulties with site selection and sediment core extraction. Given extensive study area size, a multitude of climate, landscape, and vegetation mosaics exist on latitudinal and longitudinal transects.

In the Coastal Ranges of western North America, climate varies dependent on elevation. High elevation areas receive increased precipitation and diminished temperatures as rugged mountains rise out of the Pacific Ocean, including the Coast Range of British Columbia and the Cascades of Oregon and Washington. These mountains are dominated by Pacific Douglas fir at most elevations, but intermixed with various tree species primarily belonging to the families of *Tsuga* and *Larix* at high elevations (Ricketts, 1999). South-central Idaho and southwest Montana exhibit a continental climate including xeric precipitation conditions, brief summers, and long cold winters. Mountainous regions of southwest Montana and southern Idaho consist of more drought-tolerant forest species (mosaics of lodgepole pine and Douglas fir), though give way to parklands of sagebrush, short grass, and various tree species at lower elevations. Farther north, the north central Rockies forests marks a transition from maritime to continental latitudes characterized by warm, moist summers and mild, snowy winters, given its complex and mountainous terrain. Vegetation consists of mixed-composition forests containing cedar, hemlock, spruce, and other moisture-dependent species.

Further east and inland mountain latitudes exhibit continental precipitation and temperature gradients, with warm dry summers and mild winters. Mean elevations generally decrease northward from southern Idaho and Montana, except where interrupted by low-lying basins, deep valleys, and broad, desert-like steppe (Nesser et al., 1997). Continental forest mosaics reflect distinct variation, with specific species'

abundance and occurrence depending on elevation, ranging from Ponderosa and western larch at low elevations, to lodgepole pine, Douglas fir, and white pine at mid mountain, and subalpine fir and whitebark pine at tree line. Farther east of the continental divide, a vast expanse of steppe-like grasslands is dotted with small, distinct, and scattered island mountain ranges which produce climatic gradients that influence vegetation patterns in the surrounding prairies and foothills, ranging from lodgepole pine and subalpine fir up high to assortments of sagebrush and bunchgrasses at low elevations (Nesser et al., 1997; Ricketts, 1999; Olson et al., 2001; Olson and Dinerstein, 2002).

2.6 Problem Statement and Study Hypotheses

This study used one multi-dimensional scaling technique and several multi-temporal ordination techniques to quantify spatio-temporal dynamics of vegetation communities based on relative pollen percentages. The data stemmed from three researchers' databases that included both modern and fossil pollen assemblages. These databases contained pollen and sediment records that detailed vegetative community change over time, which were used to calculate dynamics of vegetation change as driven by climate in western North America from 9000 ybp to the modern day.

While studies utilizing multivariate methods have been conducted in the study area using modern pollen surface samples, (MacDonald and Ritchie, 1986; MacDonald, 1987; MacDonald and Reid, 1989), few have used relative pollen percentages in conjunction with a host of biophysical variables to predict biome or ecoregion groundcover over large areas (Williams et al., 2004). None have used such an extensive

dataset of 596 sites, and none have used pollen percentages and biophysical variables to predict pollen assemblages spatially.

The hypothesis for the modern portion of the study is:

1. Analysis of relationships between biophysical variables and modern pollen percentages with multivariate statistical methods can effectively predict vegetation composition and be used to map it across broad geographical extents.

Although a number of paleoecological pollen analyses have been conducted within this study area (Mehringer, 1985; Thompson and Anderson, 2000; Power et al., 2006), few have utilized multidimensional scaling techniques (MDS; Prentice, 1977; Kenkel and Orloci, 1986; Kovach, 1989; Shi, 1993) within the region. This type of analysis provides several landscape metrics to effectively ascertain the magnitude and type of vegetation and climate change across the entire study area over the last 9000 years.

The hypotheses for the fossil portion include:

1. Vegetation composition changed at a similar rate due to regional climate shifts and disturbance within subgroups (regions) of the study area between 9000 ybp and modern day.
2. Shifts in vegetation composition trajectories were synchronous across the study area for all study point locations and time slices, as driven by regional changes in climate.
3. Similar vegetation assemblages and climatic conditions have been observed in previous time periods across the study area as determined by interpretation

and comparison of fossil pollen assemblages, landscape trajectory paths, paleoclimate data/models, fire occurrence proxies, geochemical, and isotope records.

3. METHODS

Methodologically, this study involved acquisition of a large set of fossil and modern pollen datasets, which usually required substantial data processing to format for comparative analysis, as well as location and manipulation of modern climatic and ecological data. Then, a series of statistical analyses were performed, on datasets much larger than those which have been previously published. Finally, these results were mapped to assess spatial patterns and trends through time.

3.1 Data Selection, Manipulation, and Processing

3.1.1 Compiling the Fossil and Modern Surface Pollen Records

Many individual paleoenvironmental reconstructions exist for western North America focused on the Yellowstone region (Baker and Richmond, 1978), Great Plains (Barnosky, 1989), Canadian Rockies (MacDonald, 1987; MacDonald and Reid, 1989), and Pacific coast forests (Brown and Hebda, 2002). However, comparatively few cumulative datasets exist that are organized by calibrated time slices (e.g. 500 year increments), contain consistent pollen taxa and data format, and possess locational information for each study site. For this study, paleopollen sites were defined as point locations where sediment cores were extracted from small lakes or fens for the purpose of pollen study and ultimately paleoenvironmental reconstruction and analysis. This study utilized 18 individual reconstruction publications and the Whitmore et al. (2005) modern

pollen dataset and Williams (2007b) fossil pollen datasets to maximize the amount of data and pollen sites in the study area.

A database containing detailed core top and fossil pollen percentages was obtained from Williams which included geographic coordinates, elevation, and pollen percentages for 61 taxa at 759 sites distributed throughout North America and Greenland (Williams, personal communication, 2007). Much of the pollen data used in that dataset were drawn from the North American Pollen (NAP) database (COHMAP MEMBERS, 1988). Unfortunately, many sites in the Northern Rocky Mountain Region were removed from the NAP dataset by Williams, due to low sampling density and the complexity of the regional topography (Williams, personal communication, 2007).

To increase sample size, distribution, and improve analytical results, the Whitmore et al. (2005) modern surface pollen dataset was also utilized. This dataset contained over 4634 sites distributed across North America and Greenland, using observed pollen count per grain type. Core tops were used to reflect modern day conditions, and followed standardized pollen processing procedures for consistent comparison of sites across North America. This modern surface sample dataset contained 134 types of pollen grains from 65 families (Whitmore et al., 2005).

Additionally, paleopollen records from another 22 sites were obtained by the author in the form of published research articles within the study area. These sites possessed sediment cores that detailed the fossil pollen record, sediment stratigraphic sequence, and in some instances, the fire-return interval from interpretation of the amount of charcoal present. However, four sites could not be used because of inadequate information such as no linear age graph present for Little Dickey Fen (Chatters and

Leavell, 1995b), or not including a pollen diagram (Poison Lake and Great Basin sites; (Doerner and Carrara, 1999; Doerner and Carrara, 2001). Most of the pollen records the author digitized were not present in the North American pollen database (NAPD) and thus had not been included in the other datasets.

The Whitmore et al. (2005) dataset, the Williams et al., (2004) data, and the supplementary pollen sites digitized by the author were merged together to form one cumulative dataset for further analysis (Table 2 and Figure 3). The additional sites digitized by the author served to increase the sample size within the study area and fill in areas with no pollen data within the confines of USFS Region One. Finally, duplicate sites in the modern day dataset were removed. Duplicates stemmed from data inconsistencies, such as where 63 surface samples collected along elevational transects were mapped using only two decimal places in decimal degrees (Davis, 1984), reducing the spatial resolution of the data below that of this study. After identification, the values for each taxon and environmental attributes for these duplicates were averaged, leaving one representative observation within the final dataset.

3.1.2 Digitizing Procedures and Temporal Resolution

The 18 supplemental sites added by the author were initially located through literature review, and then either hardcopy or digital versions of the datasets were obtained. Digital versions were particularly useful since they required no further adjustment before digitizing could take place in contrast to paper versions. Several of these sites were not previously published (Harding Lake, Little Dickey Fen, and Smeads Bench Fen; Chatters and Leavell, 1995a; Chatters and Leavell, 1995b) or were masters

theses that were not widely distributed (Sheep Mountain Bog and Marys Pond; Hemphill, 1983; Karsian, 1995).

Pollen diagrams not already in digital format were scanned using a 44 inch plotter. After scanning, the pollen diagrams were imported and rotated to horizontal alignment, but were not otherwise manipulated. These images were then digitized using Grapher 5©[1], to easily assign coordinate values based on the x and y axes for each variable (pollen taxa). The pollen diagrams from the 18 sites came in both calibrated ybp and uncalibrated. Calibrated pollen diagrams only required one x-y axis to be constructed and centered on the main axis for of the pollen diagram, since each 250-year time slice was evenly spaced (Figure 4a). However, for the uncalibrated diagrams, separate axes had to be constructed for each divisible time slice, based on logical breaks in the linear age axes available from within each paper (Figure 4b). Once the required axes were constructed, the species or taxon pollen percentages were digitized from the pollen diagram at each 250 year division. A total of 122 plant species, families, and plant taxa were originally recorded from the pollen diagrams collected and digitized by the author (Table 3).

Twenty taxon variables were selected by the author for inclusion in the model (Table 4). These 20 taxa were the result of grouping species variables (for example, individually digitized species percentages within the same family, such as *Pinus contorta* and *Pinus albicaulis,* were grouped into the variable Pinus), and selected because they were all present at most study area paleopollen sites, and provide adequate tree and groundcover species community representation.

[1] Golden Software, Golden CO (2003).

Depending on the temporal coverage of sites, 60 or more time slices were available after digitizing. However, due to technical difficulties and time constraints, just ten time periods were chosen to show species composition change over millennia in the Northern Rocky Mountain Region for this study. Time slices of 500 years were utilized between year 0 (modern time) to 3500 ybp and coarser slices from 3500 to 9000 ybp. Radiocarbon dating technology at the time of some publications used in the Williams et al. (2004) database contained too much variability, discouraging finer resolution. Additionally, 500-year intervals were deemed adequate to capture visible vegetation composition change within all habitats of the study area after initial investigations. The greater time spans from 3500 to 9000 ybp were necessary because there was too much missing data at many sites.

3.1.3 Taxon Variables

After acquiring pollen records from the various papers and databases, a uniform list of species or taxa had to be compiled that were available for all sites. To ensure consistency between the ten time periods and three datasets, methods and variable groupings utilized in Williams et al. (2004) were maintained while merging the three datasets together. For sites present in more than one source, only the Williams et al. (2004) record was maintained.

The modern surface pollen dataset (Whitmore et al. 2005) listed the raw pollen counts, while the Williams et al. (2004) dataset recorded the pollen types as percentages from the pollen sum, requiring the Whitmore et al. (2005) data be converted to pollen percentages by dividing each pollen type count by the total pollen sum for all sites. The

dataset was then winnowed such that only pollen species or families which were counted by the Williams et al. (2004) and Whitmore et al. (2005), and were included on a summary list of those digitized by the author remained. From the three datasets, 20 taxa remained as variables for use in the statistical model (Table 5a).

Within each of the databases, all pollen counts not included in the list of 20 taxa were removed, and new pollen percentages were calculated by summing the remaining amounts. No ratios were applied to sites obtained from individual papers because the pollen values were already in percentage form and required no adjustment for each pollen type recorded by the author. Once each dataset was adjusted, the three were merged.

3.1.4 Environmental Variables

Temperature, precipitation, and potential evapotranspiration are traditionally used as predictors of species distribution (Faegri and Iversen, 1989; Huggett, 2004). However, these variables can not be assumed constant through the thousands of years of time in this study. Often, estimates of past climates are inferred from the result of pollen analysis. For this study, seven environmental variables were utilized to aid in understanding the modern distribution of pollen and vegetation composition. The understanding of these modern relationships then allowed climatic gradients to be interpreted from changes in the paleopollen records over time.

Elevation was used as a proxy for temperature and the data used were from the Shuttle Radar Topography Mission (SRTM) 3 arc-second Digital Elevation Model (DEM; USGS, 2004).

Monthly and annual spatial estimates of precipitation in the complex terrain of the study area were obtained from PRISM (Parameter-elevation Regressions on Independent Slopes Model) data for the time period 1961-1990. PRISM is a spatially gridded raster climatic dataset created by Oregon State University that is downloadable free of charge for the lower forty-eight conterminous United States through the PRISM Group (http://www.ocs.orst.edu/prism/prism_new.html, accessed 2007) at 4 km × 4 km cell resolution (Daly et al., 2004; Daly et al., 2007). PRISM uses point data generated from weather stations in conjunction with a digital elevation model (DEM) to effectively capture the orographic elevation of precipitation stations (Daly et al., 1994). Other spatial and environmental factors such as coastal proximity, vertical air-mass layering, local relief, and topography are applied in the PRISM algorithm to effectively model gridded precipitation and temperature gradients. PRISM has been proven as an effective and accurate method for extrapolation of climatic gradients in mountainous terrain, including rain shadow effects and the influence of large water bodies (Daly et al., 1997). Since the study sites extended into southern Canada, PRISM data for Alberta, British Columbia, and Saskatchewan (Wang et al., 2006) was purchased from Climate Source (retrieved 30 September 2007, from http://www.climatesource.com) at 2 km × 2 km resolution. The two precipitation datasets were interpolated using inverse distance weighting and the standard atmospheric lapse rate of -2.5°C/ 700 m to 1 km × 1 km resolution to allow better estimation of site-specific conditions and then merged. Precipitation values at the study sites were then extracted, and those values included as an environmental variable in the model.

Northing and easting values were included to capture well-known North American climatic and vegetation gradients influenced by elevation, coastal proximity, and rain shadow effects driven by the Cascade and Rocky Mountains.

Thus seven variables, elevation as a proxy for temperature, annual precipitation, a manipulation of those that served as a proxy for evapotranspiration, northing and easting, as well as two variations capturing NE to SW and NW to SE gradients, were used to describe the environmental characteristics of the region (Table 5b).

3.1.5 Imputation Procedure for Missing Values

Although the Williams et al. (2004) and Whitmore et al. (2005) datasets contained pollen counts for each of the 20 taxon variables except for *Thuja*, most of the supplementary sites (Table 2) did not have pollen counts for all of the 20 taxa selected for the regional analysis, mainly due to some species not occurring within each of the ecoregions in the study area, such as *Thuja* never occurring on the Great Plains. However, most statistical gradient methods require that each site have complete pollen and environmental data for each taxon variable.

Initially, a cokriging interpolation technique using the elevation at each study site and the individual taxon pollen percentages was attempted using a moving search window measuring 300 × 300 km horizontally and 500 meters vertically (Huntley et al., 1989; McLachlan and Clark, 2004; Williams et al., 2004) throughout the study area. However, preliminary results showed very poor statistical validation, with little variance explained by the cokriging procedure. That method assumed that space was the primary driver of pollen distribution and abundance. However, plant distributions are primarily

driven by biophysical factors (such as elevation, latitude, longitude, temperature, and precipitation gradients). Imputation allows for weighting of causative factors (in this case ecological and biophysical variables as well as other pollen counts).

Several software programs perform a variety of regression- or classification–based imputation techniques including IVEWare (Ragunathan et al., 2001), the yaImpute (Crookston and Finley, 2006) and randomForests packages for R (Breiman, 2001). For this study, randomForests was chosen to impute the missing data values for those supplementary sites that were not in either of the databases. This package uses the CART regression-based classification tree method known as random forests, developed by Breiman (2001). Random forests result from a combination of random tree predictions in which each tree depends on the values of a random vector sampled independently and with the same distribution for all trees in the forest. Each tree casts a unit vote for the most popular class for a given input (Breiman, 2001). Random forests provide results competitive with boosting and bagging, but do not change the training set as it progresses.

Included within the reference matrix were PRISM-derived precipitation, geographic coordinates, elevation, and the other taxon pollen percentages (Table 5). Each time slice was processed separately so that pollen percentages from different time periods would not influence the results. Only the nine most important predictor variables were used in the imputation procedure for each missing taxon pollen percentage. (Breiman, 2001; Ragunathan et al., 2001) The iterative random forest algorithm was applied to each taxon variable, once per time slice, to predict the missing values using settings of 500 trees with three variables tried at each split. Tables 7 and 8 detail the root

mean square error (RMSE) and percent variance explained, respectively, for each predictor variable used in the imputation procedure.

Separate matrices were utilized for the modern analysis and then fossil pollen analysis. The modern pollen data matrix included 685 rows and 28 columns, while the fossil pollen matrix included between 46 to 56 rows and 28 columns, dependent on the number of sites with full pollen representation per time slice. The imputation method provided more accurate results than the cokriging technique.

3.2 Ordination Procedures for Modern Pollen Analysis

The goal of the ordination analyses was to examine the similarity (or dissimilarity) of study plots within the modern period and to temporally track species composition over time. Ordination analyses were performed using the statistical software package PCORD, version 4 (McCune and Mefford, 1999), which uses an iterative algorithm initially established by Kruskal (1964b), to find the best fit for the ordination analysis/solution. PCORD was chosen because it readily performs many of the accepted ordination methods and includes graphing functionality for multiple dimensional ordination solutions and significance testing methods.

3.2.1 Detrended Correspondence Analysis (DCA)

A detrended correspondence analysis (DCA) was performed on the modern dataset with 596 sites, the 20 taxon variables, and the seven environmental variables (Table 5b). DCA was developed as an improvement to Reciprocal Averaging (RA), and reconciles the arch or horseshoe effect which plagues RA when species are distributed non-linearly along environmental gradients, lending to more interpretable and dependable results (Hill and Gauch, 1980). The DCA analysis was executed to function as a diagnostic tool to estimate the gradient length for the environmental variables utilized in the CCA ordination. A threshold criterion of 2.5 gradient lengths was established to validate the DCA results, warranting the use of canonical correspondence analysis (CCA) (Cushman, S.A., personal communication, October 10, 2007), with biplot scaling to visually display the effect of the environmental variables on the distribution of species in the ordination diagrams.

DCA ordination was run simply as a diagnostic check to calculate gradient lengths for the environmental variables revealing whether CCA or Redundancy Analysis RDA was most appropriate for the modern day analysis, and to quantify the correlations between of the environmental variables used in the study. The DCA gradient lengths were greater than the pre-established threshold criteria of 2.5 except for Axis 3, which contained one gradient length of 1.7, allowing the use of CCA (Table 6).

3.2.2 Canonical Correspondence Analysis (CCA)

Canonical Correspondence Analysis (CCA) is a direct gradient analysis method in which assumes there is a linear relationship between causal and explanatory variables. In this case, the scores express the modern pollen species abundances as linear combinations of the environmental variables. Each CCA axis represents combinations of the environmental variables that best describe the species pollen distribution. The CCA ordination was performed on the modern dataset with the row (sites) and column (pollen species) scores standardized by centering and normalizing using biplot scaling. The resulting biplot diagram approximates weighted averages of species with respect to the environmental variables (ter Braak, 1987; ter Braak and Prentice, 1988). In other words, the site ordination scores were rescaled by optimizing the taxon pollen counts such that the species scores weighted mean is zero and the variance is one with $\alpha = 0$. Biplot scaling allows for direct spatial interpretation of the relationship between the environmental and taxon data, and was performed because it shows the best fit of species abundance to the environmental data..

Finally, a Monte Carlo test was performed with the CCA using 10,000 permutations to increase precision in the resulting p-values and significance test at the 0.05 significance level. A null hypothesis that there would be no structure in the main matrix and therefore no linear relationship between matrices was utilized in the Monte Carlo test. PCORD randomly assigned elements in the main matrix within taxa, and preserved the matrix and taxa totals (McCune and Mefford, 1999). The CCA algorithm used in PCORD is an iterative method adapted from (ter Braak, 1986).

Interpretation of the CCA ordination closely followed the suggestions and procedures presented in McCune and Grace (2002) and McCune and Mefford (1999). Unlike NMDS, CCA is a direct gradient analysis method in which there is an assumption of a linear relationship between species community composition and the environmental variables (ter Braak, 1986; ter Braak and Prentice, 1988). Thus, the CCA output includes correlations among the explanatory (environmental) variables, total variance in the species data, multiple regression results, and correlations of environmental variables with respect to the ordination axes.

3.3 Ordination Procedures for Fossil Pollen Analysis

3.3.1 Non-Metric Multi-Dimensional Scaling (NMDS)

Analysis of the paleopollen dataset focused on the 33 sites for which soil cores allowed pollen counts between modern day and 9000 ybp (Table 2). The NMDS ordination employed a multi-temporal matrix, showing the taxon pollen percentages measured at each time period at each site (Table 9). The NMDS ordination was performed using only the species variables and not the environmental variables. The NMDS analysis was performed following the suggestions of McCune et al. (2002), including an initial log transformation of the species data to normalize the rank distances from the ordination procedure and improve the ordination results and interpretation. An instability criterion of 0.00001 was applied to obtain a stable ordination solution using the Bray-Sorenson distance measure in the dissimilarity matrix.

To determine the most stable solution and appropriate dimensionality for the dataset, a preliminary six-dimensional NMDS run was selected with settings detailed in Table 10a. After examining the results of the preliminary NMDS run, a three dimensional solution was selected based on the resultant scree plot (Figure 5), the final instability, the stress levels from the various dimensional solutions in the ordination procedure, the proportion of variance explained by each axis, and the correlations of variables between the resultant axes (Table 10a). Solutions with a low number of dimensions have higher stress and instability values; however solutions with multiple axes add complexity to the ordination interpretation, lessening the likelihood of making reasonable inferences from the correlations between species variables.

Another NMDS was run (Table 10b) using the three dimensional starting configuration from the preliminary NMDS run, with no step down in dimensionality, and resulting in a minimum stress value of 9.433, meeting the stress value criteria established by (Kruskal, 1964b; Clarke, 1993), for determining reliable interpretation of ordination results, indicating a "good ordination, with no real risk of drawing false inferences" (McCune et al., 2002). The stress value indicated a good to fair ordination following Kruskal's rule of thumb (Kruskal, 1964b; McCune et al., 2002), (Table 1). The three-dimensional solution served as the base for plotting the ordination coordinates, performing the time-series analysis, and examining species composition change. A solution with greater than three dimensions was avoided to simplify the ordination interpretation, and show the strongest species gradients permitting intelligible hypotheses regarding species' distribution, abundance, and composition through time.

3.3.2 Landscape Trajectories 9000 to the Present

The landscape trajectory analysis was performed to examine the temporal change in community composition from 9000 to the present. This is vital because biophysical factors, especially climate, can change over centennial and millennial time scales. Individual and community plant distributions and migrations respond to these changes due to differing species ecological requirements. In other words, plants and plant communities spatially 'follow' their respective environmental conditions through time. By combining landscape trajectories with ordination scores, one can effectively track the rate and direction of species composition change, and thus infer climatic change, through space and time.

The ordination plots the location of taxon scores in a reduced space, and the locations of the landscapes are simply the coordinate locations resulting from the NMDS ordination analysis at each respective time slice (Cushman and McGarigal, 2007). The coordinate values make it possible to plot individual temporal landscape locations, thus creating a landscape trajectory through time (Figure 6). Of course, it is important to understand modern day ecological conditions to obtain a more thorough understanding of environment/species interactions; however, a thorough knowledge of past biophysical conditions and the resultant community composition also can serve as a reference for potential future climate scenarios. Four measurements were utilized to analyze landscape trajectories: displacement, velocity, acceleration, and divergence following McGarigal and Cushman (2007).

Displacement is measured by the Euclidean distance between the ordination (coordinate) landscape locations at any time slice from its original location. Therefore,

displacement is the Euclidean distance measured between two points in the ordination space. Displacement is expressed in the following component form equation:

$$\overline{d_i} = \Delta x_{i1} + \Delta x_{i2} + ... + \Delta x_{im}$$

where Δx_{ik} is the difference in scores between time $j=t$ and 0 for landscape i (1…n) on axis k (1…m).

Velocity quantifies a vector comprised of the direction and rate of change in the landscape trajectory, or the rate of change along each ordination axis (each dimensional gradient). Velocity is expressed in the following component form equation:

$$\overline{v_i} = (\Delta x_{i1} + \Delta x_{i2} + ... + \Delta x_{im}) / \Delta t$$

where Δx_{ik} is the difference in scores for landscape i (1…n) on axis k (1…m) for that interval.

Acceleration is a measure of the rate and direction in the community composition, where the velocity of which is shifting, and along with velocity, is a vector quantity. Acceleration is expressed in the following component form equation:

$$\overline{a_i} = (\Delta x_{i1} + \Delta x_{i2} + ... + \Delta x_{im}) / \Delta t^2$$

Here acceleration is defined as the rate of change in velocity along each dimension of the landscape structure space.

Divergence is simply a quantitative comparison between multiple landscapes, and also serves as a means to compare differences between individual landscape trajectories. Divergence is expressed in the following component form equation:

$$\overline{d_i} = \Delta x_{i1} + \Delta x_{i2} + ... + \Delta x_{im}$$

where Δx_{jk} is the difference in scores between any two landscapes at time *j* and (0…t) on axis *k* (1…m). Divergence is the difference in the landscape structure space along each dimension. The equations listed above were adapted from McGarigal and Cushman (2007).

3.3.3 Mapping NMDS Ordination Scores and Displacement

Displacement and ordination coordinate values were temporally mapped by interpolating Axes 1 and 2 displacement scores utilizing a co-kriging technique (ESRI, 2009) in conjunction with a 4 × 4 km DEM once for each time slice. The individual axis time slice interpolations were merged to form multiband composites for each time slice, enabling temporal, compositional, and climatic trend comparisons.

4. MODERN POLLEN RESULTS AND DISCUSSION

4.1 CCA Ordination Results

The CCA results yield information regarding interactions between the environmental variables, environmental gradients, and variability within the species data. Said another way, the CCA analysis provides a representation of community-level patterns of species composition variation in response to the environmental gradients. A variety of results were reported to aid in initial interpretation of the ordination diagrams themselves which are discussed in detail later in the section.

Strong correlations amongst the environmental variables themselves were observed (Table 11). In some cases this was due to their multiplicative nature, such as latitude multiplied by longitude to just longitude itself (0.992). However, other strong correlations, such as longitude to precipitation, describe the generalized modern regional climate with higher precipitation in the west.

The axes iteration report estimates convergence of a stable solution as related to a specified tolerance value of 10^{-13}. All three ordination axes met these criteria, reaching the tolerance value after few iterations (Table 12). The axis summary statistics (Table 13) calculated the total variance (inertia) in the species data at 2.5999, and revealed p-values of 0.0001 for all three axes. Comparatively, 23.2% cumulative variance is explained by the three ordination axes: 21% explained by Axes 1 and 2 alone. Similarly, Axes 1 and 2 possess the highest correlation values at 0.820 and 0.677, respectively, reporting the strength of association between species and environmental gradients depicted by each axis. The correlation values in the ordination diagram and associated

statistics portray reasonable inferences of species composition, and indicate the usefulness of the environmental variables in determining species composition at sites.

The multiple regression results (Table 14) report the effectiveness of the environmental variables in structuring the ordination, and describe the relationships of the ordination axes to the environmental variables. The coefficient of determination (r^2) expresses the strength of the relationship between the environmental variables and the site scores. The standardized scores show that the most influential environmental predictors for Axis 1 are precipitation multiplied by elevation, while Axis 2 is most closely related to variables latitude, longitude, a combination of those, and elevation.

4.2 Interpretation of the CCA Ordination Diagram

Nearly 600 sites were utilized in the CCA ordination, so to aid in interpretation of the complex graph, species scores, site scores, and the biplot vectors (of the environmental variables) were also shown (Figure 7). Only Axes 1 and 2 are discussed and displayed in the ordination diagram as the intraset correlations were insignificant for Axis 3, since the eigenvalues and percent of variance explained between the species and environmental variables were negligible for Axis 3. The distance on the ordination diagram between where a site plots relative to the species points indicates the abundance of each species at that study site. For example, sites clustered closely to Alnus should contain higher abundance of that species (Figure 7).

The ordination axes were interpreted from the correlation scores between each axis and the environmental variables (Table 15). Axis 1 is dominated by the northwest to

southeast gradient with the highest values located in the northwest (0.874) and precipitation (0.835). Also strongly significant to Axis 1 is longitude and NE to SW gradient with the highest values in the northeast. Therefore, Axis 1 is an environmental gradient driven by geographic gradients and precipitation, which is consistent with the modern day climate in which the wettest site locations are found in the northwest sector of the study area.

Table 15 shows that Axis 2 is driven predominantly by elevation (-0.692) and latitude (-0.428). Although latitude was also correlated, it was not plotted as a biplot vector since its contribution was less than the specified threshold 0.50 (-0.428). The low elevation sites located on the upper half of the diagram are valley and prairie sites, while those located on the lower half of the ordination are montane sites.

Thus, sites located on the far left side of the diagram are driest while the wettest are in the right side and upper right corner (Figure 7). This is supported by the ordination location of the species variables as well: the more drought tolerant species (S*arcobatus, Artemesia, Ambrosia,* and *Chenopodaceae/Amaranthaceae*) are located in the upper left corner of the ordination diagram, and are also generally found at low to moderate elevation ranges. Moisture and shade tolerant species (e.g. *Tsuga, Cupressaceae/Taxaceae, Pseudotsuga/Larix,* and *Alnus*) are located in the upper right of the diagram, and are generally found in the western wetter portion of the study area at higher elevations. Similarly, *Thuja, Picea, Abies,* and *Pinus* plot near the lower left quadrant, their higher elevation locations with intermediate moisture requirements (Figure 7).

Finally, a Monte Carlo test of significance was performed on the CCA output to evaluate the significance of the CCA axes. This test whether the relationship between matrices describing the environmental gradients and the species abundance data was greater than what would be expected by random chance. From Table 13 it is clear that a definite relationship exists between the first and second matrix, since the resultant p-value is 0.0001 for all three axes.

4.3 Biome Analysis

Although the initial CCA ordination results explained comparatively little variance in the overall analysis (Table 13), the ordination diagram reveals some intriguing site groupings. Species variables plotting close to the center of the ordination do not have significant weight in predicting vegetation composition or the true species optima at sites located near the species point (ter Braak, 1986). In this case, that includes *Salix, Pinus undifferentiated, Ranunculaceae,* and *Asteraceae* (Figure 7). The inclusion of more environmental and/or biophysical variables would probably increase the validity and effectiveness of further analyses. The strength of the CCA approach to define environmental gradients, however, is clearly evident when used in conjunction with GIS analysis to examine spatial patterns of the site groupings and gradients revealed by the ordination diagrams.

Figure 8 shows the geographical locations of the study sites in relation to terrestrial biomes in the study area and within the reduced ordination space. The use of broad biome groupings, defined by Olson et al. (2001) and Olsen and Dinerstein (2002),

reveal distinct relationships between sites and the environmental gradients in the ordination diagram and their spatial location within a biome. The 'High Plains' ellipse on Figure 7 corresponds to sites located in the southeast corner of the study area (eastern Wyoming, western North and South Dakota, and the Yellowstone Plateau), with the driest and lowest elevations belonging to the temperate grasslands, savannas, and shrubland biome (Figures 7 and 8).

The 'Columbia Basin' ellipse on Figure 7 shows a similar range of conditions which parallel the sites in ellipse A, but are slightly more wet and northwesterly (Figure 8). These sites are a mix of lowland biomes, including temperate grasslands, savannas, shrublands, deserts and xeric shrublands, with the lowest and driest sites in the upper portion of the ordination, including sites from the Palouse Prairie. Again, moving from upper-left to lower-right within the Columbia Basin ellipse, elevation, precipitation, and latitude increase, and geographic position is more westerly. Clustered sites of the same species within this band suggest the sites in this area may receive long distance wind-deposited pollen from contrastingly different biomes or vegetation communities given their proximity to the Cascade and Blue Mountains, the Okanagan Highlands of Washington and Oregon, and arid deserts between the mountains. The Columbia Basin ellipse may represent an ecotonal shift for areas that are moving either towards reforestation stemming from human fire suppression efforts, climate change, or various types of disturbance resulting in loss of forest cover, or a move to more xeric, open, and drought tolerant conditions, from the upper left to the lower right (Figure 8). For both respective bands, the high number of study sites throughout the plains, shrub-steppe, and dry forests of Montana, Wyoming, Oregon, Washington, and southern Canada, provided

excellent spatial representation, though may have influenced the ordination results. However, the linearity of the points within the biome designations suggests considerable capability of the CCA ordination method to define environmental gradients from a large number of environmental and species variables using relative pollen percentages, though at a coarse scale resolution.

4.4 Ecoregion Analysis

To examine finer resolution variation and distribution within the ordination space, a similar analysis was conducted using the World Wildlife Fund (WWF) ecoregions (Olson et al., 2001; Olson and Dinerstein, 2002). The 24 ecoregions were utilized to define more local variation in vegetation composition, elevation ranges, and climate regimes essentially within each of the coarse biomes described above. The ecoregions were grouped into four broad biomes to aid in interpretation and allow for comparison of study plots with analogous site characteristics and vegetation composition, including a grassland group, a xeric shrubland/steppe group, a continental inland forest location group, and a Pacific Northwest/coastal forest group, all of which plotted separately in both the ordination and geographic space (Figures 9 - 12).

4.4.1 Grasslands

Figure 9 shows the grassland grouping, comprised of seven ecoregions. All grassland ecoregions plot on the two dominant ellipses in the CCA ordination, driven primarily by longitude, latitude, precipitation, and elevation. All study plots located

within the Northern Short Grasslands and Western Short Grasslands (Figure 9) are in the upper-left sector of the High Plains/Dry Forests ellipse, and are geographically in the southeast corner of the study area. Following the High Plains/Dry Forests ellipse to the lower-right in ordination space, new ecoregion types occur reflecting the higher moisture and elevations found towards the northwest, such that the grassland ecoregions at the negative end of Axes 1 and 2 in the High Plains/Dry Forests ellipse are the higher elevation and more westward study plots in geographic space. This gradient holds especially true for the Canadian Aspen Forests and Parklands (CAFP) and Montana Valley Foothill Grasslands, (MVFG), as revealed by their close proximity location in the ordination space, reflecting that the CAFP sites are the northernmost and wettest of the grassland ecoregions. Likewise, the MVFG ecoregion displays its increased easterly location and the associated dry vegetation composition of *Artemesia*, *Poaceae*, and scattered mosaics of *Pseudotsuga* and *Pinus* (Figure 9). Finally, the Columbia Basin ellipse shows the sites from the Palouse Grassland. Even this smaller cluster of related sites reveals characteristics of enhanced dryness, high abundance of *Poaceae* and *Artemesia*, and the more westerly locations in Washington and Oregon.

4.4.2 Intermontane Forests

The intermountain forests are shown in Figure 10. Once again, a distinct geographical pattern was observed in a northwesterly direction, even within the same ecoregions. The South Central Rockies (SCR) ecoregion (which includes the Greater Yellowstone sites) plots in the center of the High Plains/Dry Forests ellipse, reflecting the relatively high elevation, increased moisture, and southeasterly location within the study

area. Other SCR sites plotted in ellipse A correspond to the longitude/elevation/precipitation gradient, with the Black Hills of South Dakota located within the upper-left of the ordination and the Bighorn/Wind River sites to the lower-right, reflecting their higher, more easterly, and wetter locations. The large diversity included within the North Central Rockies (NCR) sites are reflected by its occurrence within both Columbia Basin and High Plains/Dry Forests ellipses (Figures 7 and 10). This diversity within the NCR sites reflects the regions variable elevation, topography, climate, and excellent spatial dispersion of sites throughout the ecoregion. Finally, the Blue Mountains of Oregon cluster in ellipse A quite closely to the Palouse Prairie and steppe sites (Figure 9), reflecting their more westerly location and drier vegetation dominated by *Pseudotsuga/Larix, Artemesia,* and *Pinus.*

4.4.3 Xeric Shrublands

The xeric shrubland ecoregion comparison (Figure 11) also showed distinct grouping in both ordination and geographic space. The Wyoming Basin shrub steppe is found along a definite longitude/latitude/elevational gradient, shown by two distinct groupings in ellipse A. Similarly, the Snake-Columbia shrub steppe exhibits distinct clustering, but primarily within ellipse B. Most of the sites are located just west of the Palouse Grasslands ecoregion. Two sites are in south central Idaho and these plot along ellipse A, reflecting an ecotonal boundary (Figure 11).

4.4.4 Pacific Northwest Forests

Finally, the Pacific Northwest Forest Ecoregion sites showed the greatest amount of variation in the ordination space, though groupings are still evident. Certainly, these forest study sites are affected by their latitudinal location given the ecoregion orientations in long, slender strips running north to south. This variability is due to the dramatic precipitation gradient enhanced by elevation across the study area. The Central and Southern Cascade ecoregion and Cascade Mountains leeward forests ecoregions plot close to one another in the ordination, near the Palouse Prairie and Snake River shrublands and steppe, which is consistent with these ecoregions' westerly location, increased elevation, and latitudinal variation. The Willamette Valley forests (the only mixed broadleaf/ deciduous/coniferous forest in this analysis) cluster in the upper portion of the ordination, directly to the left of an elongated cluster of Central Pacific coastal forests, revealing their decreased elevation and moderate precipitation and significant correspondence along Axis 2. The Puget Lowland and British Columbia Mainland Coastal forests exhibit the most dispersion in the ordination, affected by high variation in latitudinal, precipitation, and elevation site values (Figure 12).

The ecoregion and biome analyses showed CCA correctly and effectively partitions geographically related study sites into definitive positions in the ordination space (Figures 9 - 12). However, the Pacific Northwest Forest Ecoregions lacked effective gradients in the ordination space, suggesting that the current environmental and species variables are not sufficient to fully differentiate environmental gradients using this technique. Likewise, given the low amount of variability described by the CCA

ordination (Table 13), the current biophysical and pollen abundance data are not adequate by themselves to predict species' pollen percentages in areas of missing data. The inclusion of more biophysical variables directly relevant to plant physiology and environmental response would improve results, though these were not further investigated in this study.

5. FOSSIL POLLEN RESULTS AND DISCUSSION

5.1 Interpretation of NMDS Ordination Axes

The three dimensional solution obtained from the NMDS ordination resulted from 33 study plots sampled at ten distinct time periods (Figure 13) can be interpreted in terms of community composition variation throughout the study area . The "+" symbols represent centroids of each species variable, and infer that sites plotting close to the species centroids have the highest abundances of that species at those sites. Species vector lengths indicate the amount of influence that species has on the ordination and aid in interpretation of the axes.

Nearly 96% of the variance within the species variables was explained in the first three ordination axes, with 91.5% explained in the first two axes alone, and Axis 3 contributing only 4.5% (Table 10b). The three axes represent different genus/species interactions. Table 16 shows the correlation scores for the ordination axes. High correlation scores indicate greater influence in terms of species composition from which inferences can be made about biophysical and vegetative characteristics at those study plots. Examination of Table 16 allowed interpretation of species gradients along each axis. R^2 represents the coefficient of determination, R is the Pearson correlation coefficient, and Tau signifies the Kendall rank coefficient (Jupp, 1987).

These results were entirely derived from pollen data and inferences about environmental gradients can only be derived from understandings between the vegetation and modern analogues as investigated in Chapter 4.

Ordination Axis 1 is predominantly dictated by tree genera (Table 16). *Pinus* undifferentiated is most highly correlated with Axis 1 (0.882), in the positive direction, while *Cupressaceae/Taxaceae*, *Pseudotsuga/Larix*, *Alnus*, and *Tsuga* have high correlation scores on Axis 1 in the negative direction. The negative tree variables plot in the upper-left quadrant of the NMDS ordination; their trajectories are aligned in the same primary direction, possess similar trajectory lengths (Figure 13), and are compositionally and phenologically much different than species within the *Pinus* undifferentiated category. Axis 1 also indicates increasing canopy openness in the positive direction (decreasing in the negative). Sites with significant abundances of *Alnus, Betula, Taxaceae, Pseudotsuga/Larix, Tsuga,* and *Cupressaceae* infer wetter, warmer, and more shade tolerant sites with denser forest canopies.

Axis 2 is a gradient that reflects shrub, herb, and grass genera. Tree genera highly correlated to Axis 2 were *Abies* (0.633) and *Tsuga* (0.771), which was also closely correlated with Axis 1 (0.744). *Alnus* and *Pseudotsuga/Larix* score high on Axis 2 (0.711 and 0.655, respectively), though their highest scores occurred on Axis 1. While Axis 1 is a gradient in tree composition and moisture, likewise Axis 2 is a moisture and grass/shrub gradient, influenced most heavily by *Artemisia* (-0.916), *Chenopodaceae/ Amaranthaceae, Poaceae, Asteraceae,* and *Ambrosia* (Table 16). All of these variables are shrub, herb, and grass genera, forming a gradient of corresponding ground cover, dryness, and canopy openness. Axis 2 also aids inferences to groundcover communities that are associated with certain tree communities. The more-closed canopy, mesic sites plot in the upper portion of the ordination space (Figure 14). Sites plotting in the upper-left quadrant are the most moist, shaded, and disturbance-tolerant variables. Sites

plotting closer to the negative end of Axis 2 possess higher abundances of *Artemisia, Chenopodaceae/ Amaranthaceae, Poaceae,* and *Ambrosia*, reflecting community composition with more drought tolerant species, less tree cover, and more herbaceous groundcover. *Abies* is closely aligned in the positive direction of Axis 2, and nearly mirrors Poaceae, indicating that the positive end of Axis 2 represents site that are wetter, more dense in canopy cover, and moisture-tolerant tree assemblages. Since Axis 3 does not indicate any strong environmental gradients, it was not further analyzed and is not discussed in this report.

Sites used in the NMDS ordination analysis were subset into 8 groups for analyses according to their proximity in the ordination diagram, their spatial location, and other biophysical similarities such as elevation and biome classification. Sites within each grouping are regionally clustered in ordination and geographic space (Figure 14) Group1 sites comprise the low-elevation, warm and moist Pacific Northwest coastal forests, Group2 the interior dry grassland Prairie sites, Group 3 the wet and mild Mid-Elevation Forest sites, Group 4 the high-elevation Yellowstone Plateau sites, Group 5 the South Central Rockies sites, Group 6 the Intermountain Forest sites, Group 7 the Northern Rockies sites, and Group 8, the High Elevation Rockies sites.

5.2 Successional Vector and Landscape Trajectory Analysis

Successional vectors display the location and direction of species composition change along axes of the NMDS ordination analysis, allowing inferences of change in vegetative groundcover, composition, climate, and other biophysical conditions. Only ordination groups 1, 2, 4, and 6 are discussed in this report. These groups were chosen

because they possess contrasting elevations, diverse community compositions, and geographically disparate locations throughout the study area, thus providing interesting ecological comparisons between groups.

While successional vectors can be easily interpreted in some cases, several additional metrics were calculated to aid in interpreting community changes through time *Displacement* measures the Euclidean distance in ordination space between the locations of a site in sequential time steps, and shows the magnitude of species composition change between each time step. *Velocity* measures the rate and direction of change in this landscape trajectory. Abrupt changes in trajectory direction can signify an ecologic threshold, resulting in alteration of community composition. *Acceleration* is the rate of change in velocity of the vegetation composition between each time slice.

Divergence trajectories quantify community composition displacement at different landscape locations though time (McGarigal and Cushman, 2007). Pronounced inaccuracies in identifying pollen grains and deteriorating radiocarbon dating accuracy in aging fossil pollen, sediment, and other macro fossils in the 6000 to 9000 ybp time period are known to exist (Kutzbach and Webb III, 1993), and may undervalue the magnitude of the landscape trajectories at those times. Successional vector and landscape trajectory graphs for groups 3, 5, 7, and 8 are listed in the Appendix.

5.2.1 Pacific Northwest Sites

The Pacific Northwest sites (Group 1) consists of low elevation, moist, coastal forest communities. Pacific Northwest vegetation displacement and divergence trajectories (Figures 15, 16, and 19) show all sites, except Site 30, had moderate

reductions in *Pinus*, grass, and shrub groundcover to increases in forest species dominated by *Tsuga, Alnus, Cupressaceae/Taxaceae,* and *Pseudotsuga/Larix*. Presumably these shifts were driven by cooler and wetter climate from 9000 to 6000 ybp, allowing colonization of locales once covered by the recently retreated Laurentide and Cordilleran ice sheets. These changes are consistent with pollen analyses focused at that time period (Barnosky et al., 1987; Barnosky, 1989). Meanwhile, velocity and acceleration trajectories were insipid during this time (Figures 17-18)

Northern Sites 30 and 33 exhibit cooler and wetter climate dominated by *Abies* and *Tsuga*; characteristic of the Pacific Northwest region, while southern Sites 31 and 32 were warmer, drier, and more open, typical of the southern Pacific Northwest region. These observations match charcoal accumulation rates (CHAR) from the Coast and Cascade Ranges of northern Oregon and southern Washington (Marlon et al., 2006), as well as consistently reduced mean *Z* scores of charcoal values from 9 ka to 3 ka in northern Washington and southern British Columbia, suggesting reduced fire occurrence, though higher intensity fires given increased biomass and fuel loads (Power et al., 2008). Pollen data and paleoclimate model comparisons are also synchronous with this trend, showing drier effective moisture between 9000 and 6000 ybp relative to the modern day, and maximum effective moisture attained around 3000 ybp throughout the Pacific Northwest (Thompson et al., 1993).

From 3000 to 1000 ybp, regional climate became warmer and drier evidenced by community displacement to *Pinus*, grass, and shrub groundcover. Velocity and acceleration trajectories deviate at 3500 ybp, as composition displacement becomes more asynchronous throughout the region. Vegetation and climate changed little until

1500 ybp, when Sites 32 and 33 accelerate abruptly in velocity to rapid forest densification, and Sites 30 and 31 exhibit more open and dry conditions given increased grass and shrub species abundance and more prolific *Pinus* forests. Regional divergence trajectories suggest accelerated and sustained drought after 1500 ybp, as revealed by decreases on Axis 1 and 2. This trend is pronounced in the southern Pacific Northwest, and coincides with the onset of the MWP, modern climate, regional forest composition, and emergence of *Tsuga* (Crowley, 2000; Whitlock et al., 2007).

The most rapid landscape trajectories occur from 500 to modern day, presumably resultant of Native American displacement, region-wide fire suppression efforts, and widespread environmental human modifications, notably logging (Brunelle et al., 2005); Figures 15-19). Inland Sites 30 and 31 indicate displacement to *Pinus* forests and more abundant grass and shrub groundcover, implying cooler and drier climes, while coastal Sites 32 and 33 turn cooler and wetter given increased abundance of *Abies* forests.

Vegetation change was largely synchronous through time within the Pacific Northwest region evidenced by analogous rate and direction of divergence trajectories driven by local climate and disturbance regimes from 9000 to 3500 ybp. Composition change became asynchronous until 1500 ybp when all Pacific Northwest sites show comparable trends toward more xeric conditions (Figure 19). Recent dry climatic trends are supported by lake level studies in southwestern British Columbia, which exhibit desiccation and minimum effective moisture in the last 1000 years (Ritchie and Harrison, 1993).

5.2.2 High Plains Prairie Sites

Figure 20 illustrates minimal successional change at all sites at all time slices for the prairie sites (Group 2). No vectors cross paths and change is inconsistent in direction, rate, and time, indicating slight climate and vegetation variation through time. Sites showing perceptible change shift from expanding forest to more prolific shrub steppe, resulting from long distance wind transport reflecting change from nearby mountains and foothills. High Plains Prairie landscape trajectories are least among the ordination groups. Axis 1 decrease is attributed to *Juniperus*, *Alnus*, and *Pseudotsuga* increase since other Axis 2 tree species are endemic to the Pacific Northwest, and have never existed on the Great Plains (Barnosky et al., 1987; Thompson et al., 2004). Displacement (Figure 21), Velocity (Figure 22), and Divergence (Figure 24) trajectories show climate slowly became wetter, allowing colonization of *Pinus* and *Abies* tree species following deglaciation from 9000 to 6000 ybp in the higher elevations. Sites 1 and 13 demonstrate similar trajectories, vegetation composition, and climate change through time.

From 6000 to 3000 ybp, all sites experienced rapidly accelerating displacement to *Cupressaceae/Taxaceae, Abies* and *Pinus* undifferentiated in the Laramie Mountains and along the Rocky Mountain Front, inferring cooler and wetter climate. Continued cooler and wetter conditions is matched by paleoclimate model and fossil pollen analyses, which show the Northern Plains were shifting from temperate grassland to xerophytic grassland, contained more chenopods and less sagebrush, while minimum effective moisture was reached at 9000 ybp, and maximum effective moisture attained at 3000 ybp, supporting forest expansion (Thompson et al., 1993). At around 3000 ybp, the High Plains region

exhibited climate and vegetation characteristics similar to modern day conditions, sharing similar rate, direction, and magnitudes of divergence paths. Grassland communities changed little during this time, suggestive of more effective moisture in higher elevations, and matched by low elevation lake-level analyses, showed aridity peaked at 6000 to 5000 ybp and lake levels rose from 5000 to 2000 ybp (Hallett and Hills, 2006). GCM model results at 3000 ybp from the southern Canadian interior also predicted the winter westerlies were stronger than today, thus increasing precipitation with cooler and wetter climate throughout the region (Ritchie and Harrison, 1993). After 3000 ybp, the high plains became warmer and wetter given denser mountain forests.

From 1500 to 1000 ybp, the region underwent sustained drought, given Sites 1 and 13 accelerate rapidly in velocity and displacement toward increased *Cupressaceae/Taxaceae* abundance and drought-tolerant grass and shrub assemblages as climate quickly became warmer and drier. Sites 3 and 15 increased in *Abies* and *Artemesia* groundcover, suggesting advancing tree line as alpine tundra gives way to pine/fir/sagebrush parkland in the mountains near those sites, coincident with the MWP, and supported by amplified and sustained salinity levels at Moon Lake, North Dakota, and high Drought Area Index (DAI) values from regional PDSI reconstructions (Cook et al., 2004).

500 to modern day revealed the most accelerated climate and vegetation change trajectories. Sites 1 and 13 rapidly shifted to increased abundance of *Pinus* undifferentiated and *Abies* forest communities with reduced herbaceous groundcover as climate became cooler and wetter, though 3 and 15 were warmer and drier given increased *Cupressaceae/Taxaceae,* sagebrush, and canopy openness, suggesting future

site conditions will have no modern analog, especially at ecotonal boundaries (Figure 23). The High Plains prairie sites possess highly synchronous divergence trajectories through time, implying the region experienced consistent and analogous climate and vegetation shifts, and was always a grassland dominated community (Figure 24)

5.2.3 Yellowstone Plateau Sites

The high elevation Greater Yellowstone sites (Group 4) possess tightly clustered successional vectors, indicating minimal though similar climate and vegetation fluctuations through time (Figure 25). Site 11 trends excessively from dry, open conditions to wet, dense, *Abies*-dominated forests (Figure 25). Greater Yellowstone displacement (Figure 26) is consistent through time. Site pairs 5 & 7 and 6 & 11 were more similar within groups. From 9000 to 6000 ybp, gradual velocity, acceleration, and displacement trajectories reveal the Greater Yellowstone area gradually underwent a prolonged period of cooler and wetter climate, reflected by reforestation of *Pinus* and *Abies* tree assemblages, marking the origination of sagebrush/pine parkland now dominant in this region. These findings do not agree with proxy record comparisons.

Site 5 increased in *Pseudotsuga, Alnus,* and *Juniperus,* indicating warmer and drier climate, while Site 7 underwent forest densification given warmer and wetter climate evidenced by *Abies, Pseudotsuga,* and *Cupressaceae/Taxaceae* resurgence and long periods of no disturbance. At Sites 6 and 11 *Pinus* and *Abies* forest expansion reflected cooler and wetter climate, coupled with minimal groundcover change (Millspaugh et al., 2000). Proxy comparisons show marked rise in CHAR (Power et al., 2008), and BCHAR (Marlon et al. 2006), resulting from large, frequent, localized

disturbance events given more combustible biomass from forest expansion (Marlon et al., 2006). This inconsistency is logical given expanding alder and Douglas Fir, and GCM model results relating temperature values 2°C warmer throughout the region (Thompson et al., 1993).

From 6000 to 3000 ybp, swift velocity, acceleration, and displacement trajectories show the Yellowstone region experienced expansion of *Pinus* (notably *Pinus Contorta*) and *Artemesia* parkland, with cool though xeric conditions, shortened fire return intervals, and larger fires (Figures 26 - 28). From 3000 to 1500 ybp, *Pinus, Alnus, Abies* and *Pseudotsuga* forests moderately expand with minimal change in shrub or herbaceous groundcover, cool climate, and wetter climate trajectories, supplemented by GCM results showing maximum effective moisture attained at 3000 ybp (Thompson et al., 1993), decreased summer insolation, less disturbance, and reduced charcoal in sediment varves supporting lengthy disturbance intervals (Power et al., 2008), and observed in geochemical, stable isotope, charcoal, and diatom records from a multi-proxy comparison of the region Whitlock et al., (2007). From approximately 1250 to 750 ybp rapid xerophytic steppe expansion and reduction in tree cover, year round anoxia and sulfate reduction resulting in minimal $CaCO_3$ deposition, increased CHAR abundance (Whitlock et al., 2007), drought indicative PDSI values (Cook et al., 2004), and resident tree ring reconstructions (Gray et al., 2007) synch with the landscape trajectory dataset, supporting the resurgence of intense and sustained drought during the MWP (Figures 26 - 29).

The last 1000 years reflect rapid displacement to *Alnus* and *Artemesia* expansion, responding to sustained drought and frequent disturbance (Figure 26), however, proxy records suggest more mesic conditions via stable isotope minima (Whitlock et al., 2007),

enhanced moisture PDSI values (Cook et al., 2004) and local tree ring studies (Gray et al., 2007) from 1000 to 500 ybp, though proxy comparisons agree during the last 500 years via high CHAR levels, prolific pine/sagebrush expansion, and xeric climate conditions (Power et al., 2008). This trend continues mildly to the present (Figures 27 and 28).

Regional synchrony was apparent along a grass/shrub gradient throughout the Greater Yellowstone area, evidenced by analogous peaks and valleys of Axis 2 trajectories, suggesting regional periods of forest expansion and contraction, driven more by localized disturbance events then regional climate shifts. The northern Greater Yellowstone area changed more similarly compared to the southern portion, though the entire region experienced extreme drought during the MWP, though the present drought is more mild (Whitlock, 1993; Millspaugh et al., 2000). The southern portion experienced rapid reforestation, suggesting significantly warmer climate in high elevations, reflecting upwardly advancing tree line.

5.2.4 Intermountain Forest Sites

The intermountain forest sites (Group 6) experienced synchronous climate and vegetation shifts through time and portrays the greatest community displacement magnitude among analyzed groups. Site 28's unique vector trajectory path is resultant of lower elevation, mesic conditions, and prolific Pacific Northwest tree, shrub, and grass species (Figure 30). Site 28 was included in this grouping due to similar community composition confirmed by its proximity to Northern Rocky Mountains sites in the ordination output (Figure 13).

Intermountain Forest displacement, divergence, and velocity trajectories from 9000 to 6000 ybp at Sites 14 -18 trended to mildly warmer and wetter climate supporting expansion of *Alnus*, *Pseudotsuga/Larix,* and *Cupressaceae/Taxaceae* forests, though Site 28 quickly shifted to more abundant *Pinus* and *Abies* forest communities with cooler and wetter climate, and is in agreement with west coast CHAR deposits, paleoclimate model scenarios showing minimum effective moisture at 9000 ybp, and like the Pacific Northwest sites, trend to dense mesic forest expansion into the middle Holocene (Thompson et al., 1993). From 6000 to 3000 ybp, at Sites 14 and 17 in west central Montana, rapid acceleration displacement to *Pinus* and *Abies* dominated forests suggest cooler and wetter climate and lack of disturbance, while Sites 16 and 18 farther north and higher in elevation, also quickly shift to more prevalent grass and shrub groundcover sustained by more xeric conditions, though may reflect down slope treeline migration. However, this result is not consistent with Thompson et al. (1993), which inferred climate was more xeric at 3000 ybp compared to 9000 ybp.

At 3000 to 1500 ybp gradual velocities to cooler climate inferred from *Pinus, Abies, Artemesia,* and *Sarcobatus* forest expansion is apparent at all sites. Sites 28 and 18 are slightly drier via higher *Pinus, Artemesia,* and *Sarcobatus* abundance, though the Bitterroot Sites continue *Pinus* and *Abies* forest growth with wetter climes until 1250 ybp, when all sites converge on Axis 2 (Figure 34b), reflecting warmer and drier regional climate, more openness, and rapid grass and shrub expansion. Modern vegetation and climate equivalents arise during this time, supported by Power et al., (2008), by matching modern day groundcover and fire regimes. From 1500 to 1000 ybp, hastened displacement, velocity, and acceleration trajectories to grass and shrub

dominance, suggests prolonged and persistent drought throughout the intermountain region, indicating rising treeline, reforesting once alpine tundra communities given expanding fir, larch, cedar, hemlock, and alder communities with short fire return intervals and open conditions (Figures 30, 32, and 33; Gerloff et al., 1995). This xeric trend is also evidenced in PDSI drought reconstructions at Burnt Knob Lake (Cook et al., 2004), and amplified BCHAR from 1200 to 900 ybp from Pintlar and Baker Lakes (Marlon et al., 2006).

Finally, the Intermountain Forests region exhibited regional synchrony, minus Site 28, from 6000 to the present. The remaining sites all diverged in similar directions on both ordination axes, suggesting the region experienced similar vegetation composition change, though at different velocities depending on elevation and latitude. Sites 28 and 14 experienced near parallel community composition change through time, regardless of the distance between them, since they are primarily composed of lodgepole pine and abundant sagebrush, suggesting consistently warmer and drier climates compared to other Intermountain Forest sites.

5.3 Regional Landscape Analysis

Divergence between representative sites from within each group provides a broad scale, regional assessment of compositional and climatic trends throughout the study area. Figure 35 shows the divergence between ordination groups, measured by utilizing the representative site from each regional divergence assessment in comparison to Group 6.

5.3.1 Divergence among Groups

The study area subregions experienced similar divergence trajectory rates, hence climate and vegetation response through time, though each group is comprised of different core vegetation assemblies. Compared to the Pacific Northwest, the intermountain forest region is consistently cooler and drier to support grass/shrub/*Pinus* parkland. Comparatively, intermountain forests tree species dominance driven by cooler and wetter climate is evidenced by the Intermountain Forests region's dual axis positive trajectory, unlike the open, dry, and warm conditions of the High Plains sites. The Yellowstone Plateau vs. Intermountain Forest trajectory shows intermountain vegetation is composed of more prolific *Alnus, Larix, Tsuga,* and *Cupressaceae/Taxaceae,* reflecting warmer and wetter climate, unlike the cool and dry climes with *Pinus/Artemesia* parkland characteristic of the Greater Yellowstone area.

According to Figure 35, all sites slowly diverge toward *Pinus* and *Abies* forest expansion and prolific grass and shrub groundcover, reflecting pine/sagebrush parkland forced by cool and moist climes from 9000 to around 3500 ybp. At 3500 ybp, the Yellowstone Plateau sites diverge more rapidly toward more open conditions and *Abies* forest contraction. The Pacific Northwest and High Plains sites experienced minimal divergence change until 500 ybp, when all sites undergo rapid dual axis increases, suggesting forest expansion, due to warmer and wetter climate, enhanced by fire suppression efforts (Hann and Bunnell, 2001; Hessburg and Agee, 2003), Native American displacement (Fiedel, 1987; Bonnickson, 2000; Hessburg and Agee, 2003), and warming climate (Woodward, 1987; Woodward and Cramer, 1996), all occurring at the

same time as the greatest divergence trajectory shift within the study area, signifying continued future warming and regional moisture shifts.

Although temporal variation exists within individual sites and site groupings as evidenced by the successional vector pathways (Figures 15, 20, 25, and 30) and NMDS ordination (Figure 13), most study plots never deviate substantially in community composition. This is evident from the temporal ordination maps showing vegetation composition at each study site (Figure 36). Diverse vegetation compositions exist across the study area, though regional trends are obvious in each ordination grouping. Traversing diagonally from northwest to southeast in geographic and ordination space, shades of dark green shift to bright red, representing the low elevation, warm, moist, dense, Pacific Northwest coastal forests to high elevation, cool, dry, and open subalpine forests/sage parkland of the Greater Yellowstone area. Likewise, progressing from the bright yellow northeast corner to the southwest reveals a change from the cool, wet, dense, mid to high-elevation sites of the Northern Rocky Mountains dominated by *Pinus* and *Abies* forest communities to dark brown-red colors showing low elevation, grass dominated, warm and dry climes of the High Plains of Montana, Wyoming, and North Dakota, located within the south-central portion of the ordination. The map and ordination show sites within regions changed little structurally in vegetation composition through time, though great differences exist between geographic regions (Figure 36).

5.3.2 Synchronousity of Vegetation Change

The study area experienced mostly synchronous directional change in vegetation and climate over millennia. Forested area is more prolific today region wide due to

reforestation from fire suppression efforts, removal of Native Americans from the landscape, and new forest growth following the large fires of 1988 and 2000 (Whitlock et al., 2003), supporting the hypothesis that vegetation composition changed synchronously throughout the region driven by regional climate and disturbance shifts over the last 500 years.

Asynchronous divergence shifts stem from varied elevation, aspect, and latitude, especially in the middle to late Holocene. These findings and observations support hypothesis 2, in that vegetation composition changed synchronously within the ordination sub grouping regions, responding to regional climatic shifts. Smaller landscape trajectory variation within groups is most likely caused by local disturbance events, differences in elevation, slope, aspect, and latitude.

The group by group divergence comparison (Figure 35) show vegetation composition throughout the study area experienced synchronous magnitude and direction of change at all time slices throughout the study area, evidenced by near parallel divergence trajectories. Note that while regions changed in synchrony, core vegetation assemblages were maintained at study sites through time. Some areas were always effectively warmer and drier than others. For example, the Intermountain Forests are always composed of more dense forest cover and less herbaceous groundcover compared to the High Plains, and were consistently cooler and wetter, though divergence trajectories change identically in direction and magnitude through time.

The displacement trajectory map exemplifies regional community composition displacement through time for the entire study area, and reveals how vegetation communities responded to sub-continental climate changes. Compositional and climatic

interpretation is identical to the ordination map (Figure 36), except for the legend. The displacement map is meant to visually illustrate community composition and climate trends from earlier to later time slices, thus showing how communities responded to large scale shifts in climate (Figure 37). To understand historic vegetation and climatic variation in the study area, one must examine both Figure 35 and 37.

For instance, from 9000 to 6000 ybp the Pacific Northwest registered composition trends reflecting cooler and drier climate given increased *Pinus* and grass/shrub abundance. The remainder of the study area largely show vegetation displacement to prolific forest expansion given cooler and wetter assemblages, and is in agreement with the landscape trajectory analysis. From 6000 to 3500 ybp, displacement between study area regions appears to be asynchronous (Figure 37), suggesting vegetation composition was changing significantly in response to continental climate change. Moving forward in time at 3500 to 3000 ybp, the Greater Yellowstone area, Pacific Northwest, Intermountain Forests, Northern Rockies, and Canadian Cordillera all respond to warmer and wetter climate given forest expansion and grassland contraction.

Beginning at 3000 ybp, areas east of the continental divide register composition displacement nearly opposite that of areas west of the divide (Figure 37). Leading to present day this trend continues, with the displacement map showing considerably different vegetation assemblages (Figure 37), though the study area divergence trajectories suggest similar climatic responses (Figure 35). The MWP is not well represented in the temporal displacement trajectory map, but is probably underrepresented at this scale since vegetation assemblages responded differently depending on elevation, latitude, and distance from the coast. This observation and

previous findings dispute the hypothesis that vegetation composition change was synchronous across the entire study area driven by sub-continental changes in climate. However, when combined with Figure 35, it is evident that climate changed in similar ways at the same times, though the vegetation composition response was asynchronous throughout the study area, depending on distance from mountains, the coast, elevation, and latitude. Therefore, continental climate changed synchronously, but vegetation responded differently throughout the study area.

5.3.3 Consistency of Vegetation Assemblages

By comparing the results of the NMDS ordination and landscape trajectory analyses to other paleoenvironmental proxy record findings, it is possible to infer similar climate conditions to present and thus likely similar vegetation assemblages, have manifested at times during the past nine millennia in the study area. In the Pacific Northwest, following consistently warm and arid conditions after 9000 ybp, all regions shifted toward slightly cooler and wetter conditions until 6000 ybp. Although 6000 ybp was considered dry, the colonization of tree species throughout the region reflects modern vegetation and climate regimes, and is supported by comparative charcoal amounts to modern times (Power et al., 2008), and from paleoclimate model output, showing similar modern temperature and moisture regimes at 6000 ybp (Thompson et al., 1993; Thompson and Anderson, 2000).

The High Plains region experienced the same trend toward cooler and drier climatic conditions from 9000 to 6000 ybp. At 6000 ybp, effective moisture was similar to modern day conditions, and divergence trajectories show compositions similar to

modern assemblages occurred at this time, though climate was still drier than present, evidenced by xerophytic grass species composition (Thompson et al., 1993). However, biome reconstructions predict modern day equivalent vegetation and climate regimes at 3000 ybp (Williams et al., 2004), although either time period is acceptable since observable change is minimal throughout the Great Plains. Although the Greater Yellowstone area also experienced drastic forest expansion with wetter climatic trends as witnessed in the Great Plains and Pacific Northwest, the Yellowstone area exhibited more variation in vegetation and climate from 6000 to 1000 ybp (Figure 29). Modern day equivalent vegetation assemblages were attained by 3000 ybp (Thompson et al., 1993), and supported by the emergence of modern day equivocal fire regimes attained by 2000 ybp (Millspaugh et al., 2000).

The Intermountain Forests also underwent similarly coupled species composition and climatic change over the last nine millennia in the Northern Rocky Mountains Analogous to the Greater Yellowstone area, the Northern Rockies around 3500 to 3000 ybp appeared most similar to modern day climate and vegetation conditions, evident from the landscape trajectory analysis, showing increasingly drier conditions leading to the present from 6000 ybp (Figures 34), further supported by modern levels of mean charcoal abundance at 3000 ybp observed in Power et al. (2008) and Whitlock et al. (2003). The Intermountain Forests are more difficult to ascertain modern day equivocal vegetation and climate in past times due to varied and asynchronous landscape trajectories, and diverse biophysical site conditions from 9000 to 3000 ybp (Figures 30-34).

The last 500 years of environmental history show hastened landscape trajectories within every region of the study area (Figures 15-34). The majority of individual sites show rapid displacement and acceleration toward warmer and climates, though differ in relative amounts of effective moisture were predicted from the landscape trajectories. The Pacific Northwest sites primarily show trends toward densification of xerophytic forests dominated by *Cupressaceae/Taxacea., Alnus, Tsuga* and *Pseudotsuga/Larix,* and dramatic contraction of shrub and grass cover, implying warmer and wetter climate. The Greater Yellowstone area showed forest increased abundance of tree species *Alnus* and *Pseudotsuga*, accompanied by increases in *Artemesia* and *Poaceae,* suggesting warmer and drier conditions (Figures 28, 29, and 35). Only the High Plains sites experienced more accelerated changes in vegetation and climate in previous time periods (from 2000 to 1500 ybp), and are more asynchronous than the other groupings during this time period, accelerating trends toward increased *Artemesia, Poaceae,* and *Sarcobatus*, and *Pinus* abundance (Figures 22 and 23), though divergence trajectories suggest of rapidly warmer and drier climes (Figures 24).

It is difficult to assert that vegetation and climate regimes similar to modern conditions occurred in the past within the study area utilizing the NMDS ordination and landscape trajectory results alone without incorporating comparisons of other proxy record findings. However, utilizing the ordination results, landscape trajectories, and proxy record comparisons together, broad similarities were found, namely between 6000 and 3000 ybp. Generally, the study area is becoming warmer, though moisture distribution varies dependent on elevation, distance from the coast, and latitude. Mountains or high elevation regions and those nearer the west coast will most likely

become warmer and wetter, while sites further in the interior will continue to become more arid with slowly increasing temperatures. Although all groups and sites most likely experienced centennial and millennial vegetation and climate regime changes within the last 9000 years, none of the previous time periods showed landscape trajectories at such amplified magnitudes, suggesting climate regimes and vegetation assemblages are changing at a rate not observed at any other time; additionally, this rate of change will likely lead to future vegetation assemblages and climate regimes that have no past analogs, making them difficult to predict.

5.4 Potential Sources of Error

A confusing and commonly encountered problem in measuring range of variation of any paleorecord is effectively and accurately accounting for the effects of human impact on the landscape. The vegetation at some or all study sites may have been so altered that no analog or similar measure is available throughout the time scale in question (Jackson and Williams, 2004). This is true for many of the paleopollen sites located on the High Plains of Montana, North Dakota, and South Dakota, as well as the Palouse regions of Oregon and Washington (Barnosky, 1989). These areas cover large tracts of land and possess fairly uniform topographic, vegetative, and climatic settings, and have all been heavily modified for intensive agricultural activities.

Native grass, shrub, and tree species composition have been replaced with “cereal grain” crops such as wheat, barley, and soy, making modern pollen assemblages difficult to compare with paleopollen assemblages, since they have not occurred at any other time

period in the pollen record. The replacement of native grasses with cereal grains is recorded in the Lost and Guardipee Lakes pollen diagrams, showing the transition to cereal grains beginning 150 years before present, revealing land use change from pre-European settlement to the modern day (Barnosky, 1989). Similar problems are encountered in areas where deforestation or selective timber cutting occurred. Although total replacement of arboreal and nonarboreal species is unlikely, the modern pollen assemblage is usually much different from past recorded pollen assemblages, and will have no functional analog for descriptive or quantitative comparison (Prentice, 1986a).

Several possible sources of error were present for this study, including initial sampling, procedural, and analytical flaws arising from the primary authors of the modern and fossil pollen sites (Williams et al., 2004; Whitmore et al., 2005) before they were combined into the cumulative dataset. Also, deleting taxa may have resulted in not exposing all ecologic and species relationships within pollen assemblages, and landscape mosaics of species composition. *Thuja* was included in the CCA ordination analysis, and occurred at few study area plots, potentially skewing the results of the ordination.

Minor misinterpretation of both ordination analyses could mislead study results, since the axis interpretations and landscape trajectory values are based from the ordination results. Ordinations using abundance data and applied to ecology are generally frustrating to use because researchers are forced to assume, with little justification, that their data correctly and accurately summarizes ecological relationships. Few guidelines or standards exist to judge ordination output, especially in studies that employ NMDS (Hirst and Jackson, 2007), leading to inconsistencies in interpretation of the results.

The use of only seven environmental variables in the CCA analysis, and 20 species variables in the NMDS analysis, may not be enough to adequately capture and analyze the community departure from past time periods to the present day. Incorporating time periods older than 6000 ybp may degrade temporal values, meaning one may assume one is observing pollen from 10,000 ybp, though one is actually analyzing assemblages from 15,000 ybp, due to inaccuracies of radiocarbon dating methods in sediments of that age. Lastly, the CCA ordination explained very little community composition variance in the modern day, thus making any conclusions drawn from its result somewhat misleading, and lending the model unfit for predicting pollen assemblages at points with unknown pollen values. However, the NMDS ordination did explain more model variance (as one would expect given it is an indirect gradient method), though many of the R^2 values obtained from the ordination used to infer environmental gradients from the ordination axes were somewhat insignificant (only *Artemesia* on Axis 2 had R^2 values over 0.90).

Lastly, other potential problems and limitations of the analysis stemmed from issues of scale and the distribution of study plots throughout the study area. The modern pollen database contained nearly 600 well-dispersed study plots, yet many portions of the study area (including whole ecoregions) contained few or no sites. Likewise, over-representation of sites in regions such as the Northern Short Grasslands along the Hi-Line of north-central Montana could potentially skew results. The modern pollen dataset is best suited to interpolate and hypothesize areas within the study area at ecoregion scales given the sampling distribution and resolution of pollen spectra at those sites (Figure 8).

The fossil pollen dataset is also adversely affected by scale. Just 33 sites scattered over the large study area creates severe limitations in terms of interpretation and inferences. One must critically evaluate all available ecological and climatic knowledge and carefully weight extrapolation of point-based findings to areas of missing data. The pollen data also degrades considerably the further one looks back in time. Known errors in radiocarbon dating and pollen identification often result in inconsistent interpretation of botanical and climatic trends. Informed evaluation of all available information about the study area is required to make reasonable inferences when working with any paleoenvironmental proxy source.

6. CONCLUSIONS AND FUTURE RESEARCH

6.1 Conclusions from the Modern Pollen Analysis

Concentrated analysis of the modern pollen biome and ecoregion study results support the first half of the modern pollen study Hypothesis 1, in that "multidimensional statistical methods combined with biophysical variables and relative modern pollen percentages can define ecological structure and associated environmental gradients across a broad area." Well-defined linearity within the biome designations (Figure 8) and ecoregion designations (Figures 9 – 12) support the ability of CCA to identify and define environmental gradients by utilizing the species and environmental variables included in this study (Table 5). The grassland, xeric shrublands, and intermountain forest ecoregion groupings revealed strong environmental gradients driven by precipitation and elevation, however, the Pacific Northwest coastal forest ecoregion group showed considerable variation in the ordination output, suggesting the CCA analysis proved most useful in predicting more xeric, continental low to mid-elevation grassland and forest ecoregion groupings, but less useful at predicting vegetation composition in high elevation areas, coastal forests, and other inherently wet, structurally complex areas (Figures 9-12)

The current CCA procedure and list of environmental and biophysical variables are probably not adequate to answer the second half of the modern pollen study hypothesis 1: CCA's ability to "predict vegetation composition spatially from point samples" in ecoregions with poor point distributions and known composition complexity (Pacific Northwest coastal forests). The resultant model output and associated variables

lacked sufficient descriptive and predictive power to effectively describe vegetative community structure and make predictions in areas of missing data (Table 13). The inclusion of more plant-specific variables (Rehfeldt, 2006) fit to relative species abundances would most likely increase the predictive capability of the CCA model.

6.2 Conclusions from the Fossil Pollen Analysis

The NMDS ordination results and landscape trajectory analysis clearly support fossil study hypothesis 1, that "vegetation composition changed at a similar rate due to regional climate shifts and disturbance within subregions of the study area through time," is supported by the regional divergence graphs (Figures 19, 24, 29, and 34), which show that sites within groupings generally responded in synch compositionally due to similar climatic fluctuations. Discrepant divergence trajectories among sites within regions are minimal, allowing persistent general patterns to be seen in the landscape trajectory analysis.

Fossil study hypothesis 2, which states that "vegetation composition change is synchronous across the study area for all study point locations and time slices, as driven by regional changes in climate," is supported by Figure 35, which shows that the analyzed ordination regions experienced similar vegetative response to regional climatic shifts, though were always comprised of core vegetation assemblages. For example, Group 2 sites were always comprised of High Plains grassland and prairie communities, though trended toward grassland and/or forest expansion synchronously with the Pacific Northwest Grouping (Group 1). This finding was consistent throughout the study area, as

observed in the region by region divergence graph (Figure 35). The displacement map (Figure 37) also supports fossil study hypothesis 2 at certain time slices, though it does reveal some regional and local scale asynchronous vegetation response to regional climate shifts (especially from 6000 to 3500 ybp) presumably due to rapidly shifting community composition. The displacement map shows vegetation change was apparent through time, though vegetation responded differently dependent on elevation, orographic effects, latitude, and distance from the coast.

Fossil study hypothesis 3, attempted to determine whether "similar vegetation assemblages and climatic conditions have been observed in previous time periods across the study area as determined by interpretation and comparison of fossil pollen assemblages, landscape trajectory paths, paleoclimate data/models, fire occurrence proxies, geochemical, and isotope records." Regional divergence graphs (Figures 19, 24, 29, and 34) and study area divergence (Figure 35) show most ordination regions may have experienced modern climatic and vegetative trends around 3000 ybp, except the Pacific Northwest region, which experienced climate and vegetation scenarios similar to modern times as far back as 6000 ybp. These findings are supported by the proxy record comparisons discussed earlier. However, it is important to note that approximation of analogous climate and vegetation regimes are not possible to assert from the ordination and landscape trajectory analyses alone. Only by reviewing and comparing the many sources of proxy records to the current study results was it possible to infer whether or not past climate and vegetation conditions were similar to those of modern times. Also, nearly all landscape trajectories in the study area reveal the largest changes in climatic and pollen abundances during the last 500 years, generally trending to warmer

temperatures, though varied moisture distribution. Therefore, future climate and vegetation scenarios may have no past analogs.

6.3 Recommendations for Future Research

In portions of the study area with a history of intensive land use, complications regarding the effective and accurate measure of vegetation variation have arisen, especially in the last 250 years. In much of western North America, European settlement was beginning or had recently taken place, resulting in dramatic vegetation composition changes and habitat alteration, stemming from intensive agriculture, fire suppression efforts, selective cutting logging practices, and other activities which changed vegetative land cover, and ultimately the modern day pollen assemblage, resulting in modified modern day vegetation mosaics and non-analogous modern and fossil pollen assemblages (Prentice, 1986a; Jackson and Williams, 2004).

To accommodate for these changes and enable comparison between modern and paleopollen spectra, studies focused on "pre-settlement" era pollen spectra throughout the High Plains, Midwest, and Palouse regions should be aggressively applied to more accurately determine the extent of vegetation alteration and departure from current conditions. Prentice et al. (1980) and Webb (1973) utilized short cores, taken from laminated sediments at study sites throughout the prairie settings of the American Midwest, to assist in tracing alterations in pollen assemblage change through more recent time periods and comparing documented changes in forest composition. Isopoll and principal component analysis patterns have surfaced in more recent studies, reflecting

changes associated with the removal of Native Americans on the landscape, changing agricultural practices, intensive timber harvesting, and drastic changes in human land use (Christensen et al., 1996; Nonaka and Spies, 2005; Power et al., 2006).

Potential future work includes incorporating the same quantitative, statistical, and analytical techniques as this study, but include all available sites from Whitmore et al. (2005), the fossil pollen sites utilized to create paleobiome maps of North America (Williams et al., 2004), include more plant taxa, and additional plant-specific environmental variables (Rehfeldt, 2006), and perform continent-scale analyses to identify continent-scale environmental and species gradients.

The inclusion of more sites over an expansive and topographically complex area would provide better interpretation for dynamic, large-scale landscape processes and complex ecologic drivers. An expansive study area would require extensive spatial datasets for modeling purposes and are often difficult to obtain and compile. A recently published spline model used to predict modern day climate parameters such as average annual precipitation, temperature, and number of degree growing days (Rehfeldt, 2006) could be combined with other climate, vegetation, and other proxy sources to provide examine widespread vegetation composition change at finer time slices as compared to this study. The inclusion of more proxy records into the ordination analysis combined with the pollen data would strengthen hypotheses concerning climate change and disturbance regime fluctuations over long time periods, with greater spatial accuracy across all of North America.

BIBLIOGRAPHY

Austin, M.P., 2005. Vegetation and environment: discontinuities and continuities. In: E. van der Maarel (Editor), Vegetation Ecology. Blackwell Publishing, Oxford, UK, pp. 52-84.

Baker, R.G., 1983. Holocene Vegetation History of the Western United States. In: H.E. Wright Jr. (Editor), Late Quaternary Environments of the United States. University of Minneapolis Press, Minneapolis, pp. 109-127.

Baker, R.G. and Richmond, M., 1978. Geology, Palynology, and Climatic Significance of Two Pre-Pinedale Lake Sediment Sequences in and near Yellowstone National Park. Quaternary Research, 10: 226-240.

Bakker, J.P., 2005. Vegetation conservation, management and restoration. In: E. van der Maarel (Editor), Vegetation Ecology. Blackwell Publishing, Oxford, UK, pp. 309-331.

Barker, R., 2005. Scorched Earth: How the Fires of Yellowstone Changed America. Island Press/Shearwater Books, Washington, 277 pp.

Barnosky, C.W., 1989. Postglacial Vegetation and Climate in the Northwestern Great Plains of Montana. Quaternary Research, 31: 57-73.

Barnosky, C.W., Anderson, P.M. and Bartlein, P.J., 1987. The northwestern U.S. during deglaciation: Vegetational history and paleoclimatic implications. In: W.F. Ruddiman, Wright Jr., H.E., (Editor), North America and adjacent oceans during the last deglaciation. Geological Society of America, Boulder, CO, pp. 289-321.

Bartlein, P.J., Anderson, K.H., Anderson, P.M., Edwards, P.M., Mock, C.J., Thompson, R.S., Webb, R.S., Webb III, T., ,Whitlock, C., 1998. Paleoclimate simulations for North America over the past 21,000 years: Features of the simulated climate and comparisons with paleoenvironmental data. Quaternary Science Reviews, 17: 549-585.

Bartlein, P.J., Edwards, M. E., Shafer, S. L., Barker Jr., E.D., 1995. Calibration of radiocarbon ages and the interpretation of paleoenvironmental records. Quaternary Research, 44: 417-424.

Bartlein, P.J., Prentice I.C. and Webb III, T., 1986. Climatic response surfaces from pollen data for some eastern North American taxa. Journal of Biogeography, 13: 35-57.

Blytt, A.G., 1876. Essay on the immigration of the Norwegian flora during alternating rainy and dry periods. Cammermeyer, Oslo, Norway.

Bonnickson, T.M., 2000. America's Ancient Forests. John Wiley & Sons, Inc., New York, NY, 594 pp.

Breiman, L., 2001. Random Forests. Machine Learning, 45: 5-32.

Brown, K.J. and Hebda, R.J., 2002. Origin, development, and dynamics of coastal temperate conifer rainforests of southern Vancouver Island, Canada. Canadian Journal of Forest Research, 32: 353-372.

Brunelle, A. and Whitlock, C., 2003. Postglacial fire, vegetation, and climate history in the Clearwater Range, Northern Idaho, USA. Quaternary Research, 60: 307-318.

Brunelle, A., Whitlock, C., Bartlein, P.J. and Kipfmueller, K., 2005. Holocene fire and vegetation along environmental gradients in the Northern Rocky Mountains. Quaternary Research, 24: 2281-2300.

Caprio, A.C. and Graber, D.M., 1999. Returning Fire to the Mountains: Can we Successfully Restore the Ecological Role of Pre-Euroamerican Fire Regimes to the Sierra Nevada? In: D.N. Cole, McCool, S.F., Bonnie, William T., O'Louglin, J. (Editor), Wilderness ecosystems, threats, and management. U.S. Department of Agriculture, Forest Service, Missoula, MT, pp. 233-241.

Chatters, J.C. and Leavell, D., 1995a. Harding Lake: A Study of Fire, Succession, and Sedimentation Since 350 AD in the Subalpine Fire Forests of the Yaak River, Northwestern Montana., Applied Paleoscience, Richland, WA.

Chatters, J.C. and Leavell, D., 1995b. Management Implications of Fire and Succession History, Smeads Bench Fen, Northwest Montana, North American Paleoscience & USDA Forest Service, Richland, WA.

Chittenden, H.M. and Richardson, A.T., 1969. Life, Letters, and travels of Father De Smet, 2. Arno Press, New York.

Christensen, N.L. et al., 1996. The report of the Ecological Society of America Committee on the scientific basis for ecosystem management. Ecological Applications, 6: 665-691.

Clarke, K.R., 1993. Non-parametric multivariate analyses of changes in community structure. Australian Journal of Ecology, 18: 117-143.

Climate Source, 2007. Temperature and Precipitation for Western Canada. Downloaded from http://www.climatesource.com on 1 October, 2007.

COHMAP MEMBERS, 1988. Climatic Changes of the past 18,000 Years: Observations and model simulations. Science, 241: 1043-1052.

Cook, E.R., Woodhouse, C.A., Eaking, C.M., Meko, D.M. and Stahole, D.W., 2004. Long-term aridity changes in the western United States. Science, 306: 1015-1018.

Crookston, N.L., 2007. Personal communication, USFS RMRS Moscow, ID.

Crookston, N.L. and Finley, A., 2006. yaImpute: An R Package for k-NN Imputation, USDA Forest Service and University of Minnesota.

Crowley, T.J., and Lowery, T. S., 2000. How warm was the Medieval Warm Period? Ambio, 29(1): 51-54.

Daly, C., Neilson, R.P. and Phillips, D.L., 1994. A statistical-topographic model for mapping climatological precipitation over mountainous terrain. Journal of Applied Meteorology, 33: 140-158.

Daly, C., Taylor, G. and Gibson, W., 1997. The PRISM approach to mapping precipitation and temperature, 10th Conference on Applied Climatology. American Meteorological Society, Reno, NV, pp. 217-218.

Davis, O.K., 1984. Pollen frequencies reflect vegetation patterns in a Great Basin (U.S.A.) mountain range. Review of Palaeobotany and Palynology, 40: 295-315.

Doerner, J.P. and Carrara, P.E., 1999. Deglaciation and postglacial vegetation history of the West Mountains, west-central Idaho, U.S.A. Arctic, Antarctic, and Alpine Research, 31: 303-311.

Doerner, J.P. and Carrara, P.E., 2001. Late Quaternary vegetation and climatic history of the Long Valley Area, west-central Idaho, U.S.A. Quaternary Research, 56: 103-111.

ESRI, 2009. ArcGIS. Earth Sciences Research Institute, Redlands, CA.
Faegri, K. and Iversen, J., 1989. Textbook of Pollen Analysis. Blackwell Scientific Publications, Oxford, UK, 328 pp.
Fiedel, S.J., 1987. Prehistory of the Americas. Cambridge University Press, New York, 422 pp.
Fox, D., 2007. Back to the no-analog future? Science, 316: 823-825.
Fries, M., 1967. Lennart Von Post's pollen diagram series of 1916. Review of Palaeobotany and Palynology, 4: 9-13.
Gavin, D.G., Oswald, W.W., Wahl, E.R. and Williams, J.W., 2003. A statistical approach to evaluating distance metrics and analog assignments for pollen records. Quaternary Research, 60: 356-367.
Gerloff, L.M., Hills, L.V. and Osborn, G.D., 1995. Post-glacial vegetation history of the Mission Mountains, Montana. Journal of Paleolimnology, 14: 269-279.
Gray, S.T., Graumlich, L.J. and Betancourt, J.L., 2007. Annual precipitation in the Yellowstone National Park region since AD 1173. Quaternary Research, 68: 18-27.
Hallett, D.J. and Hills, L.V., 2006. Holocene vegetation dynamics, fire history, lake level and climate change in the Kootenay Valley, southeastern British Columbia, Canada. Journal of Paleolimnology, 35: 351-371.
Hann, W.J. and Bunnell, D.L., 2001. Fire and land management planning and implementation across multiple scales. International Journal of Wildland Fire, 10: 389-403.
Hannah, L., Midgley, G.F. and Millar, D., 2002. Climate change-integrated conservation strategies. Global Ecology and Biogeography, 11: 485-495.
Hemphill, M.L., 1983. Fire, Vegetation, and People - Charcoal and Pollen Analyses of Sheep Mountain Bog, Montana: The Last 2800 Years. Masters Thesis, Washington State University, Spokane, WA, 70 pp.
Hessburg, P.F. and Agee, J.K., 2003. An environmental narrative of Inland Northwest United States forests, 1800-2000. Forest Ecology and Management, 178: 23-59.
Hill, M.O. and Gauch, H.G.J., 1980. Detrended correspondence analysis: An improved ordination technique. Plant Ecology, 42: 47-58.
Hirst, C.N. and Jackson, D.A., 2007. Reconstructing community relationships: the impact of sampling error, ordination approach, and gradient length. Biodiversity Research, 13: 361-371.
Holling, C.S. and Meffe, G.K., 1996. Command and Control and the Pathology of Natural Resource Management. Conservation Ecology, 10: 328-337.
Huggett, J.R., 2004. Fundamentals of Biogeography. Routledge, New York, 439 pp.
Huntley, B., Bartlein, P.J. and Prentice, I.C., 1989. Climatic control of the distribution and abundance of Beech (*Fagus L.*) in Europe and North America. Journal of Biogeography, 16: 551-560.
Huntley, B. and Birks, H.J.B., 1983. An Atlas of Past and Present Pollen Maps for Europe 0-13,000 Years Ago. Cambridge University Press, Cambridge.
Jackson, S.T., personal communication, 10 May 2006.
Jackson, S.T. and Kearsley, J.B., 1998. Quantitative representation of local forest composition in forest-floor pollen assemblages. Journal of Ecology, 86: 474-490.

Jackson, S.T. and Overpeck, J.T., 2000. Responses of plant populations and communities to environmental changes of the late Quaternary. Paleobiology, 26: 194-220.

Jackson, S.T. and Williams, J.W., 2004. Modern analogs in paleoecology: Here today, gone yesterday, gone tomorrow? Annual Review Earth Planetary Science, 32: 495-537.

Jackson, S.T. and Wong, A., 1994. Using forest patchiness to determine pollen source areas of closed-canopy pollen assemblages. Journal of Ecology, 82: 89-99.

Johnson, N.K., Agee, J. and Dale, V., 1999. Sustaining the People's Lands, USDA-Forest Service, Washington, D.C.

Jupp, P.E., 1987. A nonparametric correlation coefficient and two-sample test for random vectors or directions. Biometrika, 74: 887-890.

Karsian, A., 1995. A 6800-year vegetation and fire history in the Bitterroot Mountain Range, Montana. Masters Thesis, University of Montana, Missoula, MT, 53 pp.

Kenkel, N.C. and Orloci, L., 1986. Applying metric and nonmetric multidimensional scaling to ecological studies: some new results. Ecology, 67: 919-928.

Kovach, W.L., 1989. Comparisons of multivariate analytical techniques for use in pre-Quaternary plant paleoecology. Review of Palaeobotany and Palynology, 60: 255-282.

Kruskal, J.B., 1964a. Multidimensional scaling by optimizing goodness of fit to a nonmetric hypothesis. Psychometrika, 29: 1-27.

Kruskal, J.B., 1964b. Nonmetric multidimensional scaling: a numerical method. Psychometrika, 29: 115-129.

Kutzbach, J.E. and Webb III, T., 1993. Model Description, External Forcing, and Surface Boundary Conditions. In: H.E. Wright Jr. et al. (Editors), Global Climates since the Last Glacial Maximum. University of Minnesota Press, Minneapolis, MN, pp. 12-24.

Landres, P.B., Morgan, P. and Swanson, F.J., 1999. Overview of the use of natural variability concepts in managing ecological systems. Ecological Applications, 9: 1179-1188.

Lavorel, S. and Cramer, W., 1999. Plant functional types and disturbance dynamics. Journal of Vegetation Science, 10: 603-730.

Legendre, P. and Legendre, L., 1998. Numerical Ecology. Elsevier Publishing, New York, NY, 853 pp.

Lynch, E.A., 1998. Origin of a park-forest vegetation mosaic in the Wind River Range, Wyoming. Ecology, 79: 1320-1338.

MacDonald, G.M., 1987. Postglacial development of the subalpine-boreal transition forest of western Canada. Journal of Ecology, 75: 303-320.

MacDonald, G.M. and Reid, R.T., 1989. Pollen-climate distance surfaces and the interpretation of fossil pollen assemblages from the western interior of Canada. Journal of Biogeography, 16: 403-412.

MacDonald, G.M. and Ritchie, J.C., 1986. Modern pollen spectra from the western interior of Canada and the interpretation of late Quaternary vegetation development. New Phytologist, 103: 245-268.

Mack, R.N., Rutter, N.W., Valastro, S., 1983. Holocene vegetational history of the Kootenai River Valley, Montana. Quaternary Research, 20: 177-193.

Marlon, J., Bartlein, P.J. and Whitlock, C., 2006. Fire-fuel-climate linkages in the northwestern USA during the Holocene. The Holocene, 16: 1059-1071.
McCune, B., Grace, J.B. and Urban, D.L., 2002. Analysis of Ecological Communities, 2nd Printing. MjM Software, Glenedan Beach, OR, 301 pp.
McCune, B. and Mefford, M.J., 1999. PC-ORD. Multivariate Analysis of Ecological Data. MjM Software Design, Gleneden Beach, OR.
McGarigal, K. and Cushman, S., 2007. Multivariate Landscape Trajectory Analysis, Temporal Dimensions of Landscape Ecology, pp. 119-140.
McLachlan, J.S. and Clark, J.S., 2004. Reconstructing historical ranges with fossil data at continental scales. Forest Ecology and Management, 197: 139-147.
Mehringer, P.J., 1985. Late-Quaternary pollen records from the interior Pacific Northwest and northern Great Basin of the United States. In: V.M. Bryant Jr., Holloway, R.G. (Editor), Pollen Records of Late-Quaternary North American Sediments. American Association of Stratigraphic Palynologists' Foundation, Dallas, TX, pp. 167-189.
Mehringer, P.J., Jr., Arno, S.F. and Petersen, K.L., 1977. Postglacial history of Lost Trail Pass Bog, Bitterroot Mountains, Montana. Arctic, Antarctic, and Alpine Research, 9: 345-368.
Millspaugh, S.M., Whitlock, C. and Bartlein, P.J., 2000. Variations in fire frequency and climate over the past 17 000 yr in central Yellowstone National Park. Geology, 28: 211-214.
Nesser, J.A., Ford, G.L., Maynard, C.L. and Page-Dumroese, D.S., 1997. Ecological Units of the Northern Region: Subsections, Rocky Mountain Research Station, Missoula, MT.
Nonaka, E. and Spies, T.A., 2005. Historical range of variability in landscape structure: a simulation study in Oregon, USA. Ecological Applications, 15: 1727-1746.
Olson, D.M. and Dinerstein, E., 2002. The Global 200: Priority Ecoregions for Global Conservation. Annals of the Missouri Botanical Gardens, 89: 199-224.
Olson, D.M. et al., 2001. Terrestrial Ecoregions of the World: A New Map of Life on Earth. BioScience, 51: 933-938.
Overpeck, J.T., Webb III, T. and I.C., P., 1985. Quantitative interpretation of fossil pollen spectra: dissimilarity coefficients and the method of modern analogs. Quaternary Research, 23: 87-108.
Overpeck, J.T., Webb, R.S. and Webb III, T., 1992. Mapping eastern North American vegetation change of the past 18 ka: No-analogs and the future. Geology, 20: 1071-1074.
Palmer, M.W., 1993. Putting things in even better order: The advantages of canonical correspondence analysis. Ecology, 74: 2215-2230.
Peyron, O. et al., 1998. Climatic reconstruction in Europe for 18,000 YR B.P. from pollen data. Quaternary Research, 49: 183-196.
Peyron, O., Jolly, D., Bonnefille, R., Vincens, A. and Guiot, J., 2000. Climate of East Africa 6000 14C Yr B.P. as inferred from pollen data. Quaternary Research, 54: 90-101.
Pielou, E.C., 1992. After the Ice Age. The Return of Life to Glaciated North America. University of Chicago Press, Chicago, 366 pp.

Power, M.J. et al., 2008. Changes in fire regimes since the Last Glacial Maximum: an assessment based on a global synthesis and analysis of charcoal data. Climate Dynamics, 30: 887-907.

Power, M.J., Whitlock, C., Bartlein, P. and Stevens, L.R., 2006. Fire and vegetation history during the last 3800 years in northwestern Montana. Geomorphology, 75: 420-436.

Prentice, I.C., 1977. Non-metric ordination methods in Ecology. The Journal of Ecology, 65: 85-94.

Prentice, I.C., 1986a. Forest-composition calibration of pollen data. In: B.E. Berglund (Editor), Handbook of Holocene Palaeoecology and Palaeohydrology. John Wiley & Sons, New York, pp. 799-816.

Prentice, I.C., 1986b. Multivariate methods for data analysis. In: B.E. Berglund (Editor), Handbook of Holocene Palaeoecology and Palaeohydrology. John Wiley & Sons, New York, pp. 775-797.

Prentice, I.C., Guiot, J., Huntley, B., Jolly, D. and Cheddadi, r., 1996. Reconstructing biomes from palaecological data: a general method and its application to European pollen data at 0 and 6 ka. Climate Dynamics, 12: 185-194.

PRISM Group, 2007. Thirty-Year Mean Temperature and Precipitation, downloaded from http://www.ocs.orst.edu/prism/prism_new.html on 1 October 2007.

Ragunathan, T.E., Lepkowski, J.M., Van Hoewyk, J. and Solenberger, P., 2001. A multivariate technique for multiply imputing missing values using a sequence of regression models. Survey Methodology, 27(1): 85-95.

Rehfeldt, G.E., 2006. A Spline Model of Climate for the Western United States. United States Department of Agriculture, General Technical Report RMRS-GTR-165: 1-28.

Ricketts, T.H., 1999. Terrestrial Ecoregions of North America: A Conservation Assessment. Island Press, Washington, D.C., 485 pp.

Ritchie, J.C. and Harrison, S.P., 1993. Vegetation, Lake Levels, and Climate in Western Canada during the Holocene. In: H.E. Wright Jr. et al. (Editors), Global Climates Since the Last Glacial Maximum. University of Minnesota Press, Minneapolis, pp. 401-414.

Sankey, T.T., Montagne, C., Graumlich, L., Lawrence, R. and Nielsen, J., 2006. Twentieth century forest-grassland ecotone shift in Montana under differing livestock grazing pressure. Forest Ecology and Management, 234: 282-292.

Shi, G.R., 1993. Multivariate data analysis in palaeoecology and palaeobiogeography - A review. Palaeogeography, Palaeoclimatology, Palaeoecology, 105: 199-234.

Swetnam, T.N., Allen, C.D. and Betancourt, J.L., 1999. Applied historical ecology: Using the past to manage for the future. Ecological Applications, 9: 1189-1206.

Swetnam, T.W. and Betancourt, J.L., 1998. Mesoscale disturbance and ecological response to decadal climatic variability in the American Southwest. Journal of Climate, 11: 3128-3147.

ter Braak, C.J.F., 1986. Canonical correspondence analysis: a new eigenvector technique for multivariate direct gradient analysis. Ecology, 67: 1167-1179.

ter Braak, C.J.F., 1987. The analysis of vegetation-environment relationships by canonical correspondence analysis. Vegetatio, 69: 69-77.

ter Braak, C.J.F. and Prentice, I.C., 1988. A theory of gradient analysis. Advances in Ecological Research, 18: 271-317.

Thompson, R.S. and Anderson, K.H., 2000. Biomes of western North America at 18,000, 6000 and 0 14C yr BP. Journal of Biogeography, 27: 555-584.

Thompson, R.S., Shafer, S.L., Strickland, L.E., Van de Water, P.K. and Anderson, K.H., 2004. Quaternary vegetation and climate change in the western United States: Developments, perspectives, and prospects. In: A.R. Gillespie, Porter, S.C., Atwater, B.F. (Editor), The Quaternary period in the United States. Elsevier, New York, NY, Amsterdam, pp. 403-426.

Thompson, R.S., Whitlock, C., Bartlein, P.J., Harrison, S.P. and Geoffrey Spaulding, W., 1993. Climatic Changes in the Western United States since 18,000 yr B.P. In: H.E. Wright Jr. et al. (Editors), Global Climates since the Last Glacial Maximum. University of Minnesota Press, Minneapolis, pp. 468-514.

USGS, 2004. Shuttle Radar Topology Mission, 3 Arc second scenes, Filled Finished 2.0. Global Land Cover Facility, University of Maryland, College Park Maryland.

van Wezel, M.C. and Kosters, W.A., 2004. Nonmetric multidimensional scaling: Neural networks versus traditional techniques. Intelligent Data Analysis, 8: 601-613.

Wang, T., Hamann, A., Spillehouse, D.L. and Aitken, S.N., 2006. Development of scale-free climate data for western Canada for use in resource management. International Journal of Climatology, 26: 383-397.

Whitlock, C., 1993. Postglacial vegetation and climate of Grand Teton and Southern Yellowstone National Parks. Ecological Monographs, 63: 173-198.

Whitlock, C. and Bartlein, P.J., 1997. Vegetation and climate change in northwest America during the past 125 k yr. Nature, 388: 57-61.

Whitlock, C. et al., 2007. A 2650-year-long record of environmental change from northern Yellowstone National Park based on a comparison of multiple proxy data. Quaternary International, 188: 1-13.

Whitlock, C., Shafer, S.L. and Marlon, J., 2003. The role of climate and vegetation change in shaping past and future fire regimes in the northwestern US and the implications for ecosystem management. Forest Ecology and Management, 178: 5-21.

Whitmore, J. et al., 2005. Modern pollen data from North America and Greenland for multi-scale paleoenvironmental applications. Quaternary Science Reviews, 24: 1828-1248.

Williams, J. W., personal communication, 15 July 2007.

Williams, J.W., 2002. Variations in tree cover in North America since the last glacial maximum. Global and Planetary Change, 35: 1-23.

Williams, J.W., Shuman, B.N., Webb III, T., Bartlein, P.J. and Leduc, P.L., 2004. Late-Quaternary vegetation dynamics in North America: Scaling from taxa to biomes. Ecological Monographs, 74: 309-334.

Woodward, F.I., 1987. Climate and Plant Distribution. Cambridge University Press, New York, NY, 174 pp.

Woodward, T.I. and Cramer, W., 1996. Plant functional types and climate change. Journal of Vegetation Science, 7: 305-430.

Wright Jr., H.E., 1993. *Global Climates since the Last Glacial Maximum*. University of Minnesota, Minneapolis.

FIGURES

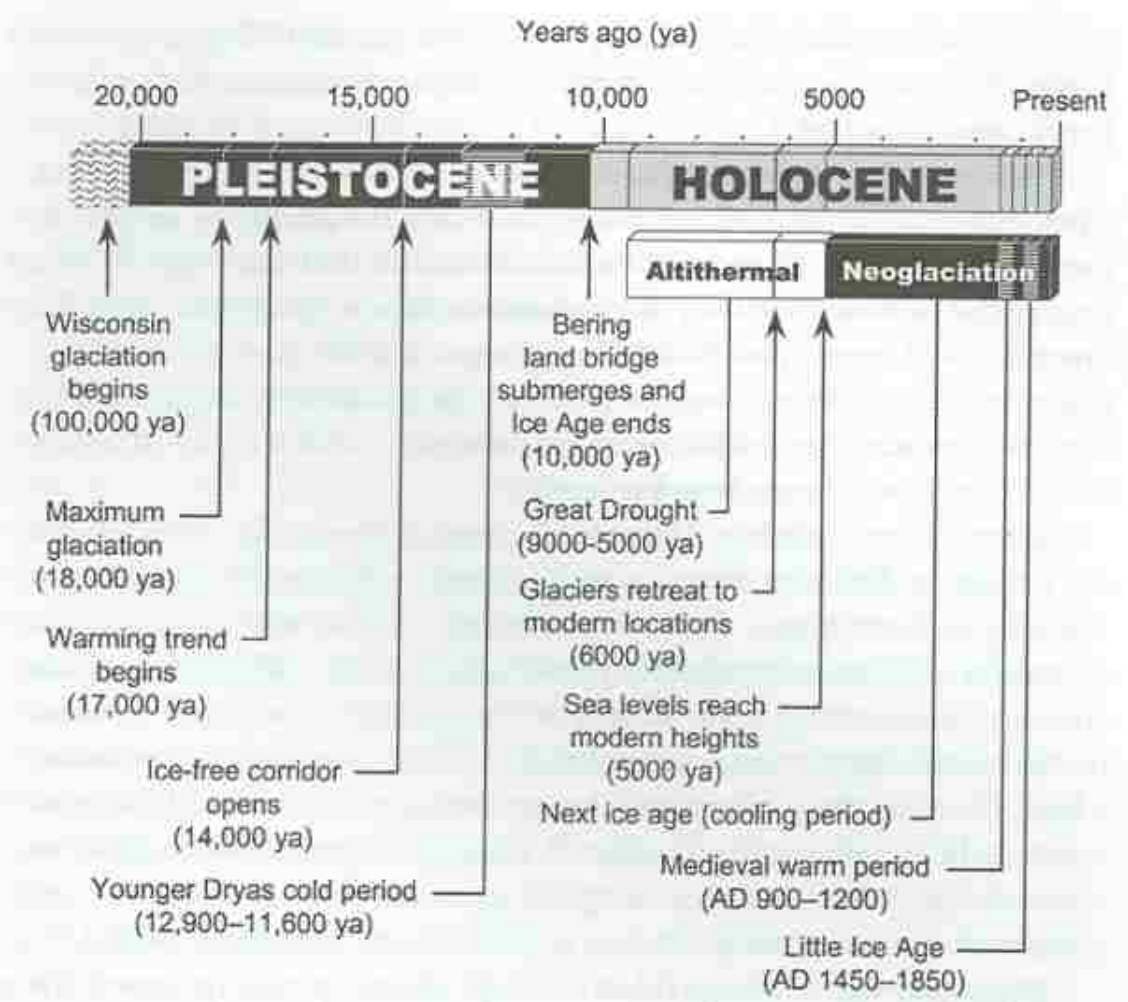

Figure 1. Temporal sequence of events as witnessed in the Holocene from 10,000 ybp to the modern time (Reproduced from Bonnickson, 2000).

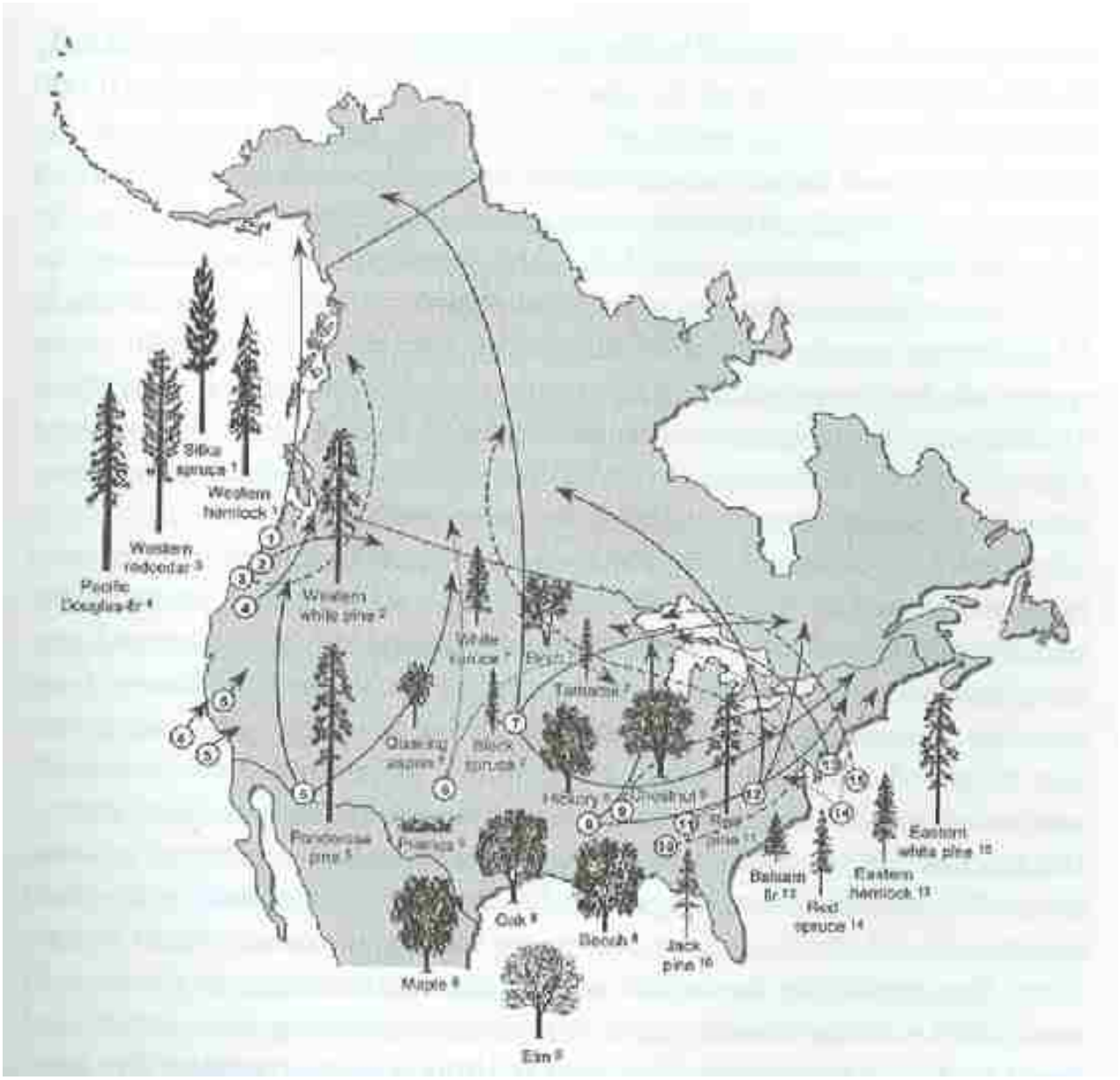

Figure 2. Generalized map of important tree species migration movements at the end of the last ice age (Reproduced from Bonnickson, 2000). The numbers refer to tree species listed above.

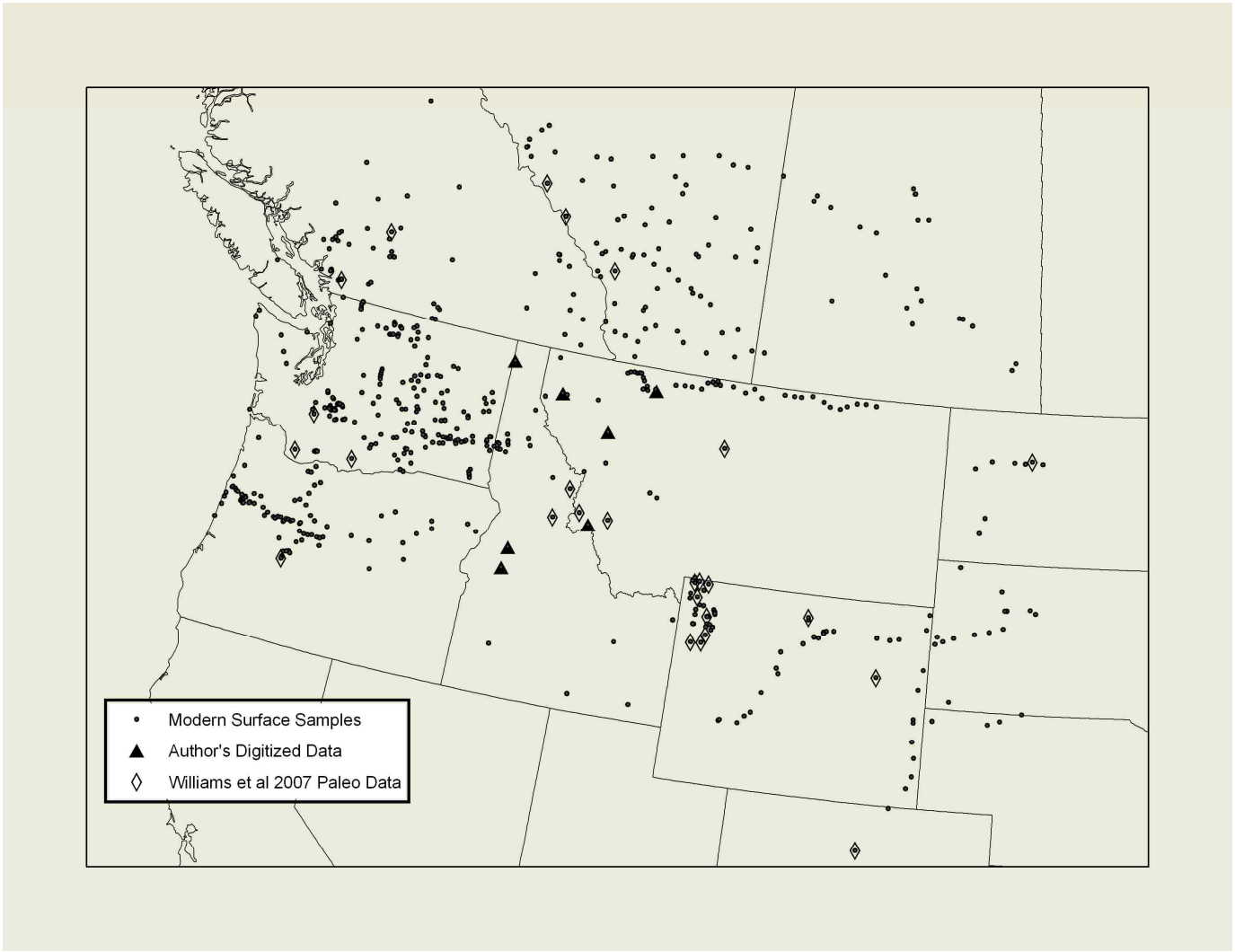

Figure 3. Study area extent and locations of modern day surface samples and sediment core fossil pollen sites. Modern samples are from Whitmore et al. (2005). For references for digitized data see Table 2. Fossil pollen database from Williams et al. (2007).

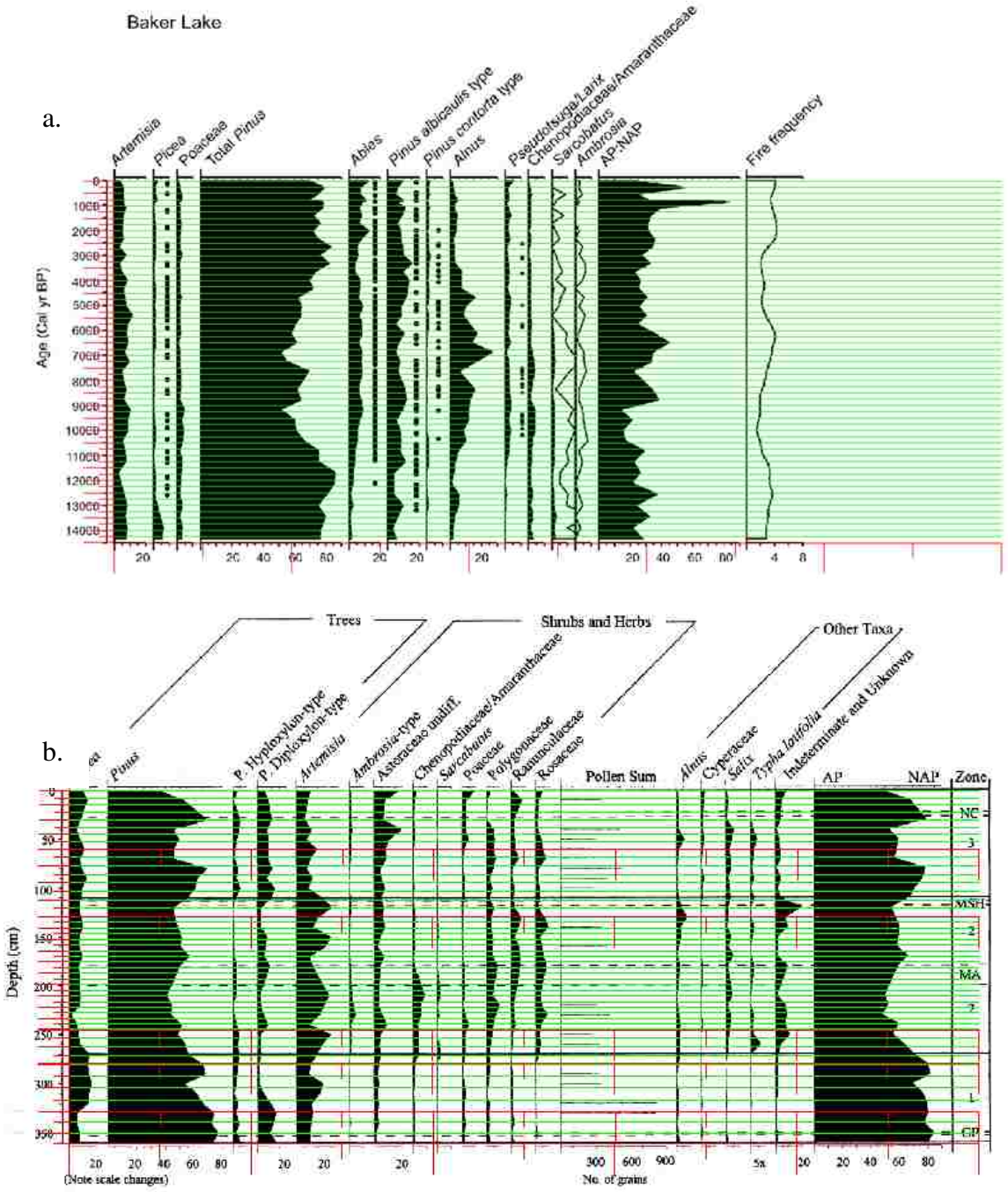

Figure 4. Example of pollen diagrams with (a) unadjusted (adapted from Brunelle et al., 2005) and (b) adjusted axes (adapted from Doerner and Carrara, 2001) to obtain pollen values. The carbon 14 ages have already been calibrated to calendar years before present in (a) but not in (b).

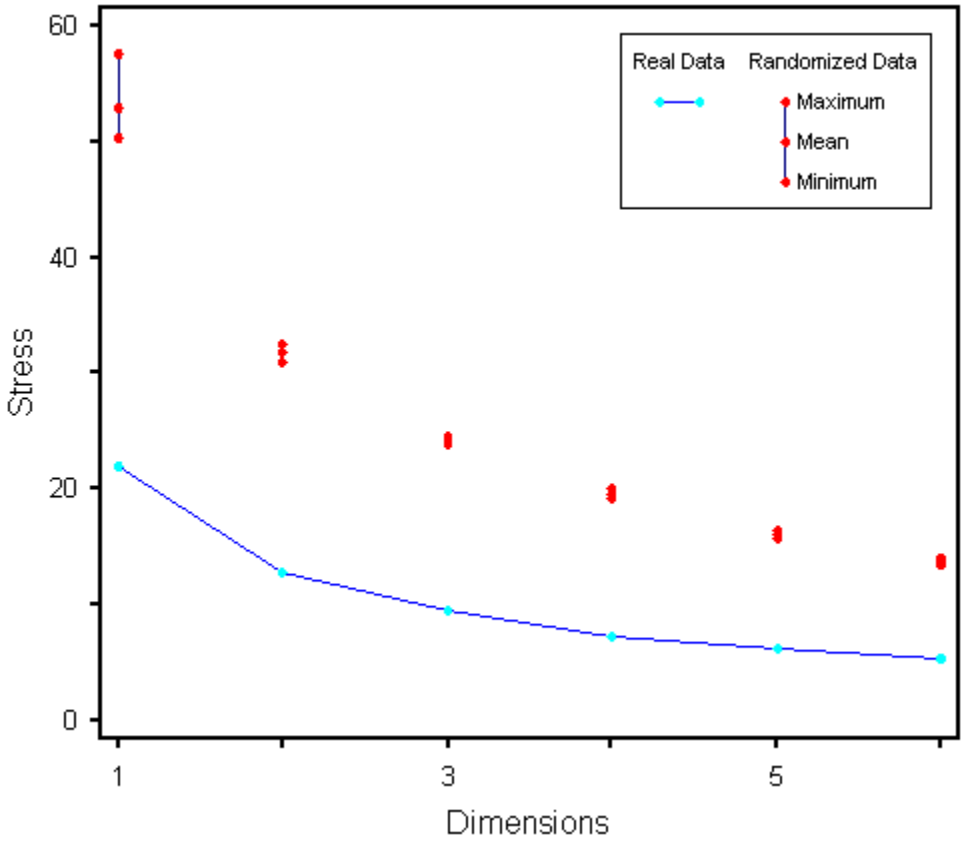

Figure 5. Scree plot from the initial 6-dimensional test NMDS run to determine the most appropriate dimensional solution for the remainder of the NMDS analysis. A three dimensional solution was chosen since stress changed very little with increased dimensionality at three dimensions.

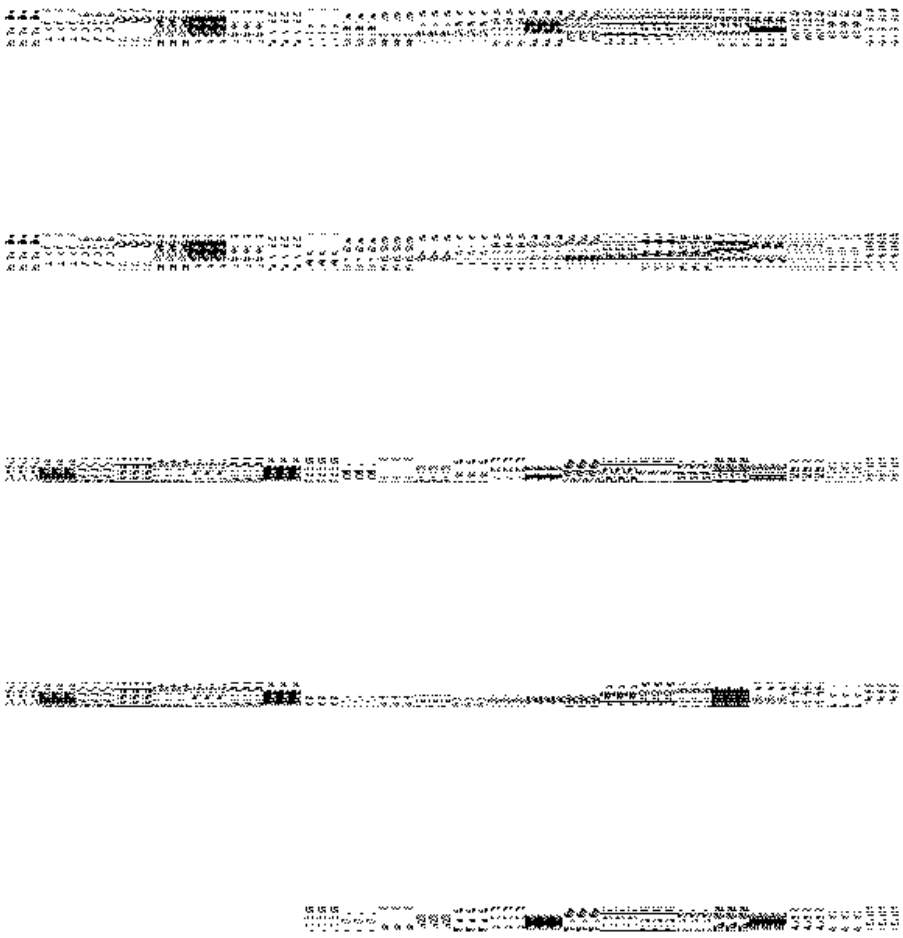

Figure 6. Example of a location coordinate landscape vector. The different locations of the coordinate pairs for linked sites indicate different time periods, and hence different species composition at three broadly similar composition study plots.

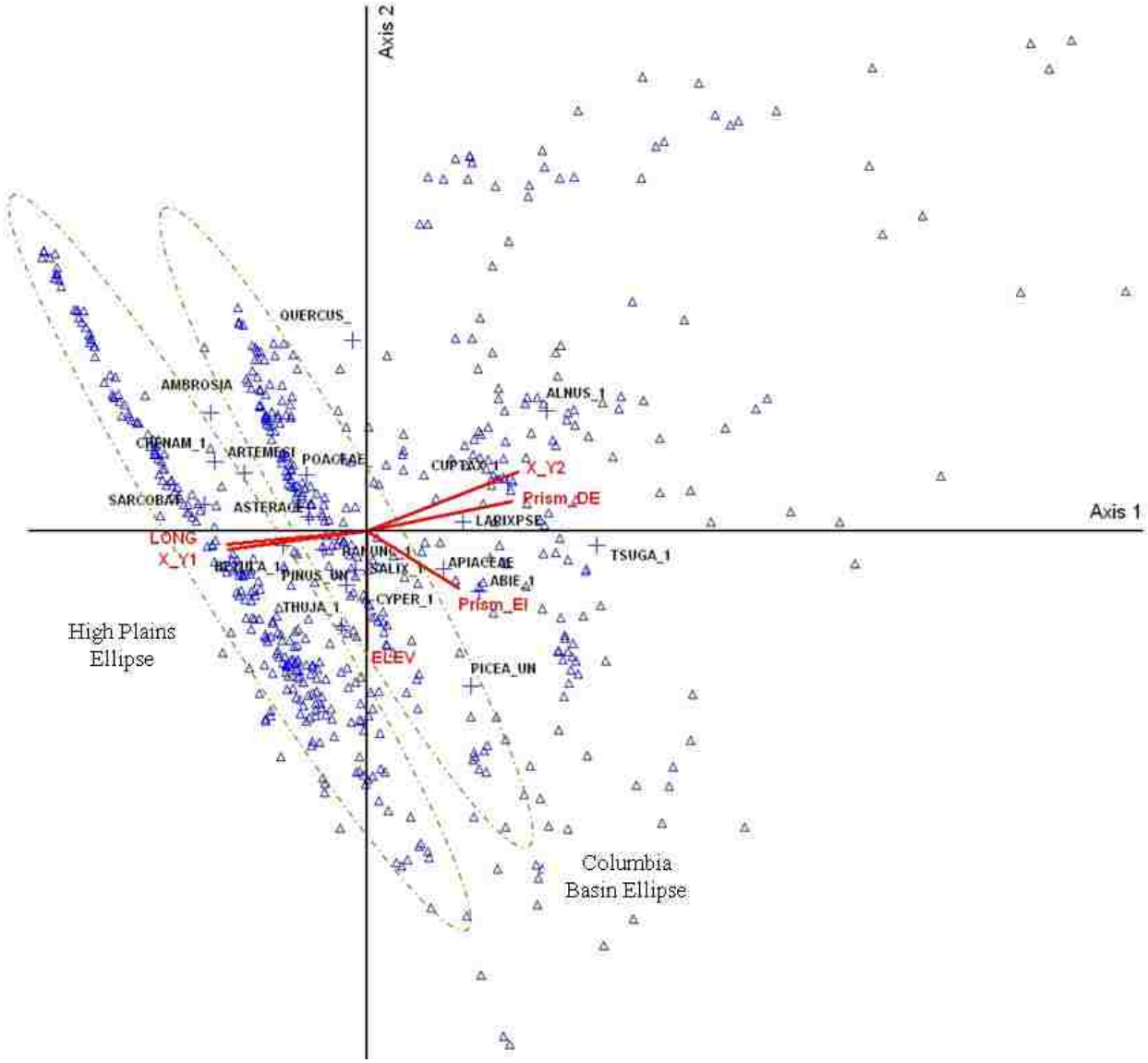

Figure 7. CCA ordination diagram showing species variable locations along environmental gradients (axes). Centroids of species variables are shown as '+' symbols. Sites falling close to a respective species point indicate the highest abundance of those species at those sites, aiding in deductions about species composition. The red radiating lines are environmental (biplot) vectors showing the relative influence of each environmental variable. Higher elevation, more precipitation, northerly and westerly locations are found to the right on Axis 1, while more arid, southerly, and easterly locations are located towards the bottom of Axis 2. The High Plains ellipse includes mainly grassland prairie communities, while the Columbia Basin ellipse includes sites from the Columbia Steppe grass and shrubland communities.

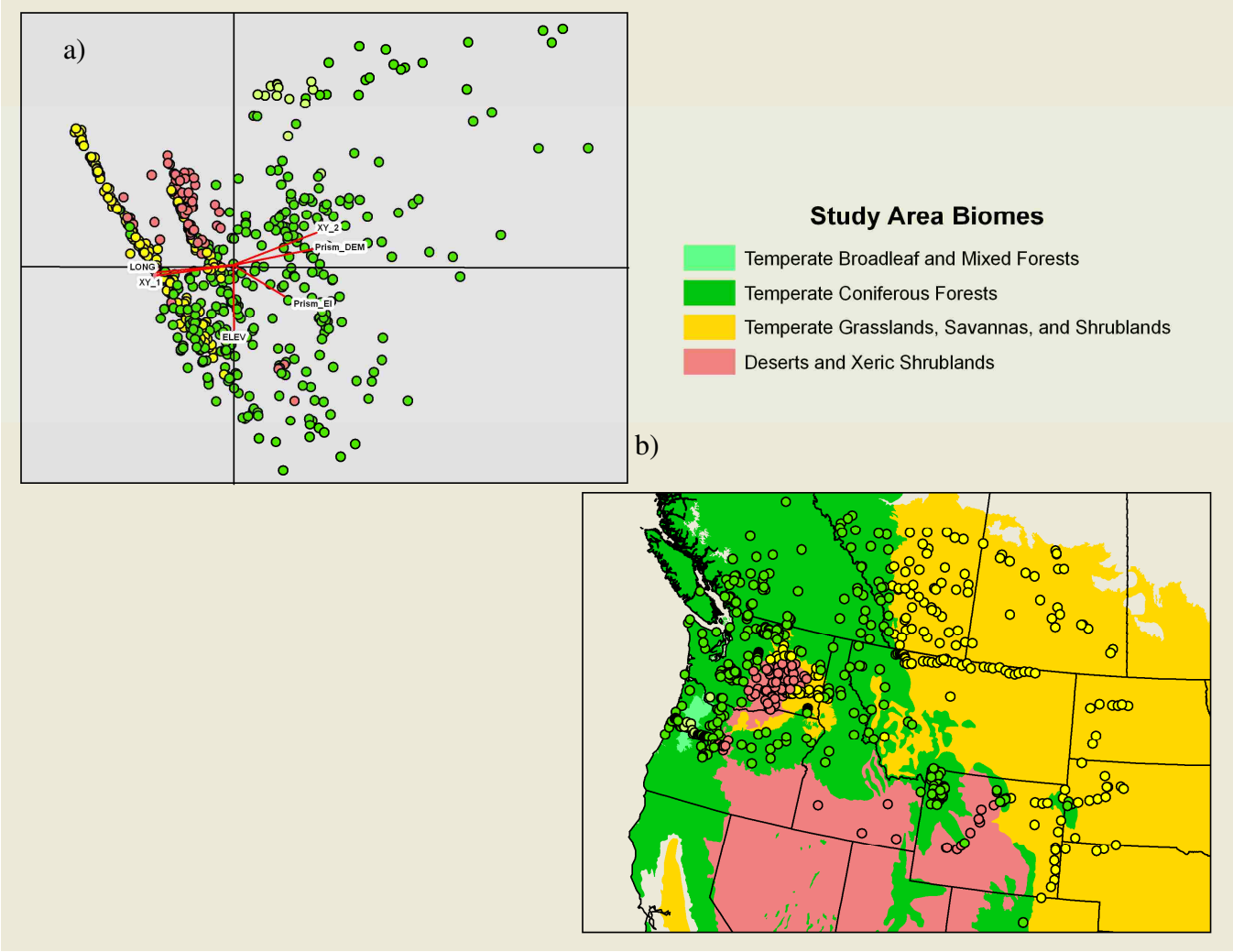

Figure 8. Location of study plots in (a) ordination space and (b) geographic space, delineated by biome type. Circles indicate site locations. Distinct groupings occur for all biome types in the modern day, controlled by the effects of the environmental gradients derived from the ordination analysis. Biomes are from Olson et al. (2001), Olson and Dinerstein (2002).

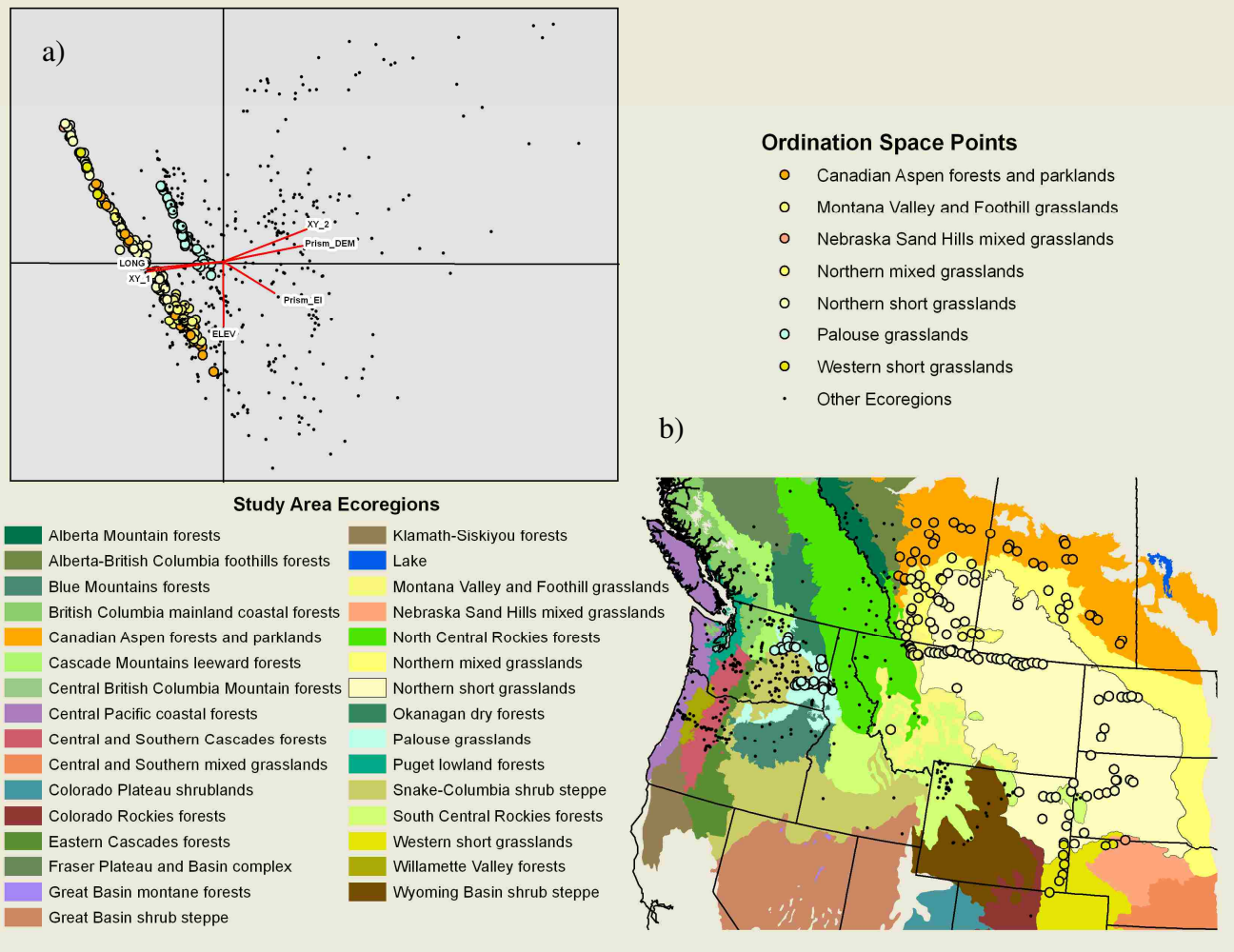

Figure 9. Location of study plots in (a) ordination space and (b) geographic space for the grassland ecoregion type. Circles indicate site locations, while dots represent 'other' ecoregion types. Distinct groupings occur for the grassland ecoregion types, influenced primarily by longitude, elevation, and precipitation gradients in the ordination analysis.

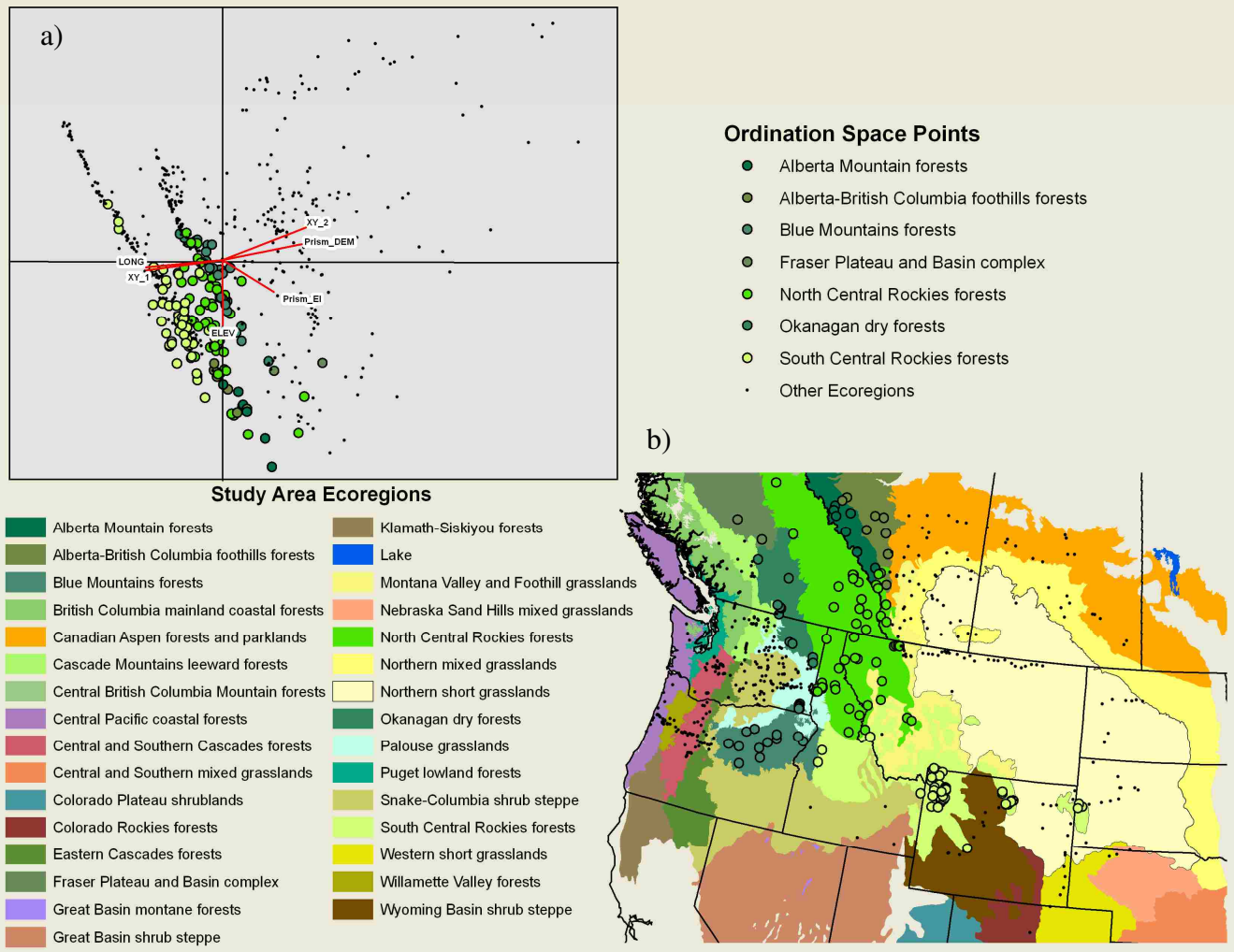

Figure 10. Location of study plots in (a) ordination space and (b) geographic space for the intermountain forest ecoregion type. Circles indicate site locations, while dots represent 'other' ecoregion types. Distinct groupings occur for the intermountain forest ecoregion types, influenced primarily by longitude, elevation, and precipitation gradients in the ordination analysis.

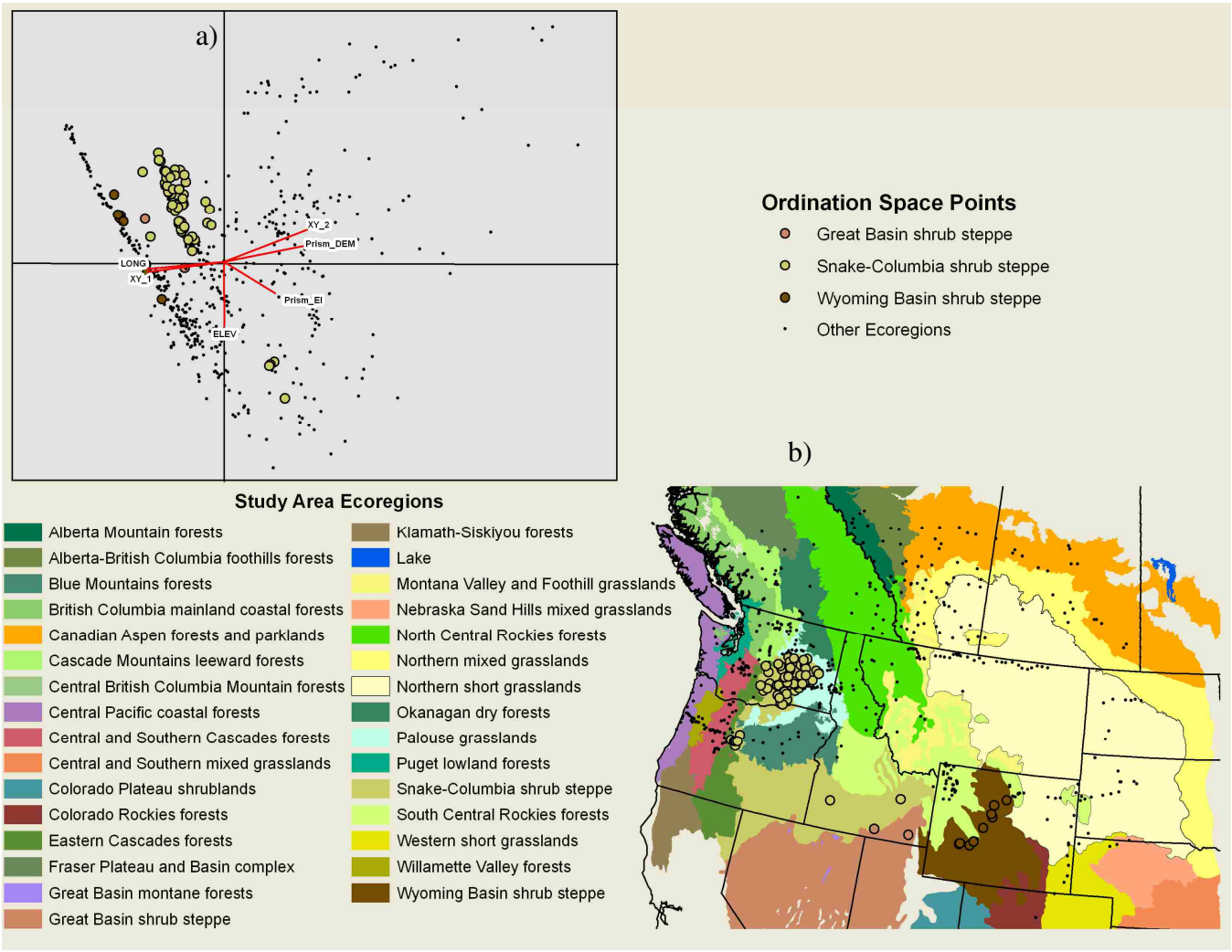

Figure 11. Location of study plots in (a) ordination space and (b) geographic space for the xeric shrubland steppe ecoregion type. Circles indicate site locations, while dots represent 'other' ecoregion types. Distinct groupings occur for the xeric shrubland steppe ecoregion types, influenced primarily by longitude, elevation, and precipitation gradients in the ordination analysis.

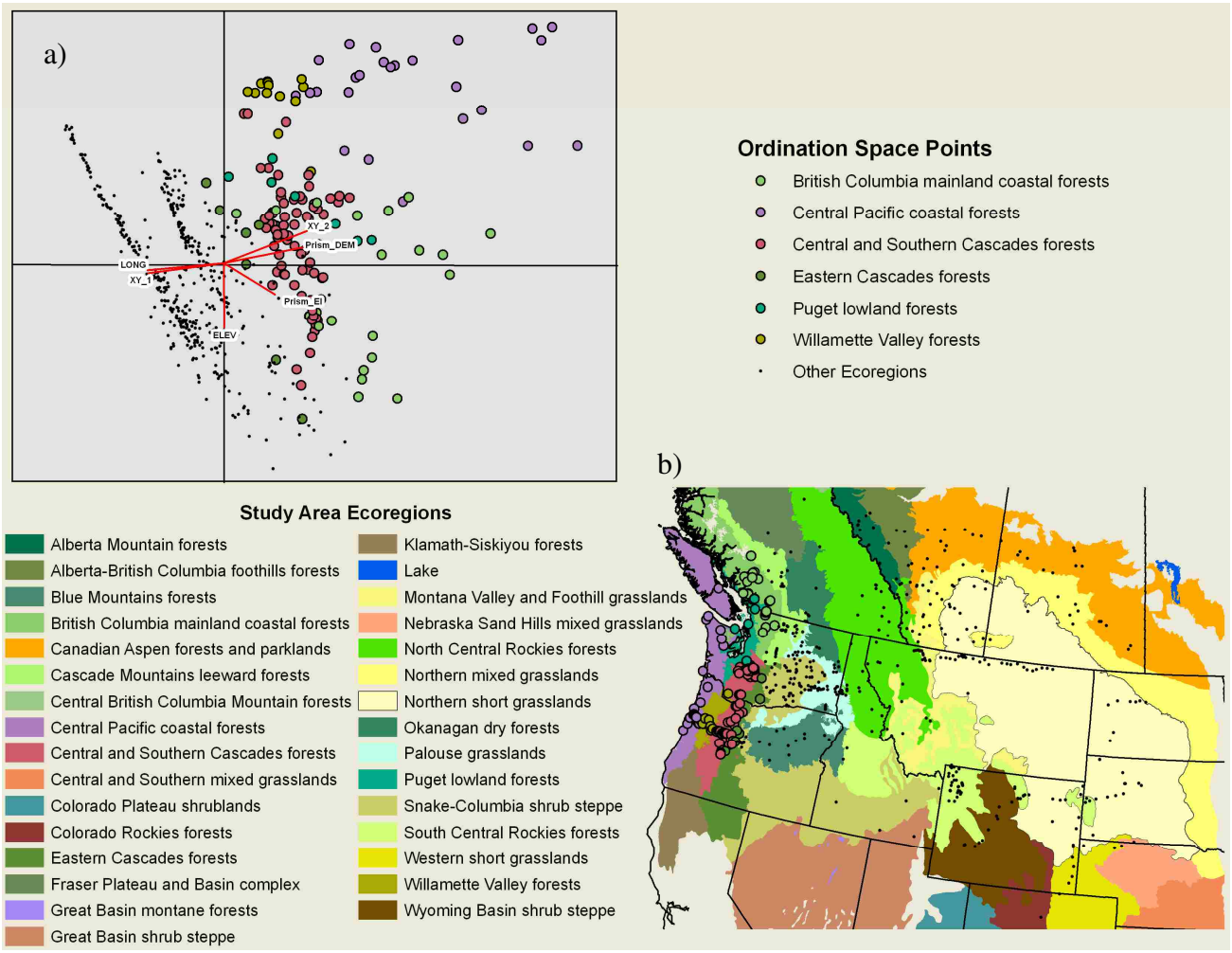

Figure 12. Location of study plots in (a) ordination space and (b) geographic space for the coastal forest ecoregion type. Circles indicate site locations, while dots represent 'other' ecoregion types. Distinct groupings occur for the coastal forest ecoregion types, influenced primarily by longitude, elevation, and precipitation gradients in the ordination analysis.

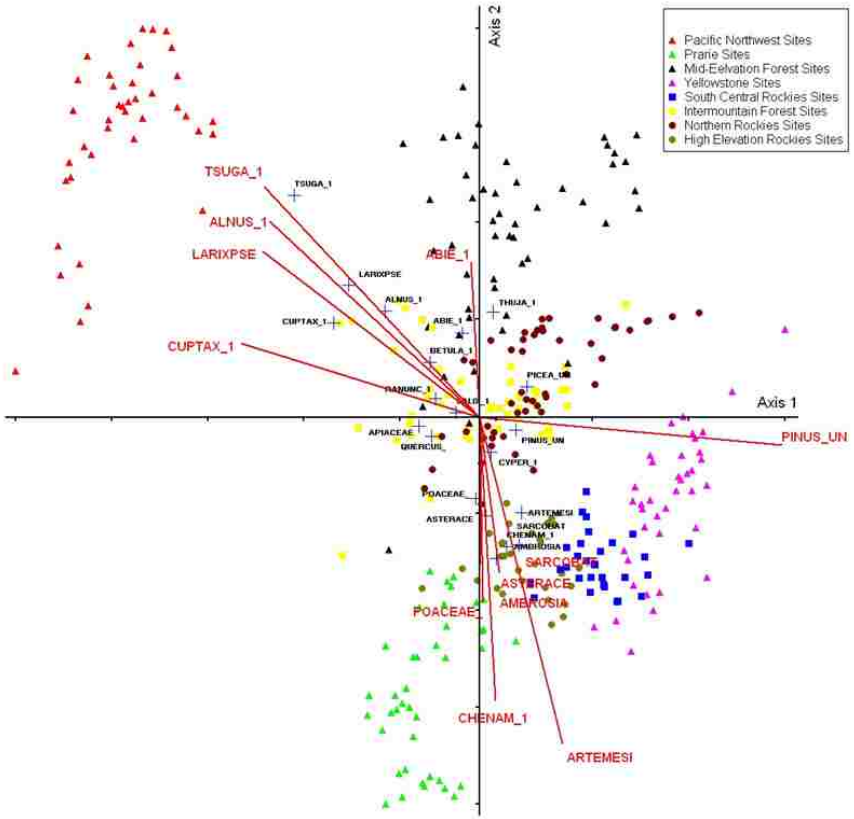

Figure 13. NMDS ordination showing the locations of each of the 10 time slices for each of the 33 study plots classed into eight groups. The "+" symbols are centroids of each species variable. Sites that plot close to the species centroids have the highest abundances of that species at those sites. The corresponding species vectors are shown in red. The length of the species vector indicates the influence that species on the ordination and aid in interpret the axes. Groupings were based on proximity in the ordination diagram, spatial location, and biophysical similarities.

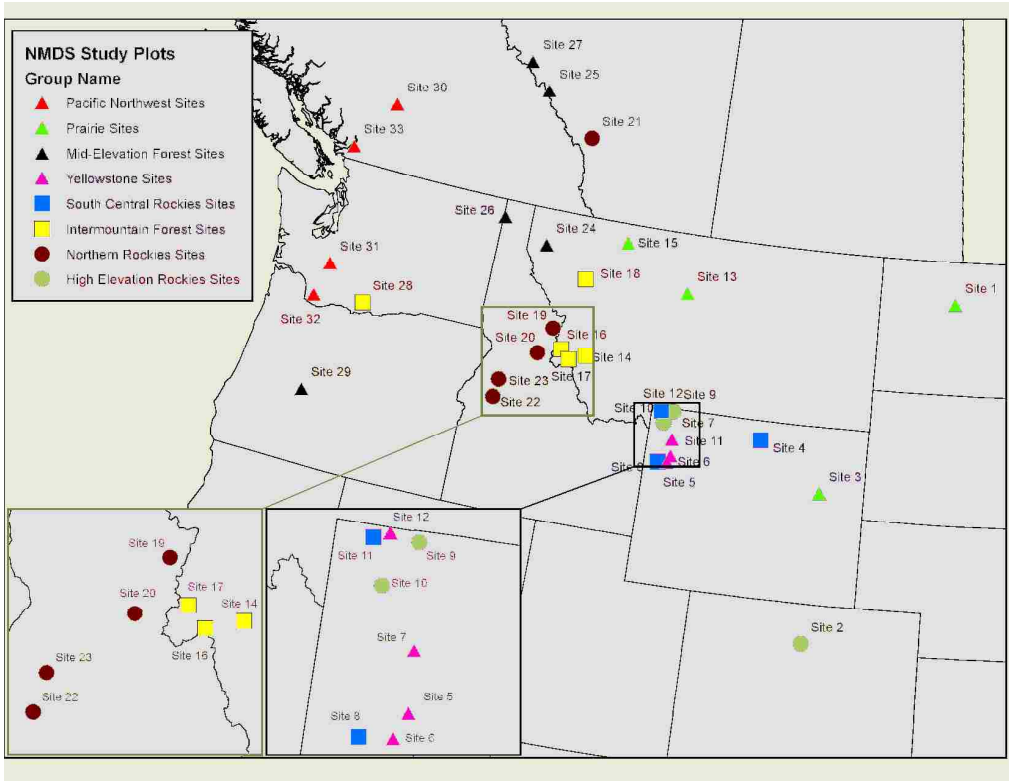

Figure 14. Map of the eight ordination groupings. See Table 2 for site names.

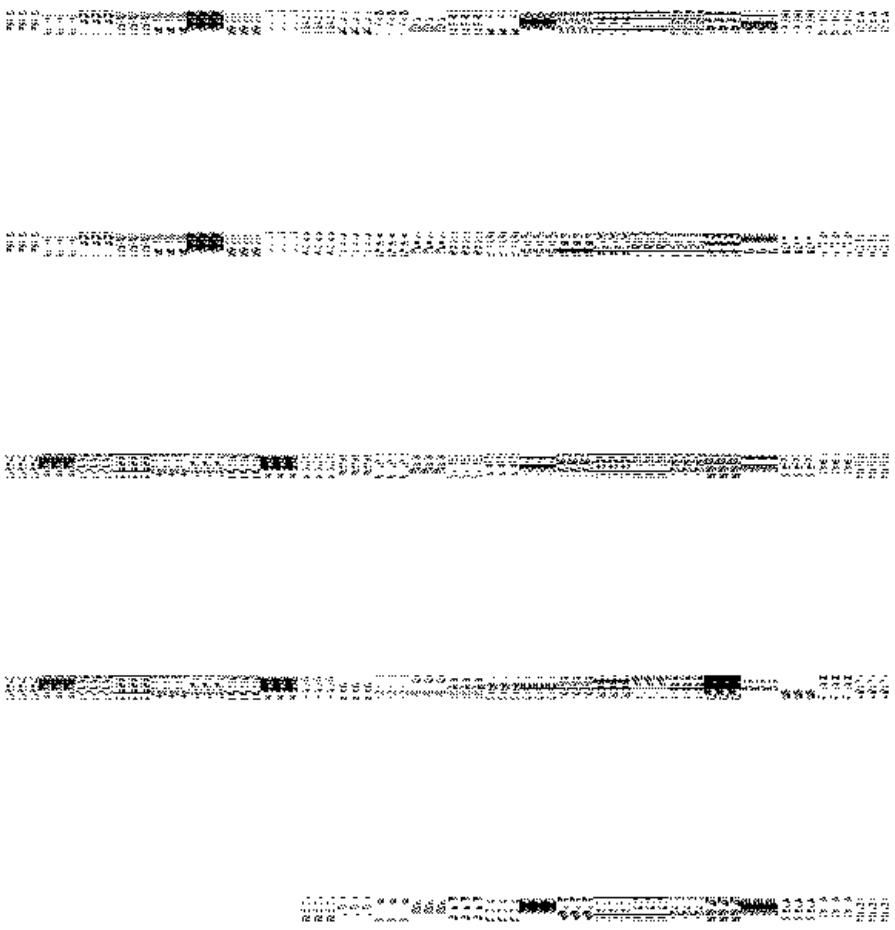

Figure 15. Successional vector pathways for ordination Group 1, the Pacific Northwest sites. Symbol locations and line vertices show each respective time slice from 0 to 9000 ybp. Closed circles represent the starting points (Time 0) and closed arrows indicate the continued trajectory beyond 9000 ybp. Axes change position, but maintain equal scaling.

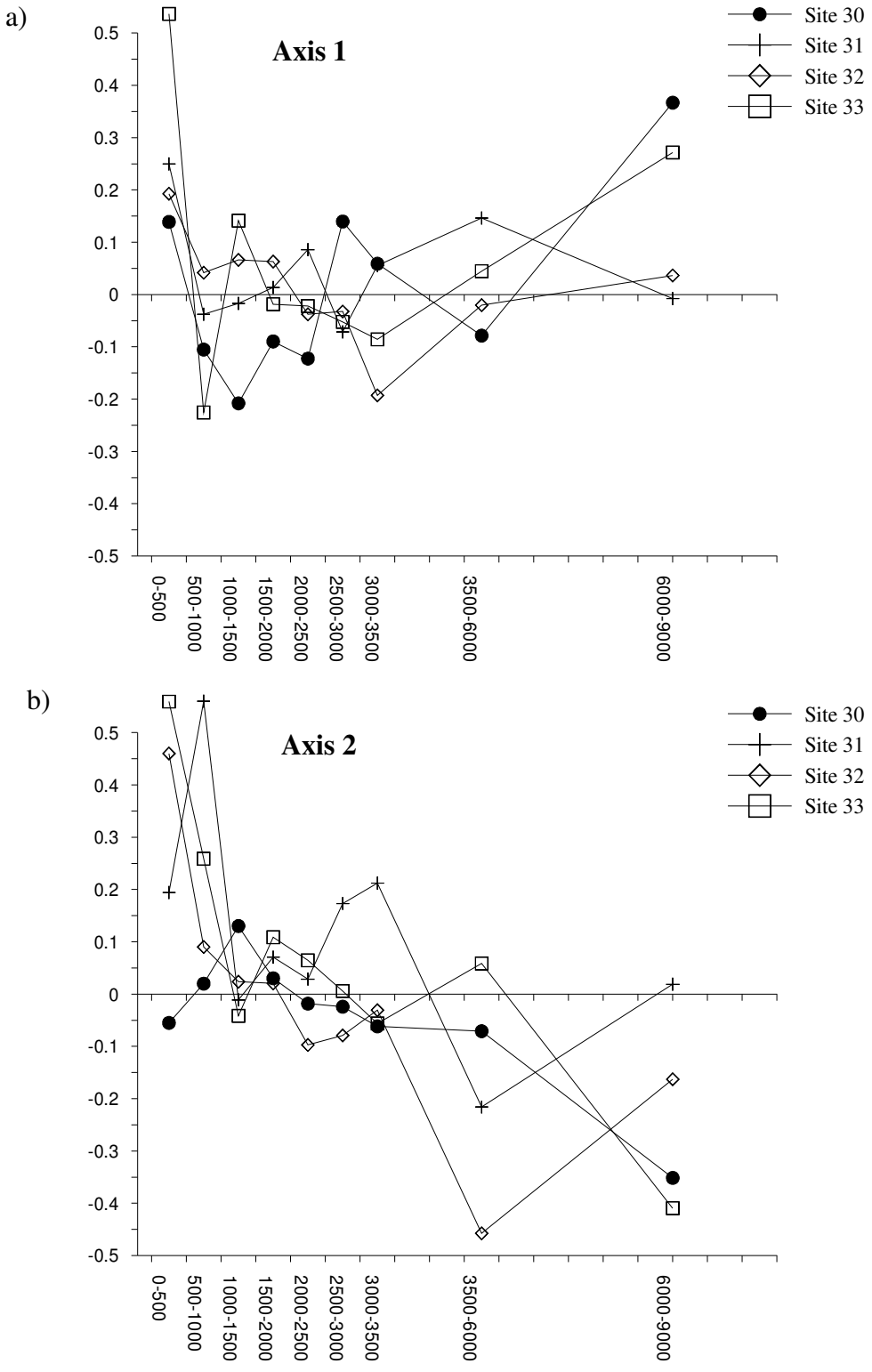

Figure 16. Displacement of community composition change for the paleopollen sites belonging to ordination Group 1, the Pacific Northwest sites, from the present to 9000 ybp on (a) ordination axis 1 and (b) on ordination axis 2. Note scale on the y-axis varies depending upon grouping and landscape trajectories for all landscape trajectory graphs.

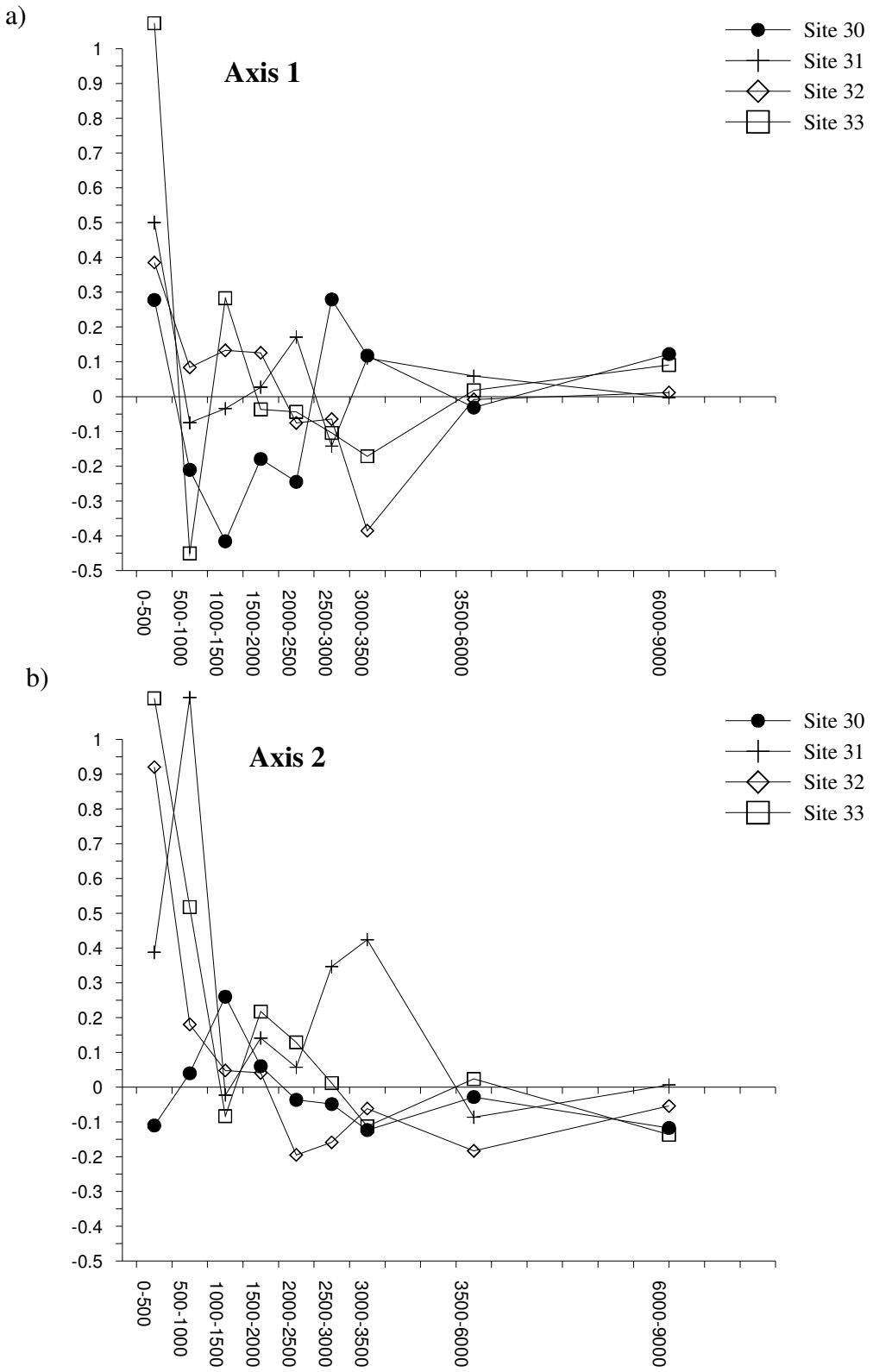

Figure 17. Velocity of community composition change for the paleopollen sites belonging to ordination Group 1, the Pacific Northwest sites, from the present to 9000 ybp on (a) ordination axis 1 and (b) on ordination axis 2.

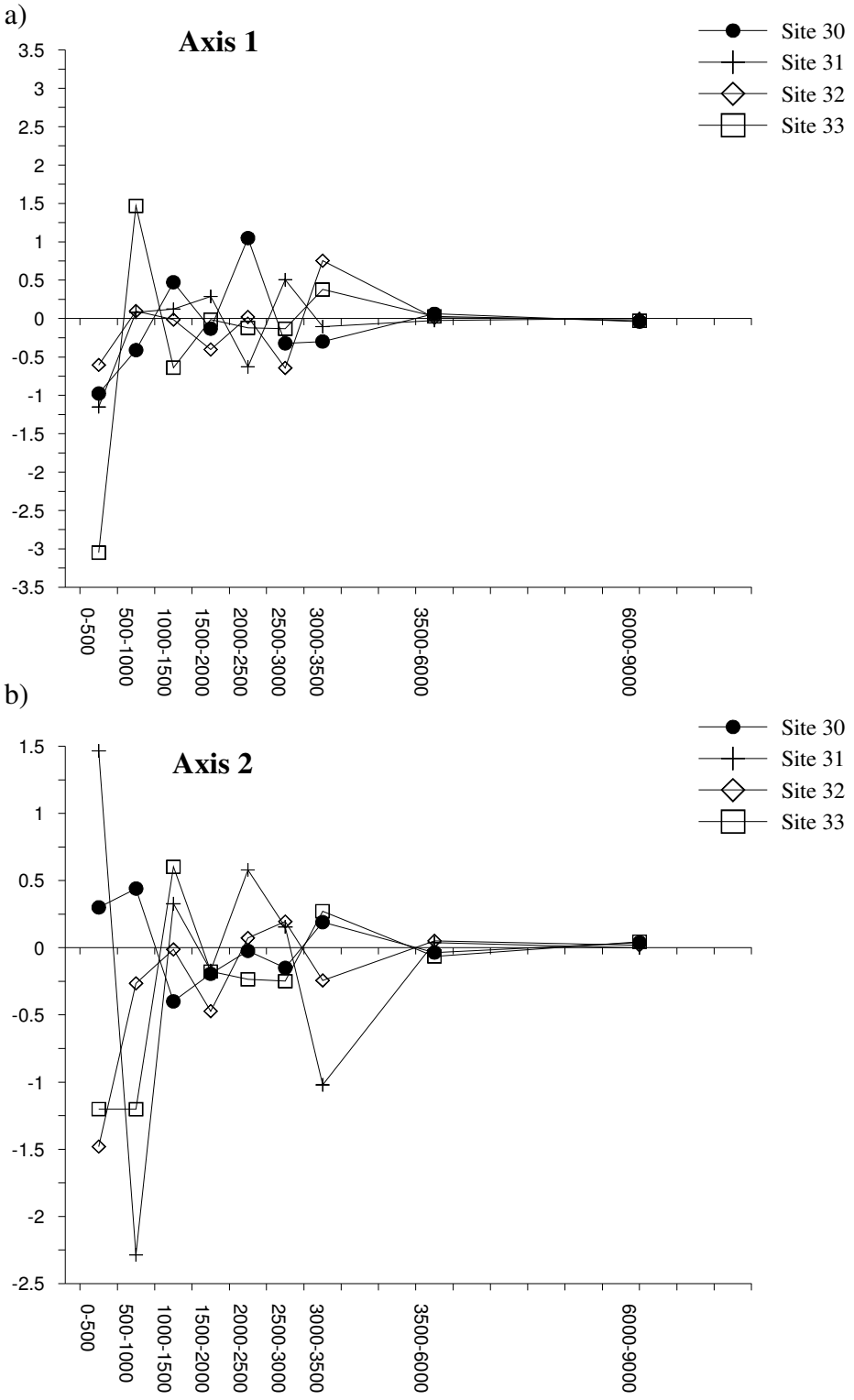

Figure 18. Acceleration of community composition change for the paleopollen sites belonging to ordination Group 1, the Pacific Northwest sites, from the present to 9000 ybp on (a) ordination axis 1 and (b) on ordination axis 2.

a)

b)

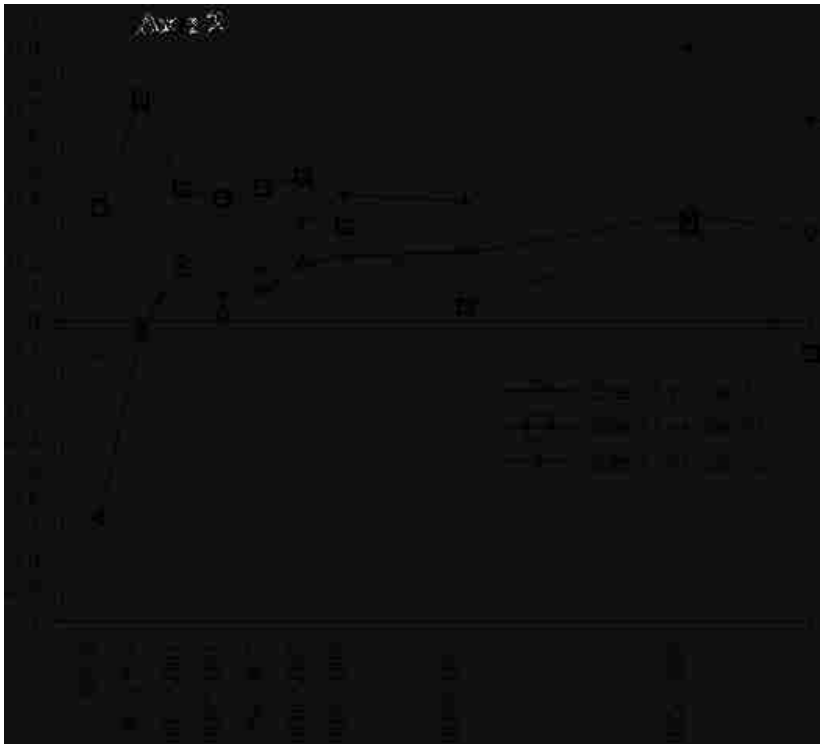

Figure 19. Divergence trajectories within ordination Group 1, the Pacific Northwest sites. Site 33 was the representative site and plotted against the remaining sites to compare divergence trajectories between sites.

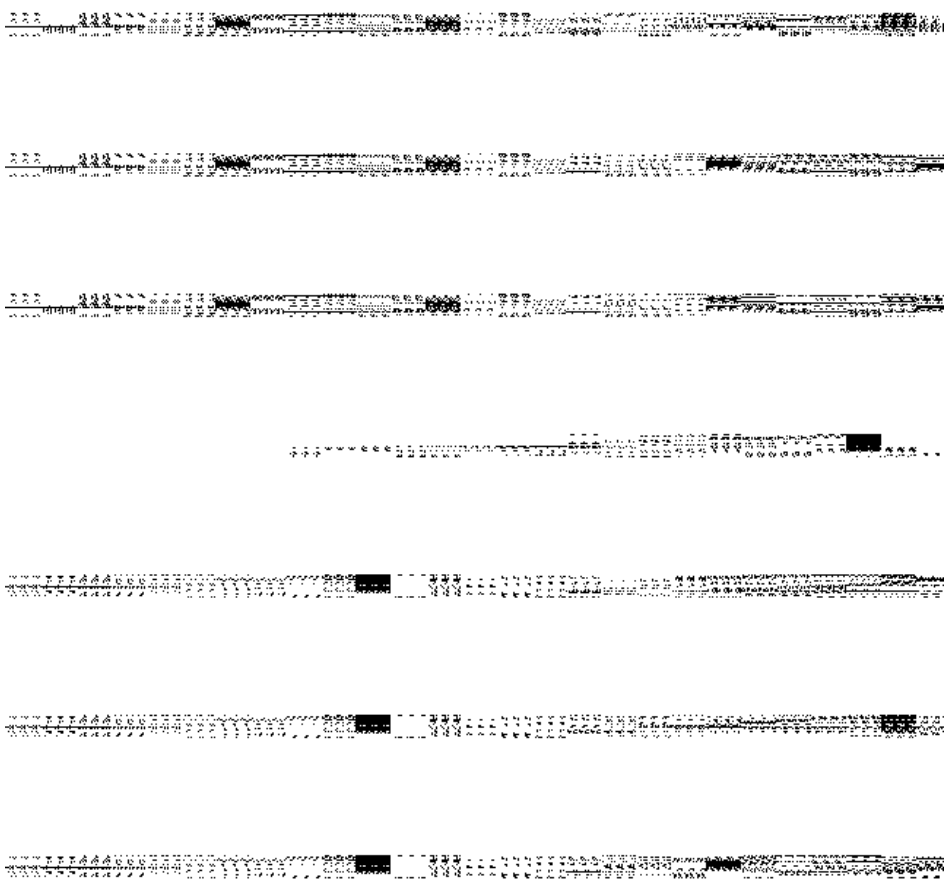

Figure 20. Successional vector pathways for ordination Group 2, the high plains prairie sites. Symbology as in Figure 15.

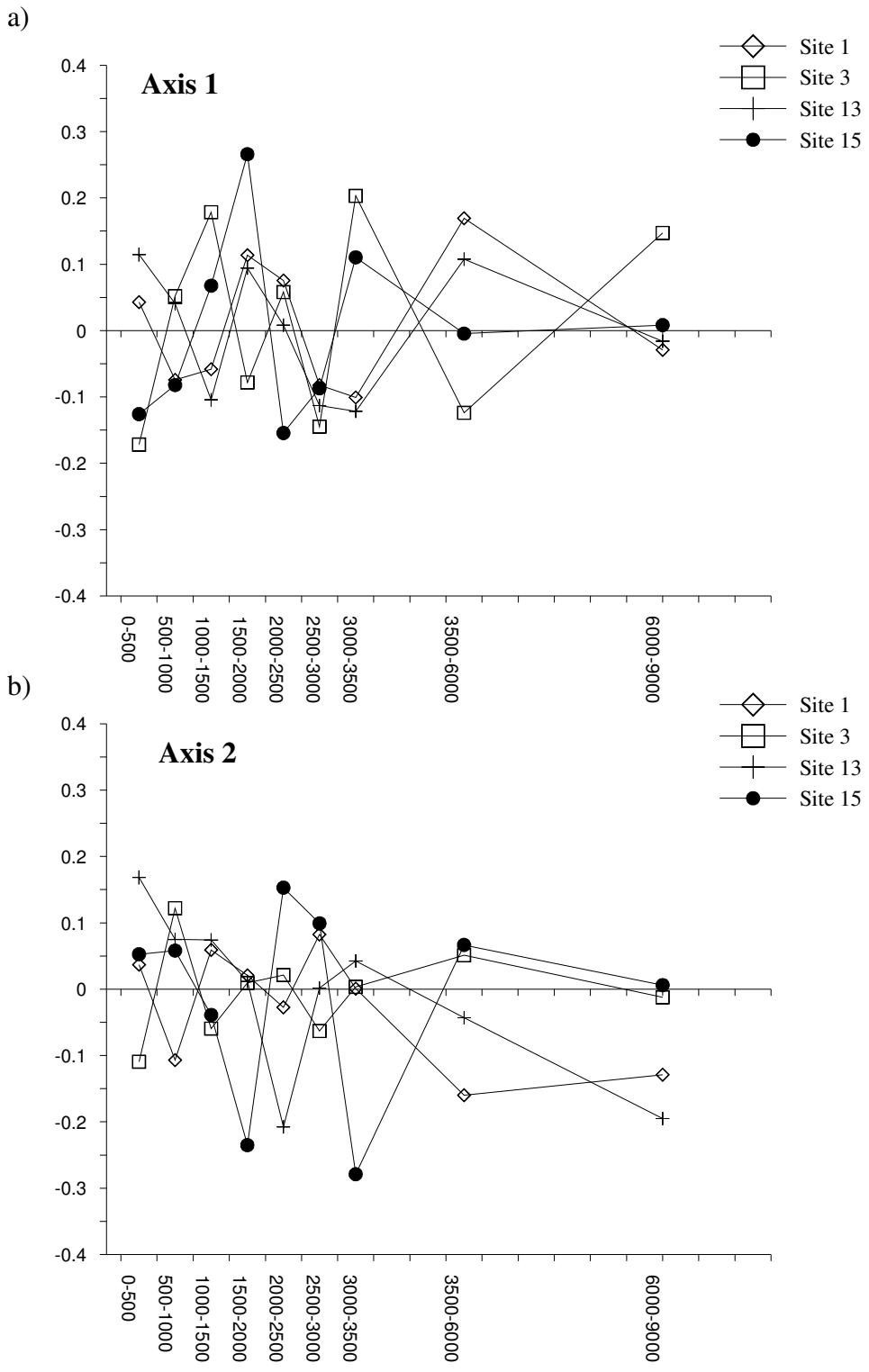

Figure 21. Displacement of community composition change for the paleopollen sites belonging to ordination Group 2, the High Plains Prairie sites, from the present to 9000 ybp on a) ordination axis 1 and on b) ordination axis 2.

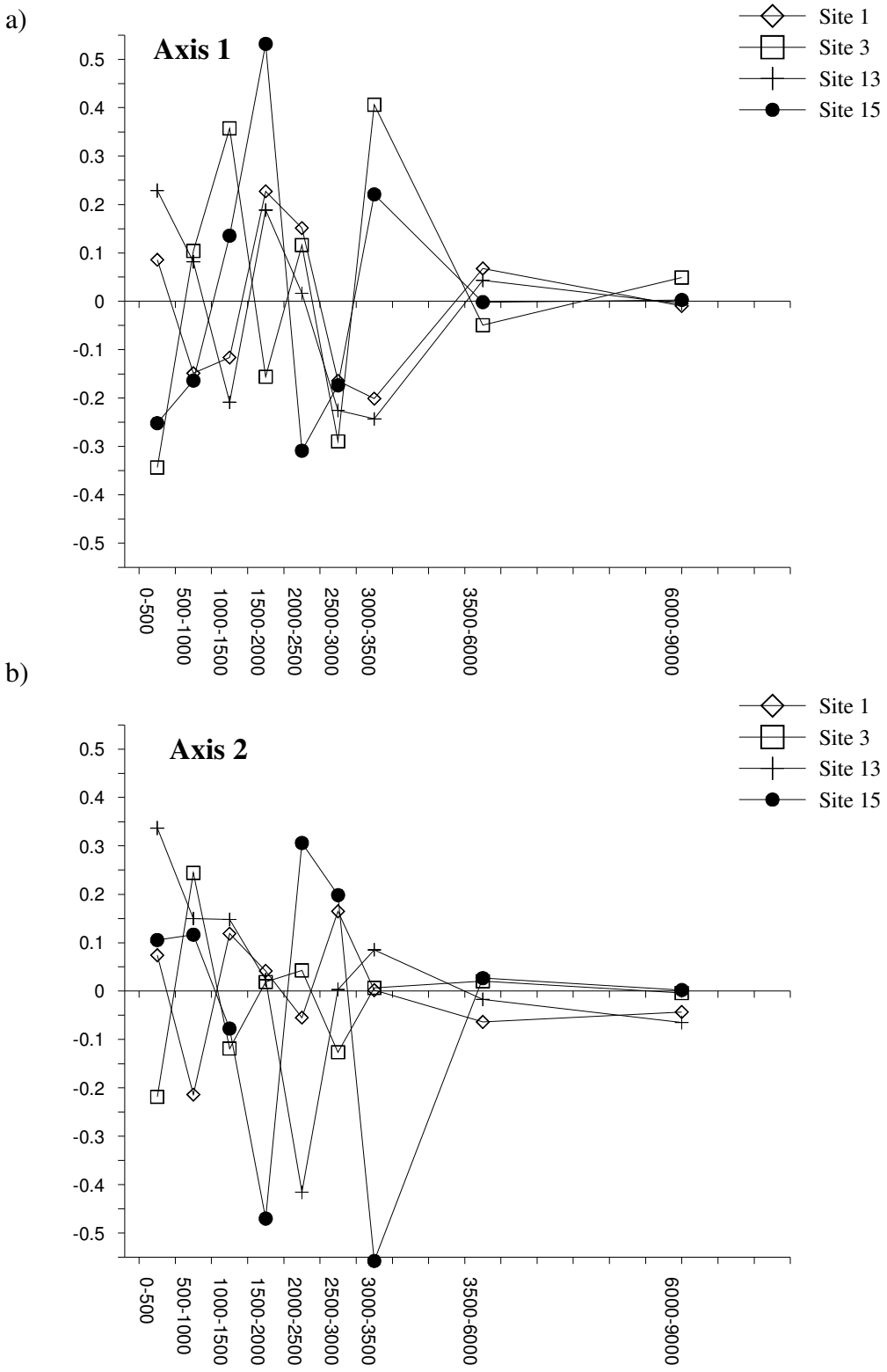

Figure 22. Velocity of community composition change for the paleopollen sites belonging to ordination Group 2, the High Plains Prairie sites, from the present to 9000 ybp on a) ordination axis 1 and on b) ordination axis 2.

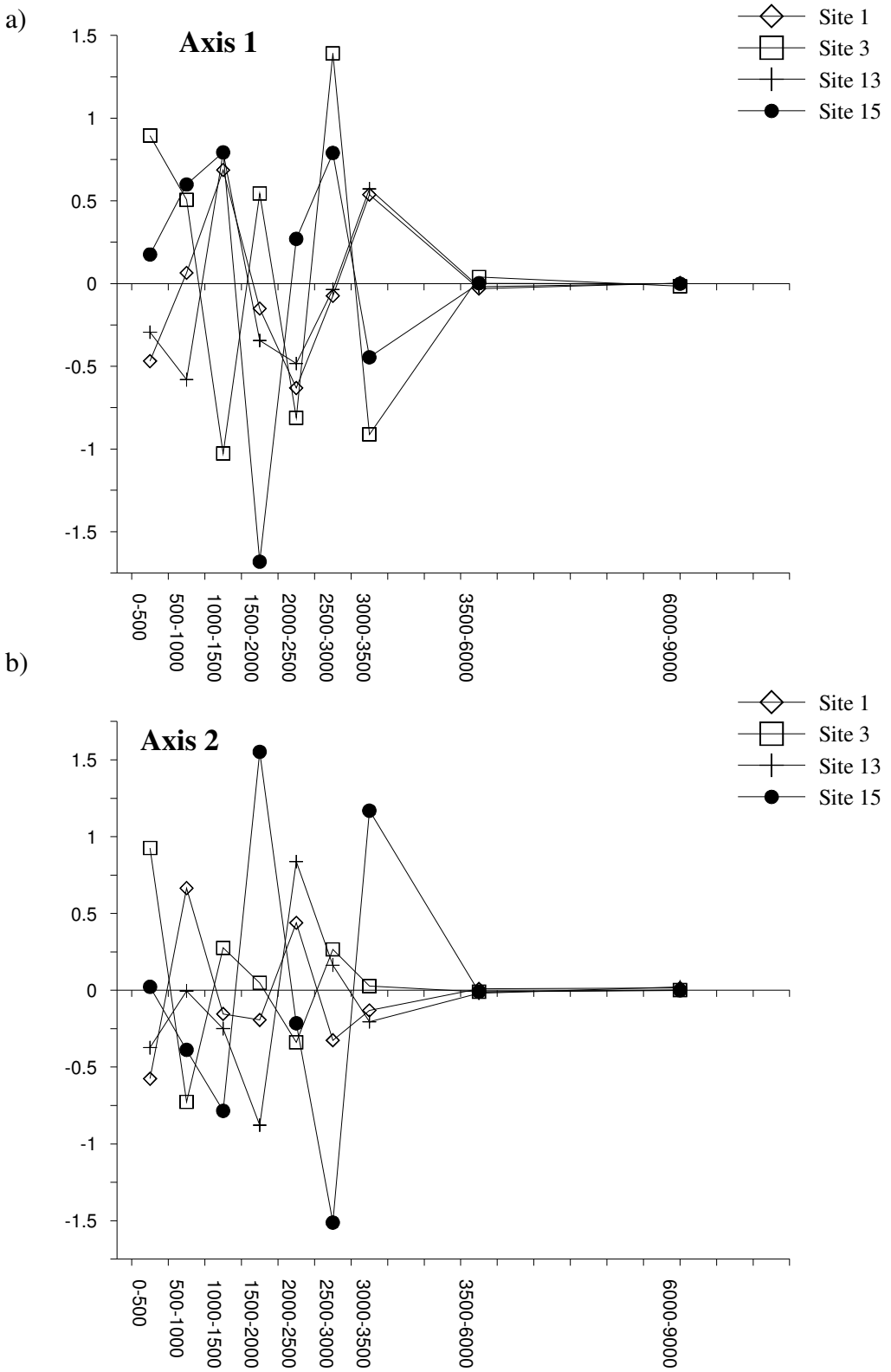

Figure 23. Acceleration of community composition change for the paleopollen sites belonging to ordination Group 2, the High Plains Prairie sites, from the present to 9000 ybp on a) ordination axis 1 and on b) ordination axis 2.

a)

b)

Figure 24. Divergence trajectories within ordination Group 2, the Prairie sites. Site 13 was chosen as the representative site for the High Plains Prairie region comparison.

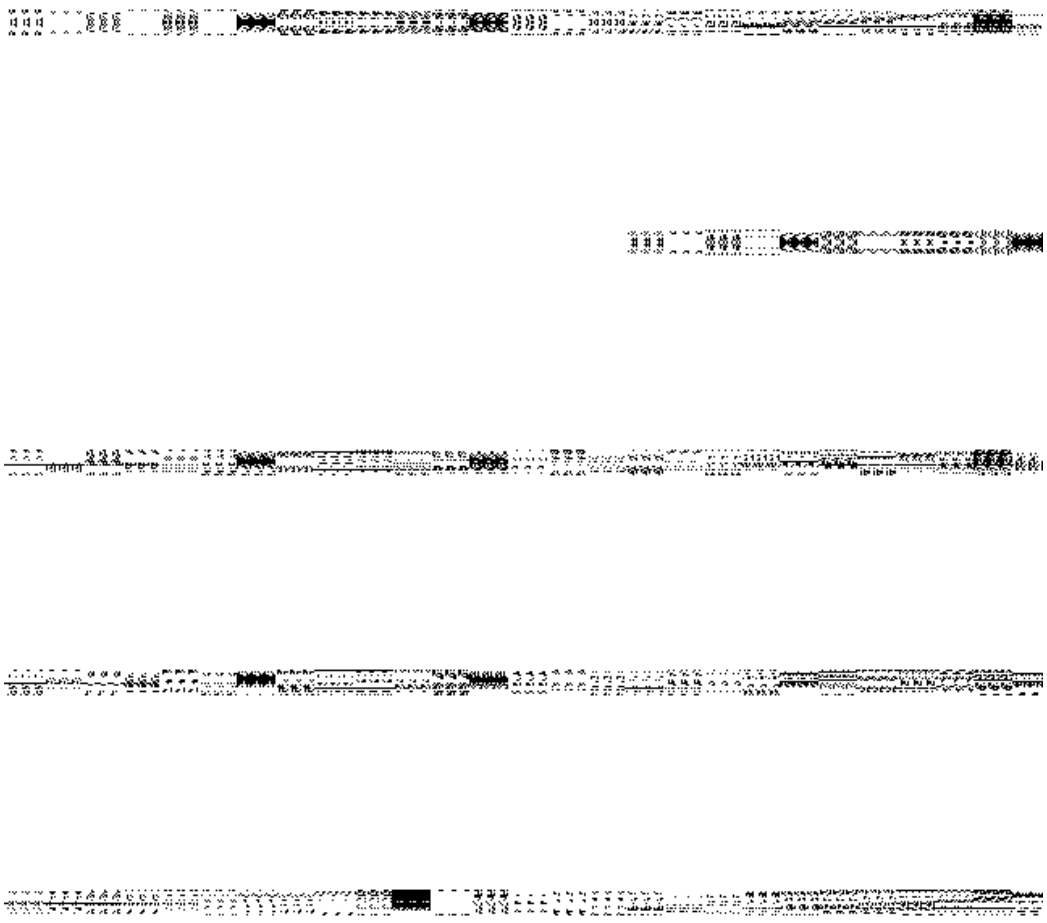

Figure 25. Successional vector pathways for ordination Group 4, the Yellowstone sites. Symbology as in Figure 15.

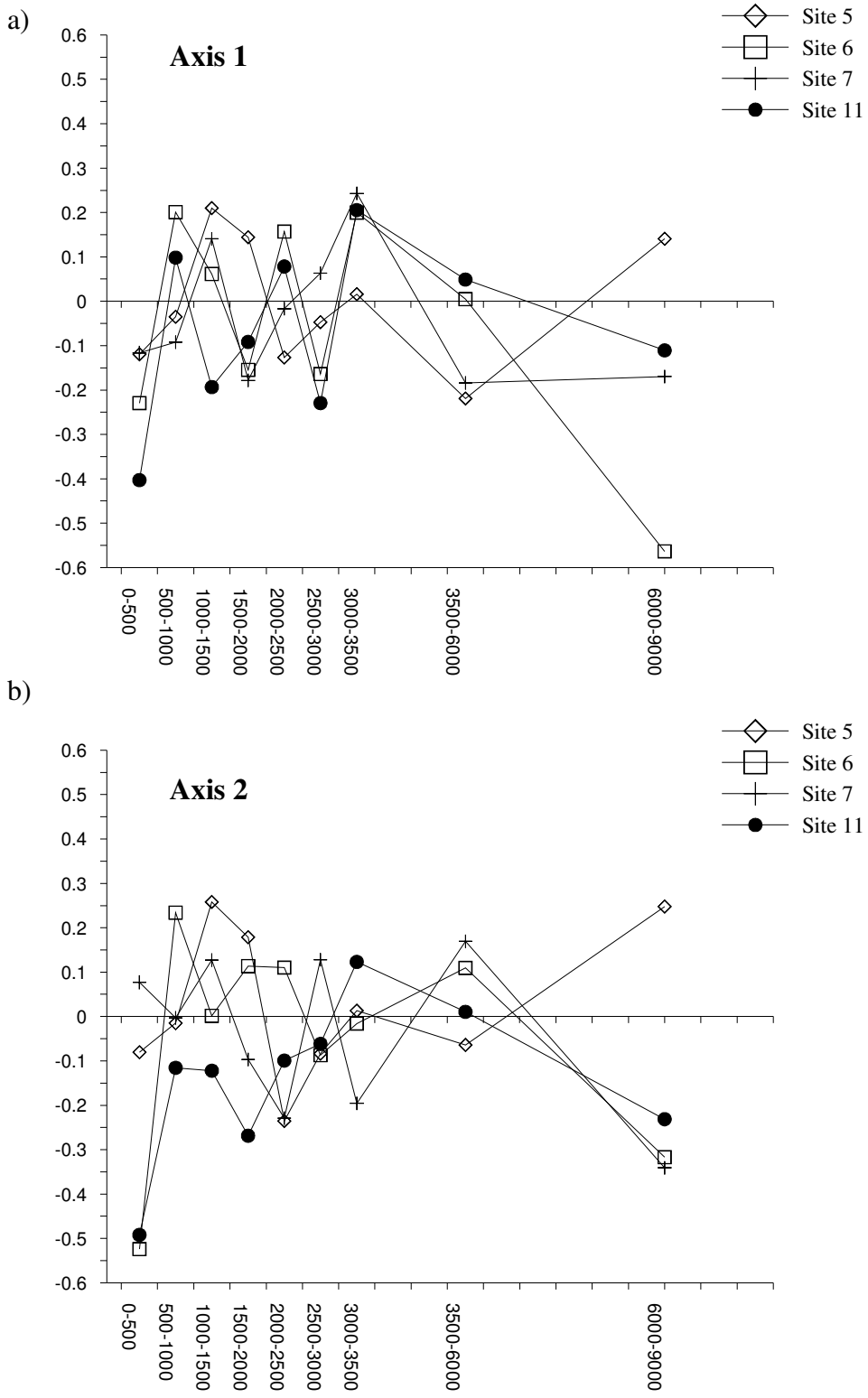

Figure 26. Displacement of community composition change for the paleopollen sites belonging to ordination Group 4, the Yellowstone sites, from the present to 9000 ybp on a) ordination axis 1 and on b) ordination axis 2.

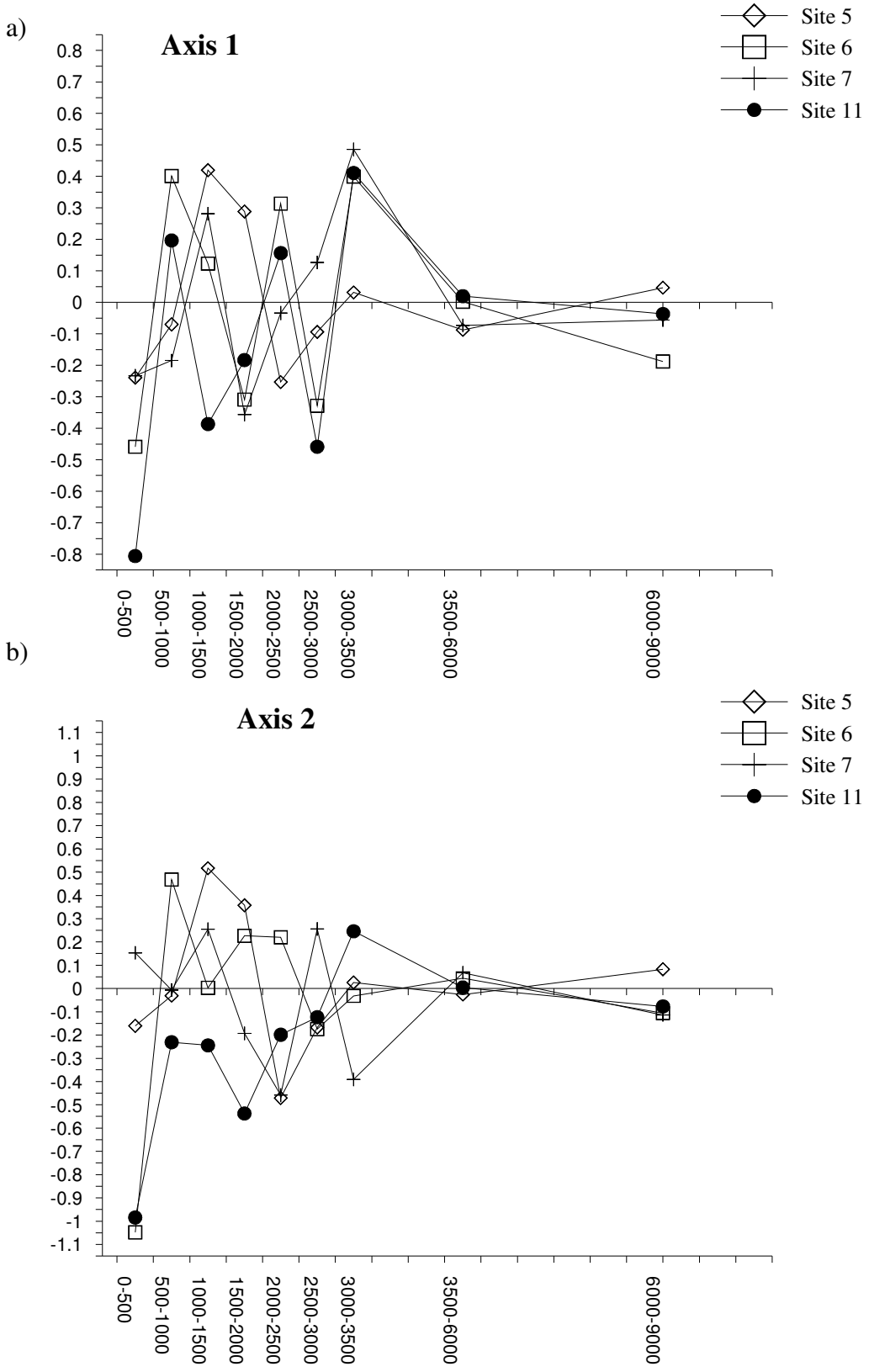

Figure 27. Velocity of community composition change for the paleopollen sites belonging to ordination Group 4, the Yellowstone sites, from the present to 9000 ybp on a) ordination axis 1 and on b) ordination axis 2

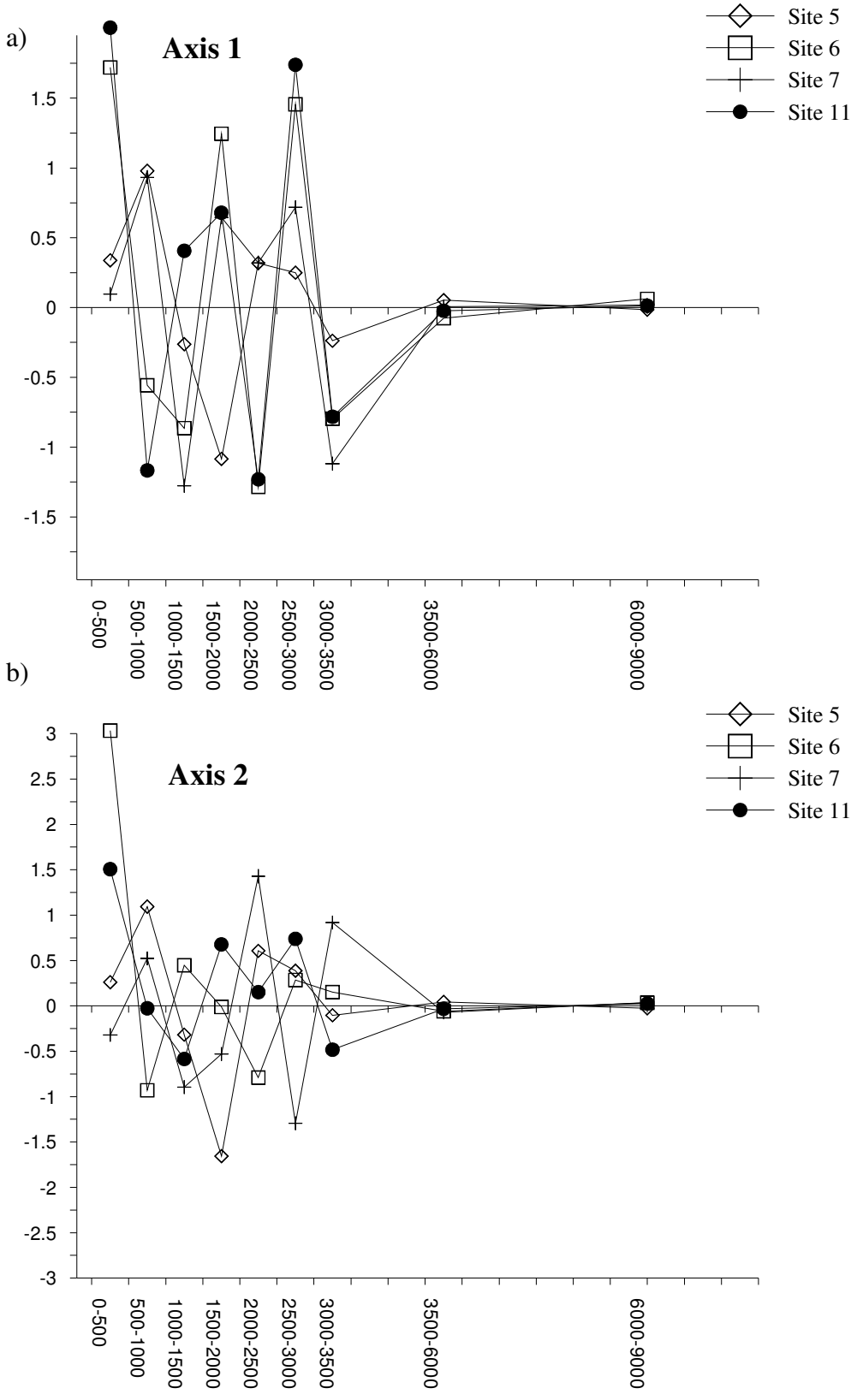

Figure 28. Acceleration of community composition change for the paleopollen sites belonging to ordination Group 4, the Yellowstone sites, from the present to 9000 ybp on a) ordination axis 1 and on b) ordination axis 2.

a)

b)

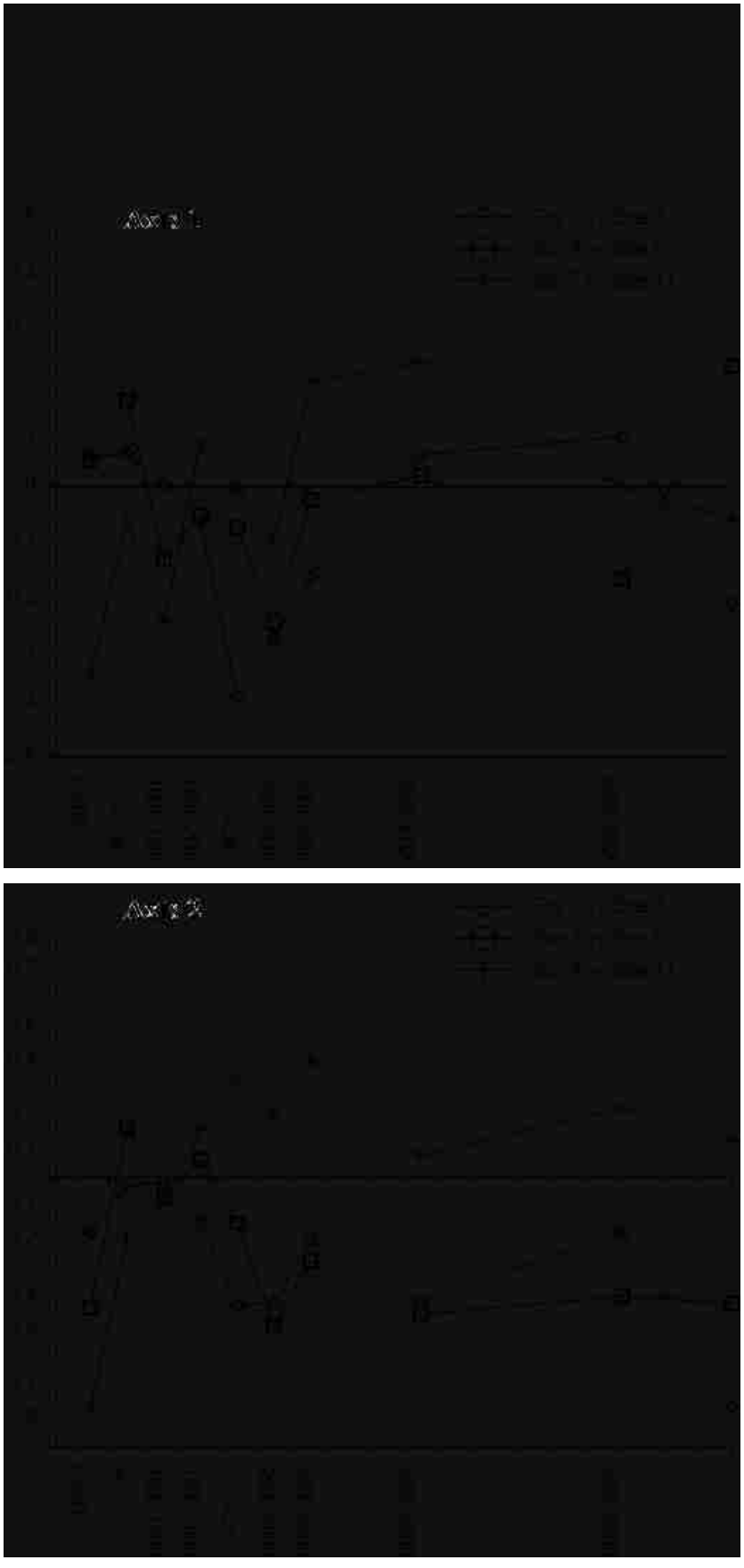

Figure 29. Divergence trajectories within ordination Group 4, the Yellowstone sites. Site 7 was chosen as the representative site for the Yellowstone area.

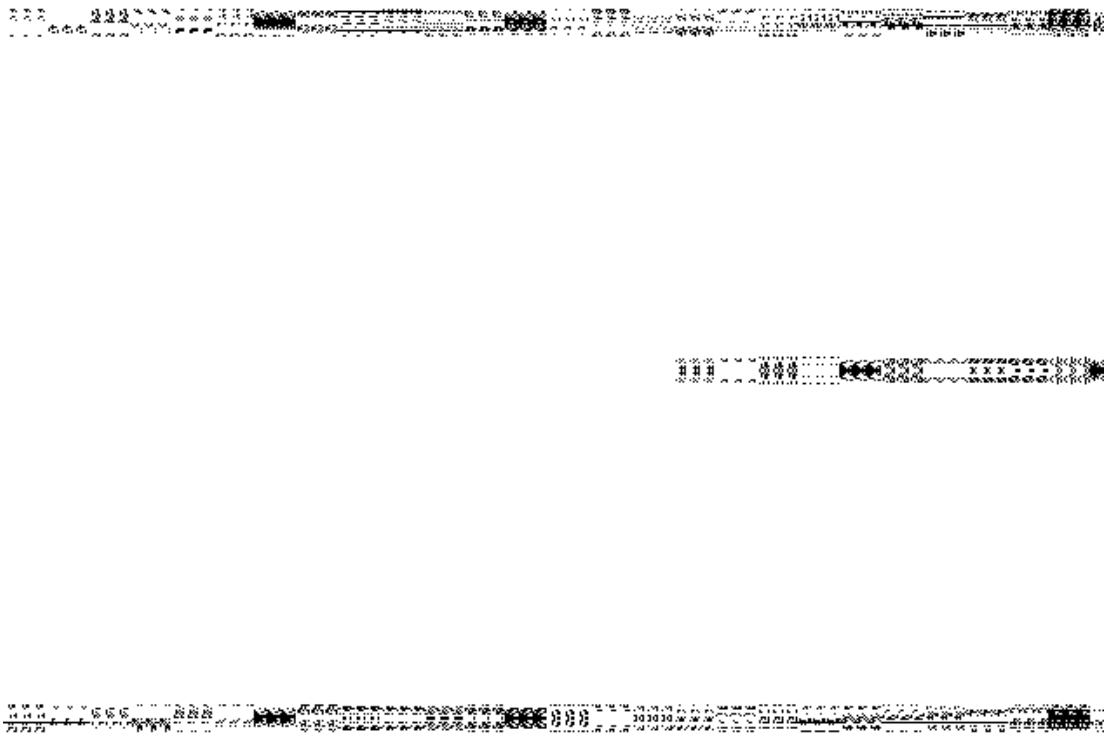

Figure 30. Successional vector pathways for ordination Group 6, the Intermountain Forest sites. Symbology as in Figure 17.

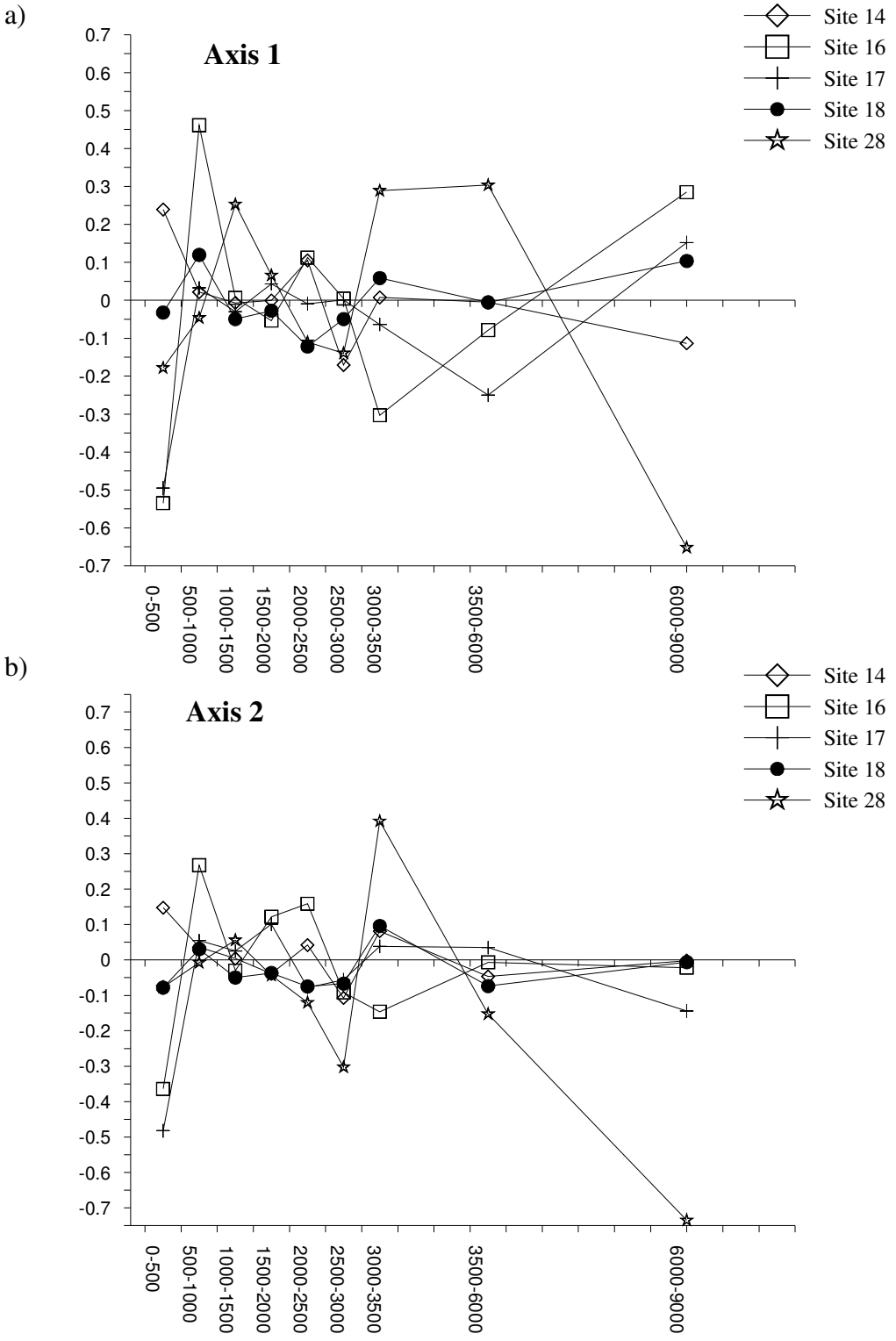

Figure 31. Displacement of community composition change for the paleopollen sites belonging to ordination Group 6, the Intermountain Forest sites, from the present to 9000 ybp on a) ordination axis 1 and on b) ordination axis 2.

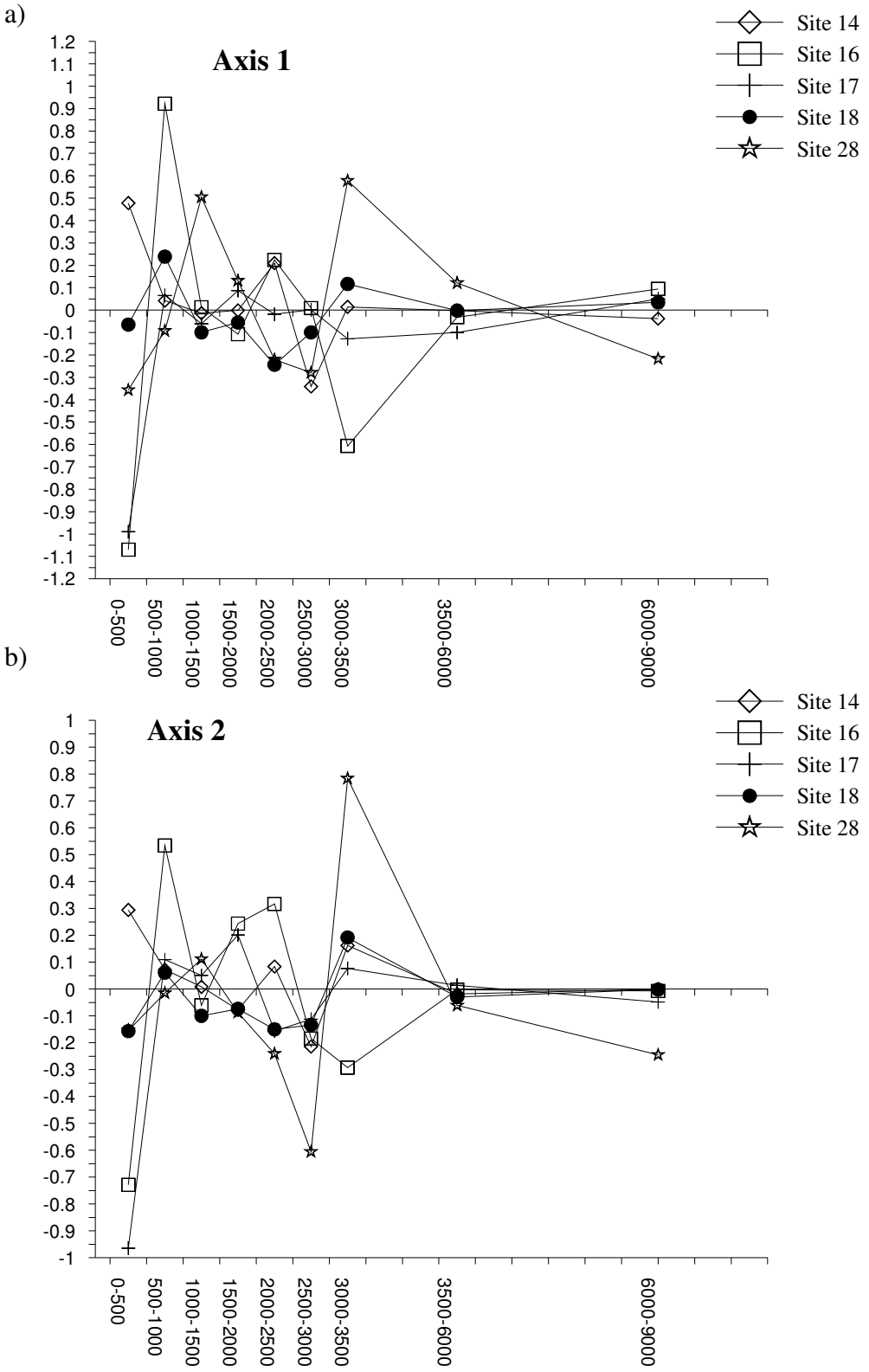

Figure 32. Velocity of community composition change for the paleopollen sites belonging to ordination Group 6, the Intermountain Forest sites, from the present to 9000 ybp on a) ordination axis 1 and on b) ordination axis 2.

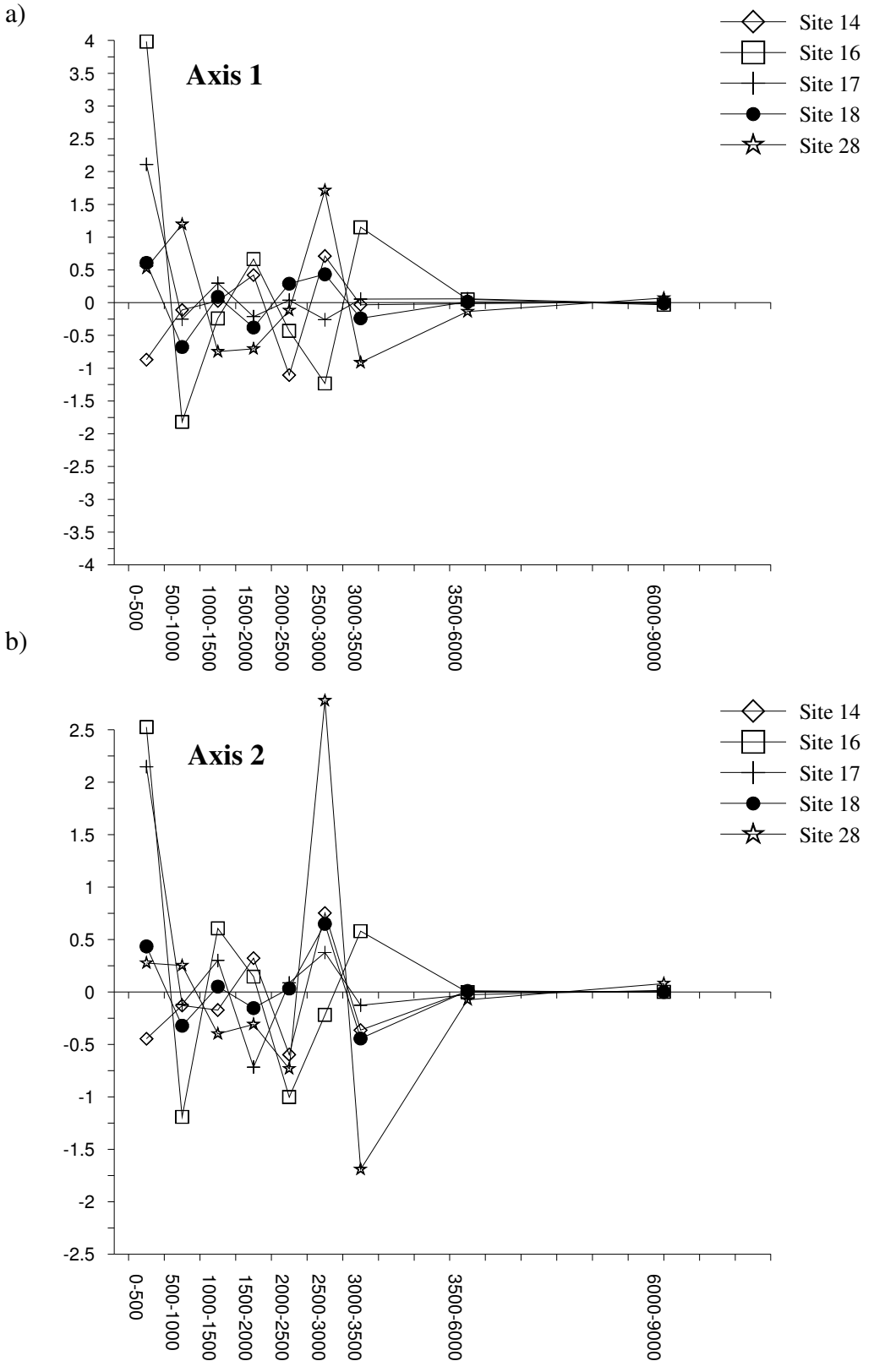

Figure 33. Acceleration of community composition change for the paleopollen sites belonging to ordination Group 6, the Intermountain Forest sites, from the present to 9000 ybp on a) ordination axis 1 and on b) ordination axis 2.

a)

b)

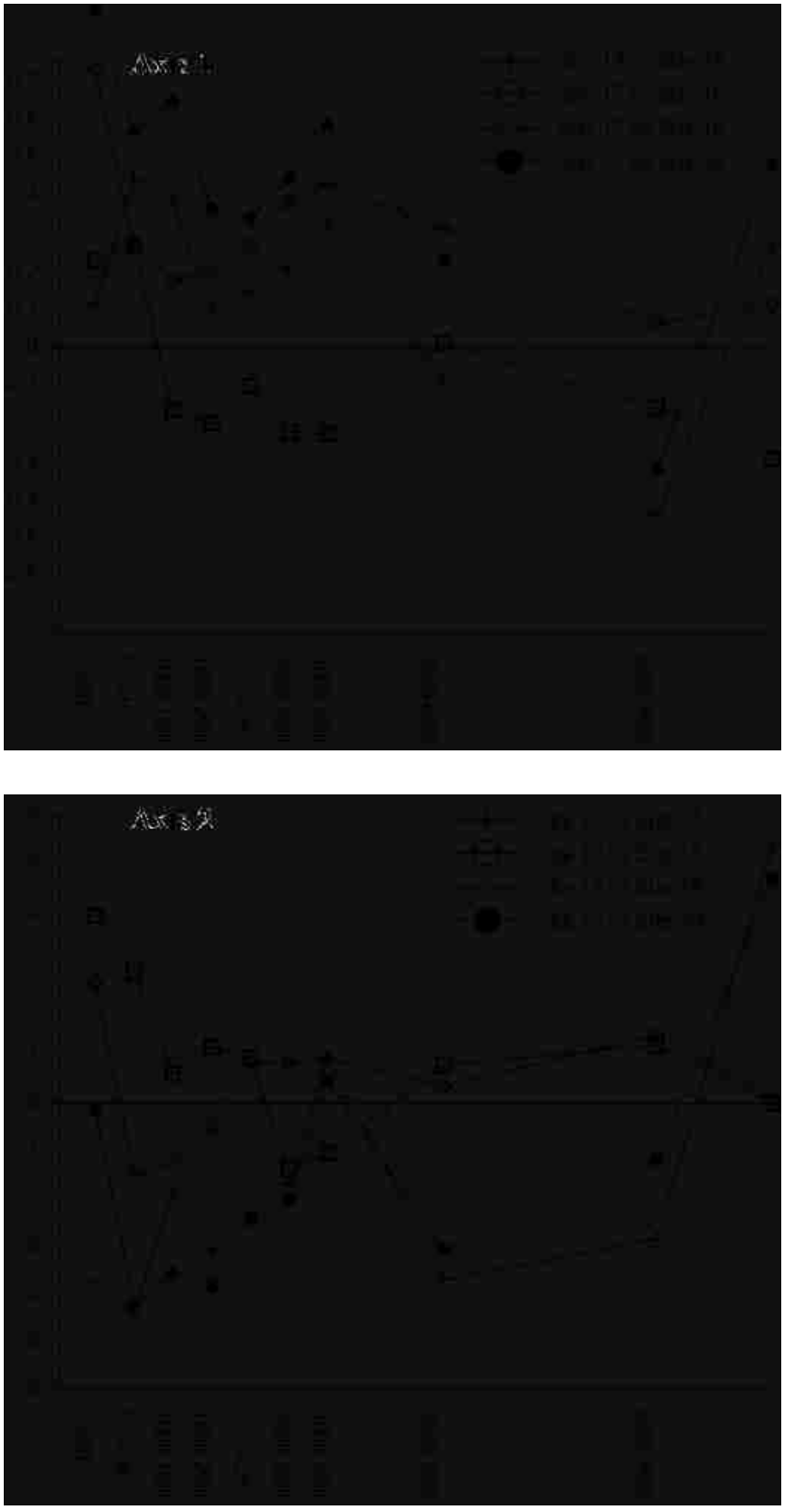

Figure 34. Divergence trajectories within ordination Group 6, the Intermountain Forest sites. The Group 6 sites follow very similar rates of divergence along both axes throughout time, suggesting analogous regional climate and vegetation changes.

a)

b)

Figure 35. Divergence trajectories of all groups through time. Group 6 was used as the comparative group. This graph shows synchronous climate and vegetation composition shifts through time within the groups discussed in the thesis. Divergence trajectory shifts are relative to a site's biophysical setting at 'x' time period, though are not relative to one another.

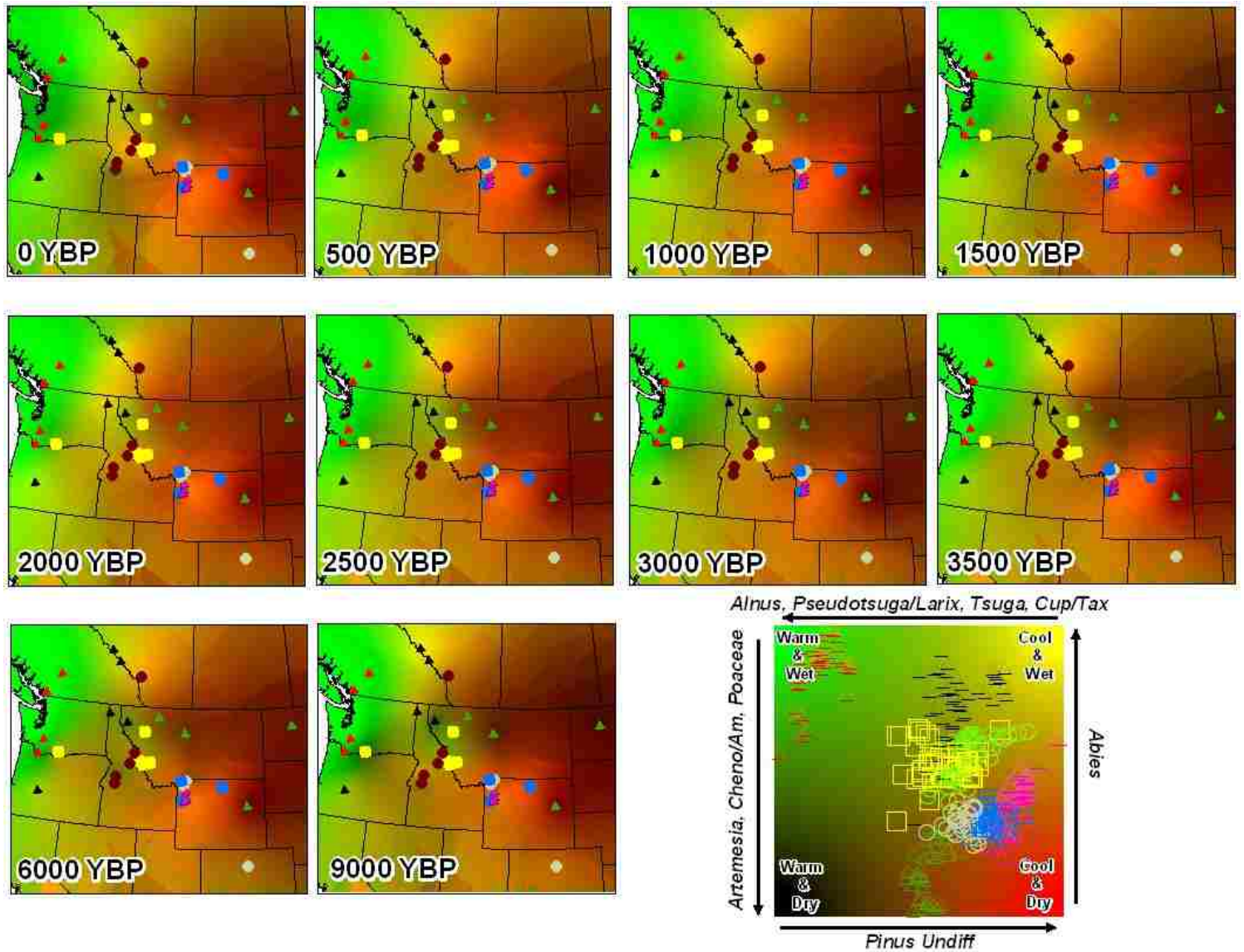

Figure 36. Interpolated ordination axis scores depicting climate and vegetation composition throughout the study area as inferred from relative fossil pollen percentages. Each map is a distinct time slice. Paleosite symbology matches the NMDS ordination symbology in Figure 13.

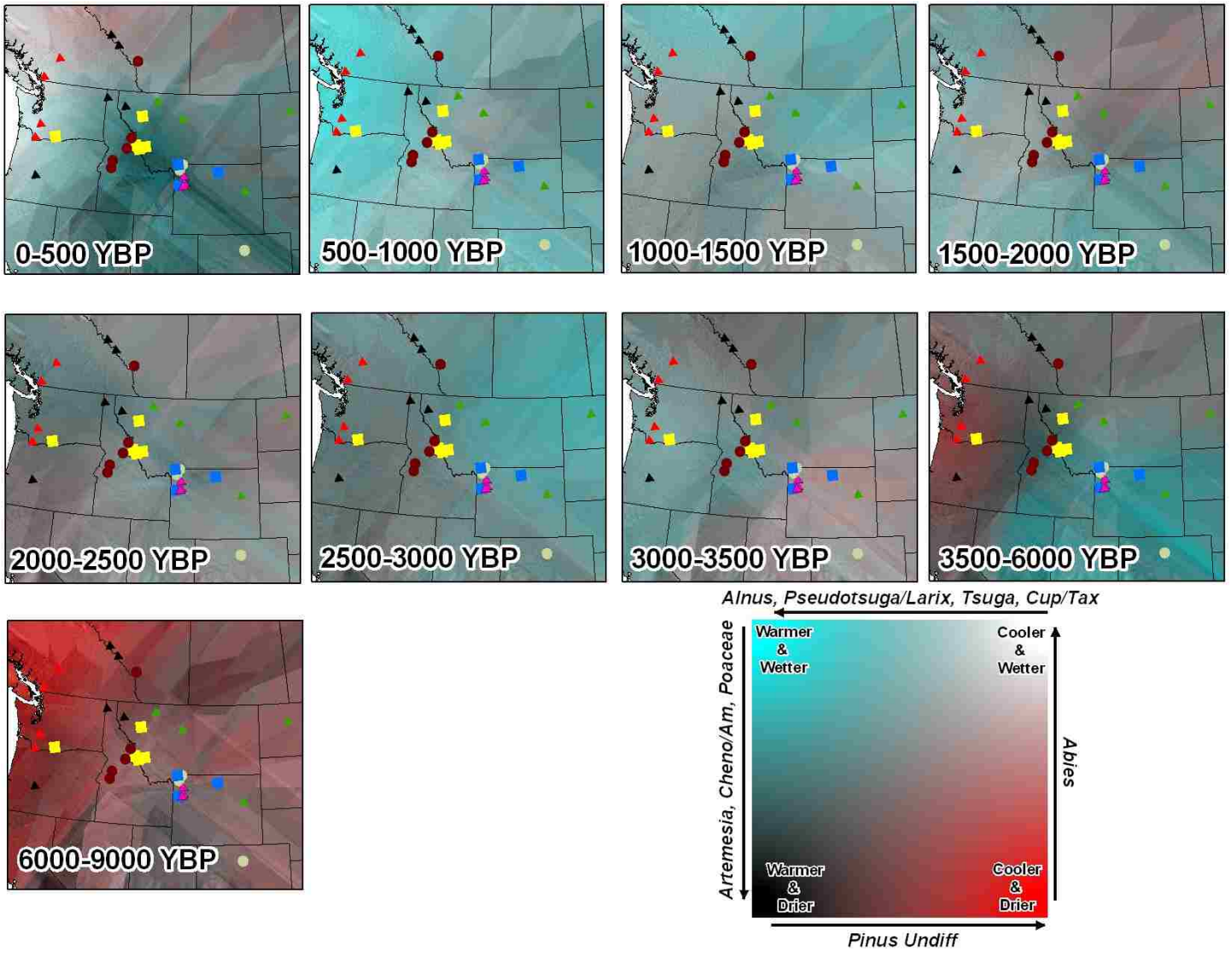

Figure 37. Interpolated community composition displacement scores for inferring climate and vegetation trends through time. Each map is the transition from the earlier time period to the next later time slice, (e.g. vegetation displacement from 9000 to 6000 ybp). Paleosite symbology matches the NMDS ordination symbology in Figure 13.

TABLES

Table 1. Kruskal's (1964a) and Clarke's (1993) rules of thumb for determining validity of NMDS ordination results as based on stress (adapted from McCune and Grace, 2002).

Kruskal's Rules of Thumb	
Stress	
0.0-2.5	Excellent
2.51-5.0	Good
5.01-10.0	Fair
10.01-20	Poor

Clarke's Rules of Thumb	
<5	An excellent representation with no prospect of misinterpretation. This is rarely achieved.
5 to 10	A good ordination with no real risk of drawing false conclusions.
10 to 20	Can still correspond to a usable picture, though values at the upper end suggest a potential to mislead.
>20	Likely to yield a plot that is relatively dangerous to interpret. Samples are placed essentially at random.

Table 2. Paleopollen sites included in the cumulative pollen database. N/I represents digitized sites not included in the analysis and N/A means the citation was not available. Detailed citations are in the bibliography. Stump under source reflects sites digitized by the author, and Williams infers sites provided by Williams (2007).

Site Number	Pollen Sample Site	Citation	Source
1	Rice Lake, ND	N/A	Williams
2	Eldora Fen, CO	N/A	Williams
3	Antelope Playa, WY	Markgraf and Lennon, 1986	Williams
4	Floating Island Lake, WY	Burkhart, 1976	Williams
5	Divide Lake, WY	Steventon and Kutzbach, 1987	Williams
6	Lily Lake, WY	Whitlock and Bartlein, 1993	Williams
7	Buckbean Fen, WY	Baker, 1976	Williams
8	Hedrick Pond, WY	Whitlock and Bartlein, 1993	Williams
9	Slough Creek Pond, WY	Whitlock and Bartlein, 1993	Williams
10	Cygnet Lake Fen, WY	Whitlock, 1993	Williams
11	Blacktail Pond, WY	Gennet and Baker, 1986	Williams
12	Gardiner's Hole, WY	Bender et al, 1971	Williams
13	Lost Lake, MT	Barnosky, C., 1987	Williams
14	Pintlar Lake, MT	Brunelle et al., 2005	Williams
15	Guardipee Lake, MT	Barnosky, C., 1987	Stump
16	Lost Trail Pass Bog, MT	Mehringer et al., 1977	Stump
17	Baker Lake, MT	Brunelle et al., 2005	Williams
18	Rock Lake, MT	Gerloff et al., 1995	Stump
19	Hoodoo Lake , ID	Brunelle et al., 2005	Stump
20	Burnt Knob Lake, ID	Brunelle et al., 2005	Williams
22	Van Wyck, ID	Doerner and Carrara, 1999	Stump
23	McCall Fen, ID	Doerner and Carrara, 2001	Stump
24	Tepee Lake, MT	Mack et al., 1983	Stump
26	Hager Pond, ID	Mack et al., 1978	Stump
27	Wilcox Pass, AB	Beaudoin, 1984	Williams
28	Carp Lake, WA	Barnosky, C., 1985	Williams
29	Gold Lake Bog, OR	Sea and Whitlock, 1995	Williams
30	Pinecrest Lake, AB	Mathews and Rouse, 1975	Williams
31	Davis Lake, WA	Barnosky, C., 1981	Williams
32	Battle Ground Lake, WA	Barnosky, C., 1985	Williams
33	Marion Lake, BC	Mathews and Heusser, 1981	Williams
N/I	Marys Pond, MT	Karsian, 1995	Stump
N/I	McKillop Creek	Mack et al., 1983	Stump
N/I	Sheep Mountain Bog, MT	Hemphill, 1983	Stump
N/I	Smeads Bench Fen	Chatters and Leavell, 1995	Stump
N/I	Harding Lake	Chatters and Leavell, 1995	Stump
N/I	Foy Lake, MT	Powers et al., 2006	Stump

Table 3. All taxa recorded from the pollen diagram digitizing procedure at the supplemental paleopollen sites.

Abies	*Ericaceae*	*Plantago*	*Tsuga*
Acer	*Erigonum*	*Poaceae*	*Tsuga heterophylla*
Algae	*Eupatorium*	*Polygonaceae*	*Tsuga mertensiana*
Alnus	*Fabaceae*	*Polygonum*	*Tubuliflorae*
Ambrosia	*Fenestrate*	*Populus*	*Typha*
Amelanchier-type	*Galium aparine*-type	*Potentilla*	*Ultricularia*
Apiaceae	*Galium Boreale*	*Potomagoten*	*Umbelliferae*
Arceuthobium	*Geum-type*	*Primulaceae*	*Vaccinium*
Artemisia	*Helianthus*-type	*Prunus*	
Asteraceae	*Holodiscus*	*Pseudotsuga-Larix*	
Athyrium	*Isoetes*	*Pteridium*	
Bayophyta spores	*Juniperus*	*Quercus*	
Berberis	*Kalmia*	*Ranunculaceae*	
Betula	*Labiatae*	*Rhamnaceae*	
Botryococcus	*Lamiaceae*	*Ribes*	
Brassicaceae	*Larix Lyalli*	*Rosaceae*	
Bryophyta	*Liguliflorae*	*Rumex*	
Caprifoliaceae	*Liliaceae*	*Ruppia*	
Carcocarpus-type	*Lycopus*	*Salix*	
Carex	*Menyanthes*	*Sarcobatus*	
Caryophyllaceae	Monolete undiff.	*Saxifraga*	
Ceanothus	Moss spores	*Scenedesmus*	
Centaurea	*Myriophyllum*	*Scheuchzeria*	
Cercocarpus-type	*Nuphar*	*Scirpus*	
Cereal-type	*Onagraceae*	*Scrophulariaceae*	
Chenopodiacea/Amarath	*P. araneosum*	*Selaginella*	
Compositae (Other)	*P. balsamifera-type*	*Shepherdia*	
Cornus	*P. contorta/P. ponderosa*	*Sorbus*	
Corylus	*P. Integrum*	*Sphaeralcea*	
Cruciferae	*P. obstusum*	*Spirea*	
Cupressaceae	*P.boryanum var. longicorne*	*Spirogyra*	
Cyperaceae	*Pediastrum*	*Stellaria*	
Cystopteris	*Petalostemum*	*Symphoricarpos*	
Dodecatheon	*Phacella*	*Taxus* (brevifolia)	
Drosera	*Picea*	*Thalictrum*	
Dryopteris	*Pinus*	*Thuja Plicata*	
Ephedra virdis	*Pinus albicaulis*	*Tofieldia*	
Equisteum	*Pinus Contorta*	*Trilete* undiff.	

Table 4. The list of plant taxa used in the analysis to determine vegetation composition change. Individually digitized species were grouped via family designation to form the variables below.

Abies	*Picea*
Alnus	*Pinus*
Ambrosia	*Poaceae*
Apiaceae	*Pseudotsuga-Larix*
Artemisia	*Quercus*
Asteraceae	*Salix*
Betula	*Sarcobatus*
Chenopodiacea/Amarath	*Ranunculaceae*
Cupressaceae	*Thuja*
Cyperaceae	*Tsuga*

Table 5. Final (a) vegetation and (b) environmental variables selected for inclusion in the analysis.

Taxa Variables	Taxon Alias	Description
ABIE_1	Abies	Pollen types grouped belonging to the Family *Abies*
ALNUS_1	Alnus	Pollen types grouped belonging to the Family *Alnus*
AMBROSIA_1	Ambrosia	Pollen types grouped belonging to the Family *Ambrosia*
APIACEAE_1	Apiaceae	Pollen types grouped belonging to the Family *Apiaceae*
ARTEMESIA_	Artemesia	Pollen types grouped belonging to the Family *Artemesia*
ASTERACE_1	Asteraceae	Pollen types grouped belonging to the Family *Asteraceae*
BETULA_1	Betula	Pollen types grouped belonging to the Family *Betula*
CHENAM_1	Cheno./Am.	Pollen types grouped belonging to the Families *Chenopodaceae* and *Amaranthaceae*
CUPTAX_1	Cupress./Taxac.	Pollen types grouped belonging to the Families *Cupress.* and *Taxac.*
CYPER_1	Cyperaceae	Pollen types grouped belonging to the Family *Cyperaceae*
LARIXPSE_1	Pseudotsuga/Larix	Pollen types grouped belonging to the Families *Pseudo/Larix*
PICEA_UND_	Picea	Pollen types grouped belonging to the Family *Picea*
PINUS_UND_	Pinus	Pollen types grouped belonging to the Family *Pinus*
POACEAE_1	Poaceae	Pollen types grouped belonging to the Family *Poaceae*
QUERCUS_1	Quercus	Pollen types grouped belonging to the Family *Quercus*
RANUNC_1	Ranunculaceae	Pollen types grouped belonging to the Family *Ranunculaceae*
SALIX_1	Salix	Pollen types grouped belonging to the Family *Salix*
SARCOBATUS	Sarcobatus	Pollen types grouped belonging to the Family *Sarcobatus*
THUJA_1	Thuja	Pollen types grouped belonging to the Family *Thuja*
TSUGA_1	Tsuga	Pollen types grouped belonging to the Family *Tsuga*

Environmental Alias	Environmental Variable	Description
LAT	Northing	Latitude of site location
LONG	Easting	Longitude of site location, zeroed to minimum
ELEV	Elevation	Elevation in meters
Prism_DEM	Precipitation	Precipitation value obtained from PRISM manipulation procedures
X_Y1	NE to SW Gradient	Latitude * Longitude
X_Y2	NW to SE Gradient	Latitude (inverse of Longitude)*10,000
Prism_El	Precipitation / Elevation Gradient	Precipitation value * Elevation value

Table 6. DCA parameters utilized in the study.

DCA Study Parameters:			
Eigenvalues:		**Gradient Lengths:**	
Axes	Value:	Axis 1:	
Axis 1	0.562608719	3.013	3.57
		3.379	3.581
		Axis 2:	
Axis 2	0.265315205	2.622	2.671
		2.711	2.708
		Axis 3:	
Axis 3	0.18626608	1.691	2.009
		2.737	2.844
Total Variance in Species Data: 2.5999			

Table 7. Root mean squared error per variable used in the randomForest imputation procedure.

RMSE per Variable Time Slice										
Variable	**0**	**500**	**1000**	**1500**	**2000**	**2500**	**3000**	**3500**	**6000**	**9000**
LAT	2.82	1.70	1.75	1.92	1.97	2.15	2.03	1.64	2.26	1.90
LON	5.45	3.47	3.76	4.59	4.68	5.38	4.18	4.94	3.87	5.93
ELEV	157471.80	99948.90	111329.60	101517.60	142304.00	112472.30	106953.00	73089.61	104000.70	80506.52
ABIE_1	5.93	9.73	5.75	7.35	7.98	3.58	14.48	10.79	6.90	2.74
ALNUS_1	61.96	86.89	33.95	28.16	61.98	123.70	109.42	100.60	104.98	169.21
AMBROSIA_1	3.06	2.36	2.46	1.61	1.29	1.50	1.10	3.02	3.52	8.79
APIACEAE_1	0.03	0.12	0.01	0.02	0.07	0.06	1.61	1.55	0.80	0.46
ARTEMESIA_	14.27	40.95	43.12	38.27	39.56	37.07	46.49	43.35	48.31	33.96
ASTERACE_1	3.35	1.35	2.02	1.45	1.90	1.45	2.04	2.46	1.00	28.67
BETULA_1	21.26	14.25	5.51	8.41	3.76	3.80	9.91	11.86	15.50	13.59
CHENAM_1	20.51	11.64	13.24	23.01	15.10	21.13	49.27	31.21	18.19	68.73
CUPTAX_1	79.25	95.36	90.64	142.01	122.93	109.91	131.27	157.03	62.11	18.58
CYPER_1	122.82	40.97	43.17	95.72	108.32	193.87	42.62	20.35	110.73	95.53
LARIXPSE_1	20.75	13.39	34.14	55.53	43.78	37.45	22.17	33.12	17.40	46.15
PICEA_UND_	8.29	11.56	12.45	15.08	24.34	25.01	22.69	21.88	16.85	16.78
PINUS_UND_	288.10	256.97	241.94	271.64	226.07	245.20	220.64	239.41	304.95	167.83
POACEAE_1	51.05	40.78	21.98	51.60	33.86	33.44	25.11	29.01	30.85	30.78
QUERCUS_1	1.07	0.39	0.08	0.15	0.16	0.50	0.53	0.92	1.67	1.61
RANUNC_1	0.20	0.37	2.53	0.08	0.18	0.36	0.50	0.11	4.74	2.01
SALIX_1	0.49	0.88	6.29	1.24	1.06	2.08	1.34	1.25	0.29	0.37
SARCOBATUS	0.38	0.49	0.31	0.25	0.27	0.13	0.70	0.23	0.32	0.48
THUJA_1	0.00	0.01	0.02	0.01	0.00	0.00	0.08	0.00	58.69	0.06
TSUGA_1	23.50	21.69	9.66	9.27	13.89	11.69	15.91	14.72	36.82	4.25
Prism_DEM	413036.50	151335.90	149610.90	181400.90	195723.00	179202.70	181151.20	136295.90	131498.40	122629.10
X_Y1	37890.12	25244.65	26482.24	30366.17	26613.97	38571.76	44725.89	35010.56	42892.23	37424.28
X_Y2	30390.99	26068.03	24151.79	26735.63	26716.20	29879.70	26285.44	26230.37	21032.09	25135.44
Prism_Elev	232000000.00	339000000000.00	3220000000.00	30.00	3790000000.00	34500000000.00	3620000000.00	3530000000.00	385000000.00	3080000000.00

Table 8. The variance (r^2) explained per variable used in the randomForest procedure.

Variance Explained per Variable										
	Time Slice									
Variable	**0**	**500**	**1000**	**1500**	**2000**	**2500**	**3000**	**3500**	**6000**	**9000**
LAT	71.74	86.37	85.55	84.33	81.95	80.32	81.48	84.98	78.49	79.18
LON	86.44	90.48	90.16	88.4	88.74	87.05	89.95	88.11	90.46	85.15
ELEV	81.02	87.34	85.95	87.03	82.03	85.8	86.49	90.77	86.85	89.99
ABIE_1	4.44	27.24	47.72	33.56	30.08	42.92	9.4	23.99	44.88	64.49
ALNUS_1	72.46	46.98	50.71	56.17	51.11	39.83	45.18	47.52	52.34	57.17
AMBROSIA_1	31.94	29.66	50.07	42.92	43.7	41.05	53.2	36.12	10.75	3.92
APIACEAE_1	-0.13	-7.47	9.6	-20.83	-25.81	-28.85	-25.35	-15.24	-20.46	-27.93
ARTEMESIA_	79.86	60.31	67.45	64.64	65.07	68.48	60.11	66.95	59.24	52.87
ASTERACE_1	22.04	41.03	42.41	31.6	36.06	40.72	29.36	41.91	55.21	-25.95
BETULA_1	20.04	16.71	11.38	31.82	36.96	34.18	27.89	25.72	-8.07	-5.52
CHENAM_1	60.63	34.81	48.54	14.53	36.7	21.42	6.14	14.95	45.65	33.37
CUPTAX_1	16.9	13.64	45.58	21.55	32.41	24.86	23.4	20.59	-1.29	-25.35
CYPER_1	-13.71	-3.75	-15.55	-22.68	-26.45	-30.73	-7.89	2.33	-18.99	-14.07
LARIXPSE_1	6.13	44.22	53.89	47.36	42.63	26.76	49.23	27.32	58.94	51.47
PICEA_UND_	40.2	42.66	38.03	48.57	26.39	37.07	43.81	46.97	47.29	17.22
PINUS_UND_	67.33	64.49	68.29	64.07	66.57	66.26	69.64	70.39	61.32	78.64
POACEAE_1	33.05	12.92	39.11	17.4	44.26	39.7	39.61	35.09	18.86	28
QUERCUS_1	-13.16	-4.44	40.87	23.36	15.49	-3.62	3.51	7.16	1.8	2.38
RANUNC_1	-28.12	-20.88	-33.85	-17.44	-27.7	-24.4	-13.06	-14.4	-34.01	-37.71
SALIX_1	55.26	-1.42	-21.2	-13.3	18.7	10.41	-0.83	-6.86	-8.2	-19.47
SARCOBATUS	21.97	23.01	44.13	20.93	23.75	54.51	-3.85	25.91	29.98	18.93
THUJA_1	NaN	-30.84	-31.32	-29.5	-27.16	NaN	-34.79	-41.41	-30.32	-47.59
TSUGA_1	50.41	57.6	78.49	73.73	60.82	67.17	67.06	67.46	44.24	31.74
Prism_DEM	36.1	58.85	59.75	53.72	52.27	56.3	55.83	66.76	60.88	60.68
X_Y1	85.08	91.76	91.37	90.17	90.61	86.39	84.22	87.65	85.68	87.19
X_Y2	73.43	75.57	76.83	75.23	75.38	72.46	75.77	75.83	75	61.58
Prism_Elev	68.26	65.1	67.76	72.8	63.16	66.46	64.8	65.69	64.47	70.26

Table 9. Example of the multi-temporal matrix utilized in the ordination procedures and temporal landscape metric analysis.

Study Point * Time	**Variable 1**	**Variable 2**	**Variable *m***
Site1_Time1	23	5	**…..**
Site1_Time2	14	55	**…..**
Site1_Time3	46	34	**…..**
Site1_Time4	21	76	**…..**
Site1_Time5	11	6	**…..**
…	**…..**	**…..**	**…..**
Site *n*_Time *o*	**…..**	**…..**	**…..**

Table 10. NMDS parameters examined in the (a) initial run and (b) the final utilized in the study.

NMDS Study Parameters:			
a) Initial 6 Axes Solution NMDS Run:			
500 Iterations .20 Step Length 50 Runs with Real Data 25 Runs with Randomized Data 0.000010 Stability Criterion			
Stress			
Axes	Real Data	Random Data	P
Axis 1	44.513	51	0.0385
Axis 2	13.018	31.672	0.0385
Axis 3	9.65	24.1888	0.0385
Axis 4	7.352	19.416	0.0385
Axis 5	6.204	16.118	0.0385
Axis 6	5.442	13.656	0.0385
b) Secondary 3 Axes Solution NMDS Run:			
253 Iterations .20 Step Length 1 Run with Real Data 0 Runs with Randomized Data 0.000010 Stability Criterion			
Stress			
9.43308 = Final Stress .000001 Final Instability			
Percent of Variance (R^2) in Distance Matrix			
Axes	Increment	Cumulative	
Axis 1	0.568	0.568	
Axis 2	0.346	0.915	
Axis 3	0.046	0.960	

Table 11. Listing of the correlations among the environmental variables obtained from the CCA analysis. Descriptions of the variables are in Table 5b. Correlations greater than 0.5 or less than -0.5 are in bold.

Weighted Correlations Among Environmental Variables (weighted by row totals in main matrix)							
	LAT	LONG	ELEV	Prism_DEM	X_Y1	X_Y2	Prism_El
LAT	1	-0.006	-0.281	-0.134	0.108	-0.01	-0.169
LONG		1	0.223	**-0.502**	**0.992**	**-0.761**	-0.274
ELEV			1	0.050	0.177	-0.304	**0.601**
Prism_DEM				1	**-0.514**	**0.654**	**0.701**
X_Y1					1	**-0.759**	**1**
X_Y2						1	0.235
Prism_El							1

Table 12. Iteration report from the CCA analysis, which reveals the convergence on a stable solution from a specified tolerance (0.100000^{E-12}) after fewer than 30 iterations for each axis (McCune and Mefford, 1999, 100).

Iteration Report Obtained from the CCA analysis			
	Axis 1	Axis 2	Axis 3
Solution Tolerance	$0.1E^{-12}$	$0.1E^{-12}$	$0.1E^{-12}$
Number of Iterations	21	8	26

Table 13. CCA axis summary obtained from the ordination.

CCA Study Parameters:		
Monte Carlo Results -- Eigenvalues:		
Axes	Real Data: Eigenvalues:	Randomized Data Based on 9999 Runs:
Axis 1	0.368	0.01
Axis 2	0.176	0.176
Axis 3	0.059	0.059
All share a p-value of 0.0001		

Monte Carlo Results -- Species-Environment Correlations:		
Axes	Real Data: Eigenvalues:	Randomized Data Based on 9999 Runs:
Axis 1	0.82	0.23
Axis 2	0.677	0.195
Axis 3	0.525	0.169
All share a p-value of 0.0001		

Percent of Variance (R^2) Explained in Species Data & Axis Summary Statistics			
Axes	Increment	Cumulative	
Axis 1	14.2	14.2	
Axis 2	6.8	20.9	
Axis 3	2.3	23.2	
	Axis 1	Axis 2	Axis 3
Pearson	0.82	0.677	0.525
Kendall	0.689	0.485	0.391
Total Variance in Species Data: 2.5999			

Table 14. Multiple regression results obtained from the environmental variables used in the CCA ordination analysis. Descriptions of the variables are in Table 5b. Correlations greater than 0.5 are in bold.

MULTIPLE REGRESSION RESULTS: Regression of Plots in Variable space							
	Standardized Units			Original Units			
Variable	Axis 1	Axis 2	Axis 3	Axis 1	Axis 2	Axis 3	St. Dev.
LAT	0.190	**-0.889**	**-0.678**	0.071	-0.332	-0.235	0.268E+01
LONG	-0.389	**-1.54**	**-2.817**	-0.064	-0.252	-0.461	0.612E+01
ELEV	0.407	**-0.963**	0.445	0.001	-0.001	0.001	0.692E+03
Prism_DEM	**0.614**	-0.008	**0.824**	0.001	0.000	0.001	0.975E+03
X_Y1	0.000	**2.002**	**1.586**	0.000	0.007	0.006	0.287E+03
X_Y2	0.374	0.347	**-1.359**	0.000	0.000	0.000	0.283E+07
Prism_El	-0.305	0.195	**-0.896**	0.000	0.000	0.000	0.132E+07

Table 15. Correlation scores of environmental variables with the ordination axes. Intraset correlations were used (LC scores) for graphing the site and species scores. The intraset correlations indicate which environmental variables were more influential in structuring the ordination. Descriptions of the variables are in Table 5b. Correlations greater than 0.5 or less than −0.5 are in bold.

Correlations and Biplot Scores for the Environmental Variables Used in the CCA Analysis			
	Correlations		
Variable	Axis 1	Axis 2	Axis 3
LAT	0.044	-0.428	**-0.559**
LONG	**-0.808**	-0.077	-0.274
ELEV	0.001	**-0.692**	0.203
Prism_DEM	**0.835**	0.169	0.02
X_Y1	**-0.801**	-0.109	-0.327
X_Y2	**0.874**	0.341	-0.22
Prism_El	**0.533**	-0.333	0.043

Table 16. Correlation scores from the NMDS ordination of the species variables used to interpret the ordination axes. R is the coefficient of correlation, and measures the correlation between two variables. R^2 is the coefficient of determination (and square of R), and indicates the strength of fit between two variables. Tau is Kendall's tau, a nonparametric statistic used to measure the degree of correspondence between two rankings and assess the significance of correspondence. Correlations above 0.50 or below −0.5 are in bold.

NMDS R^2 Correlation Scores Used to Infer the Ordination Axes Gradients									
Axes:	1			2			3		
Species Variables	R	R^2	Tau	R	R^2	Tau	R	R^2	Tau
Abies	-0.148	0.022	-0.098	**0.633**	0.401	**0.501**	0.105	0.011	0.100
Alnus	**-0.734**	**0.539**	-0.445	**0.711**	0.505	0.491	0.303	0.092	0.160
Ambrosia	0.093	0.009	0.034	**-0.689**	0.474	**-0.561**	-0.436	0.190	-0.351
Apiaceae	-0.179	0.032	-0.261	-0.022	0.000	0.010	-0.059	0.003	-0.120
Artemesia	0.462	0.213	0.170	**-0.916**	**0.839**	**-0.739**	-0.471	0.222	-0.316
Asteraceae	0.044	0.002	-0.012	**-0.614**	0.377	**-0.506**	**-0.611**	0.373	-0.496
Betula	-0.294	0.087	-0.198	0.283	0.080	0.188	0.163	0.027	0.072
Cheno/Amaranth.	0.203	0.041	0.063	**-0.853**	**0.727**	**-0.713**	-0.459	0.211	-0.329
Cup./Tax.	**-0.783**	**0.613**	-0.410	0.437	0.191	0.093	0.337	0.114	0.094
Cyperaceae	0.120	0.014	-0.088	-0.318	0.101	-0.221	-0.105	0.011	-0.064
Pseudotsuga/Larix	**-0.747**	**0.557**	-0.414	**0.655**	0.429	0.471	0.47	0.221	0.317
Picea Undiff.	0.430	0.185	0.301	0.244	0.060	0.197	**-0.545**	0.297	-0.351
Pinus Undiff.	**0.882**	**0.777**	**0.527**	-0.266	0.071	0.021	-0.155	0.024	0.176
Poaceae	-0.042	0.002	-0.152	-0.690	0.477	-0.507	-0.424	0.180	-0.329
Quercus	-0.193	0.037	-0.128	-0.067	0.005	-0.089	0.037	0.001	-0.058
Ranunculaceae	-0.150	0.023	-0.095	0.056	0.003	-0.015	-0.309	0.096	-0.274
Salix	-0.165	0.027	-0.175	0.027	0.001	0.019	-0.269	0.072	-0.159
Sarcobatus	0.224	0.050	0.148	**-0.631**	0.399	**-0.512**	-0.321	0.103	-0.257
Thuja	0.012	0.000	-0.064	0.083	0.007	0.054	0.103	0.011	0.031
Tsuga	**-0.744**	**0.554**	-0.436	**0.771**	**0.594**	**0.646**	0.503	0.253	0.251

APPENDIX

a)

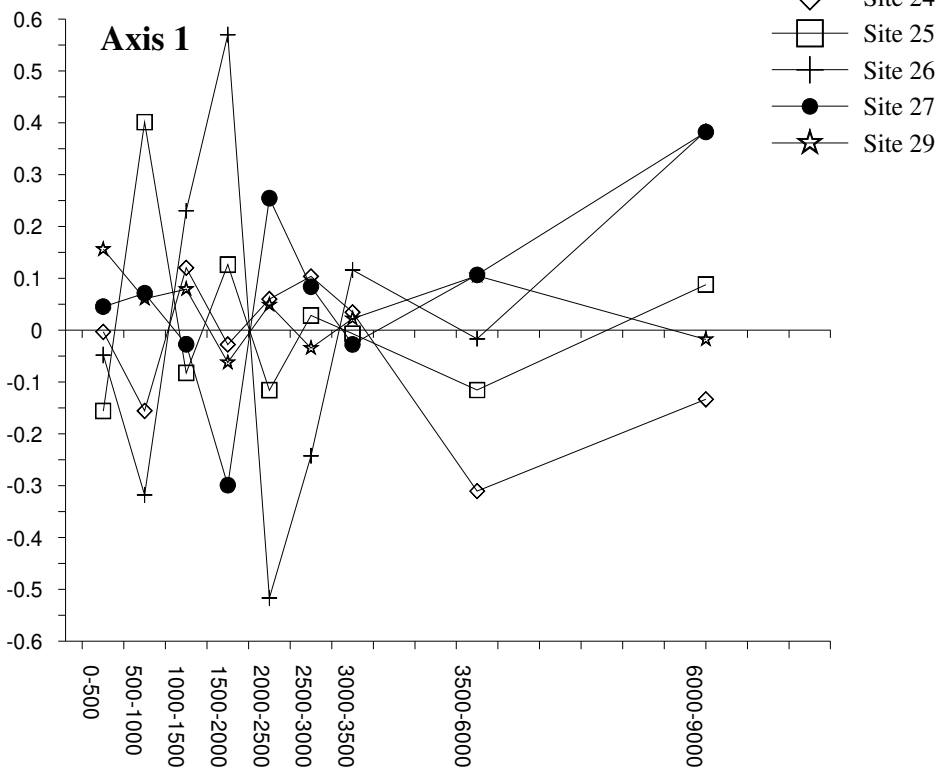

b)

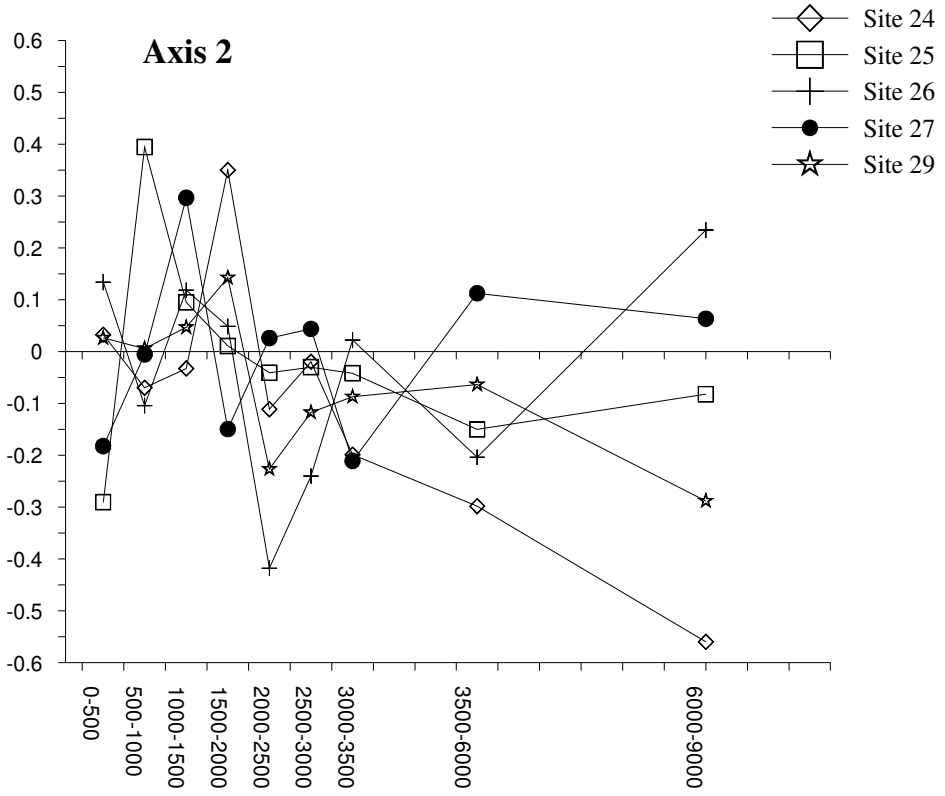

Figure A. Displacement of community composition change for the paleopollen sites belonging to ordination Group 3, the Mid-Elevation Forest sites, from the present to 9000 ybp on a) ordination axis 1 and on b) ordination axis 2.

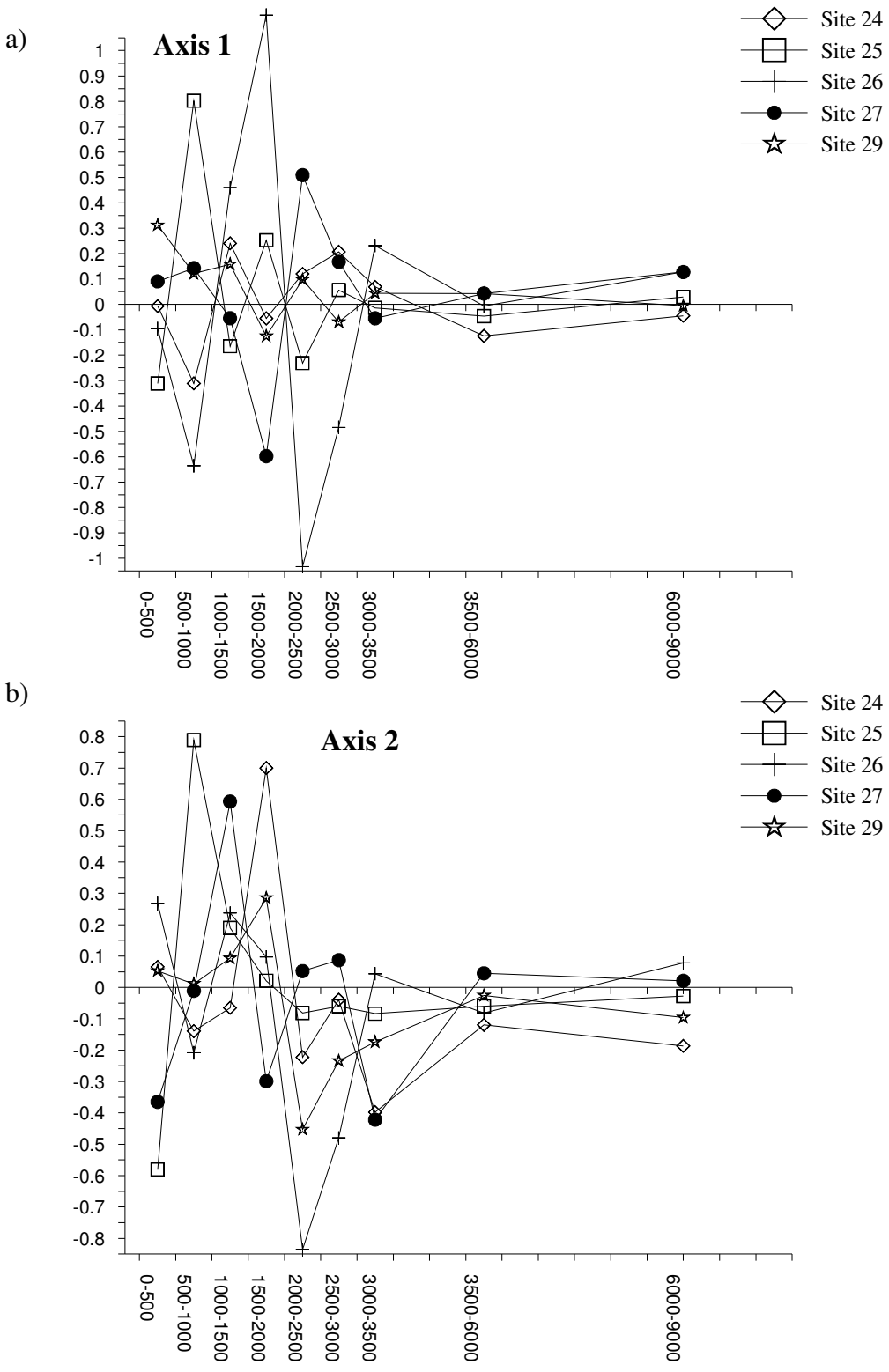

Figure B. Velocity of community composition change for the paleopollen sites belonging to ordination Group 3, the Mid-Elevation Forest sites, from the present to 9000 ybp on a) ordination axis 1 and on b) ordination axis 2.

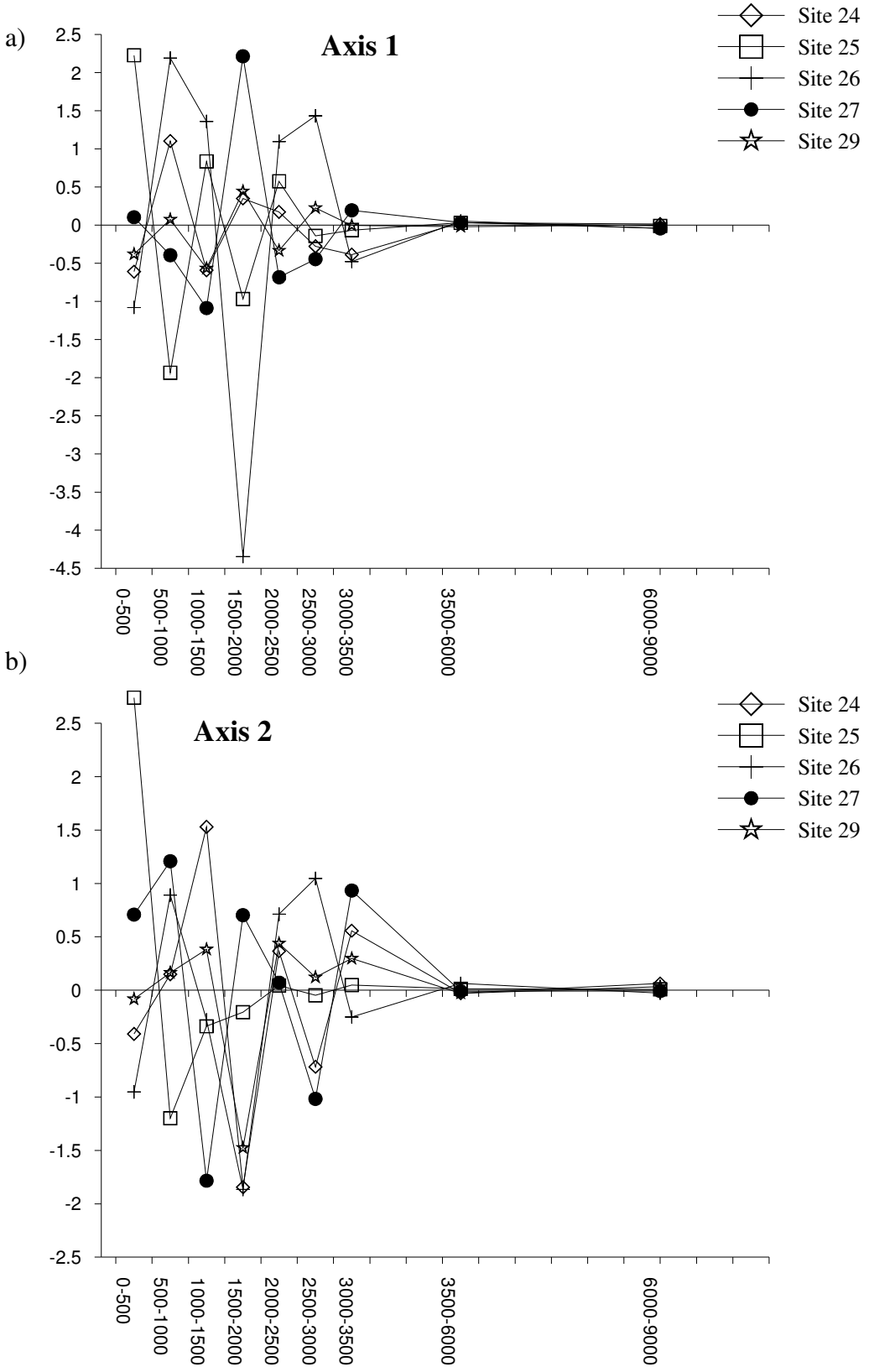

Figure C. Acceleration of community composition change for the paleopollen sites belonging to ordination Group 3, the Mid-Elevation Forest sites, from the present to 9000 ybp on a) ordination axis 1 and on b) ordination axis 2.

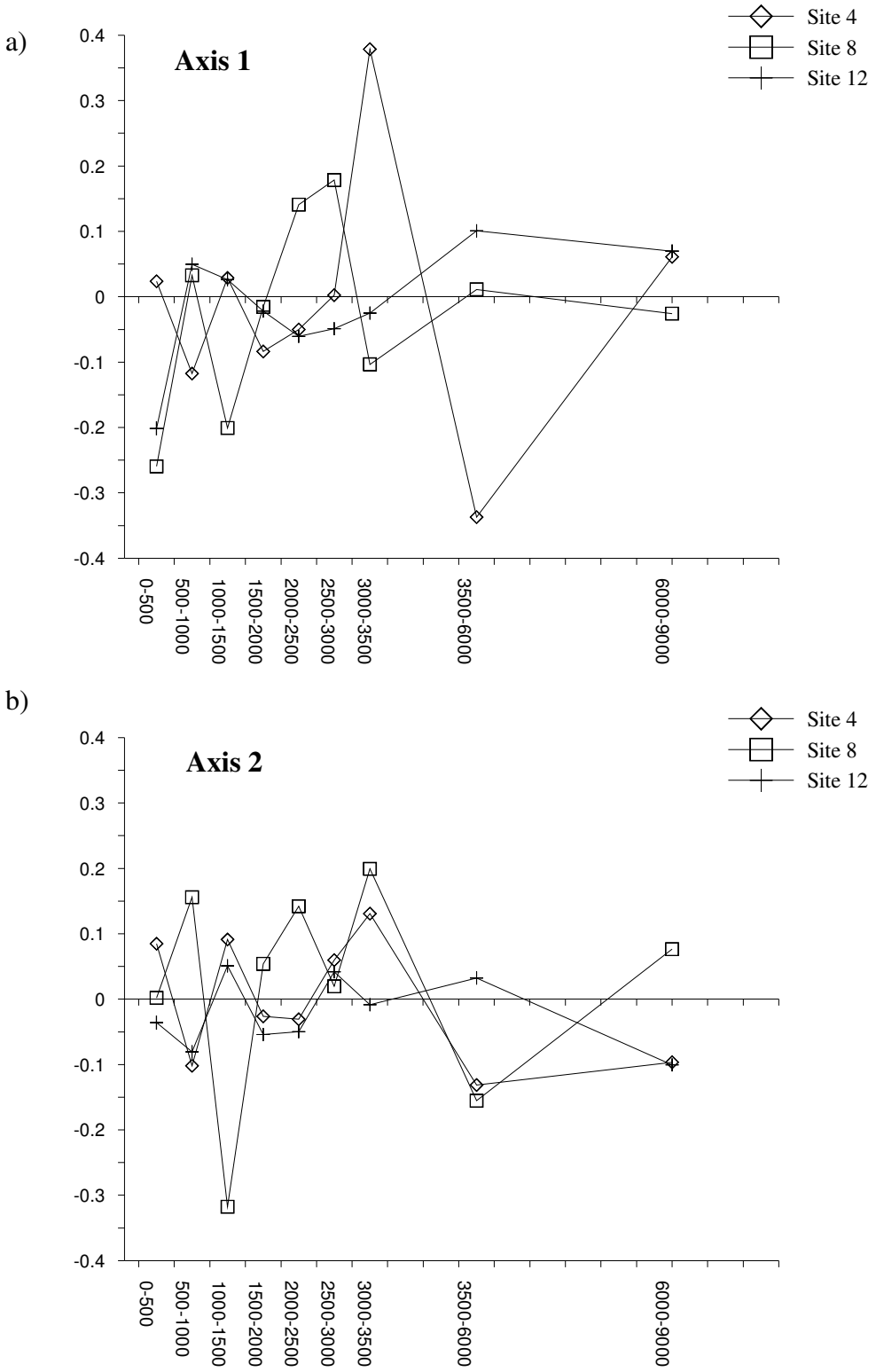

Figure D. Displacement of community composition change for the paleopollen sites belonging to ordination Group 5, the South Central Rockies sites, from the present to 9000 ybp on a) ordination axis 1 and on b) ordination axis 2.

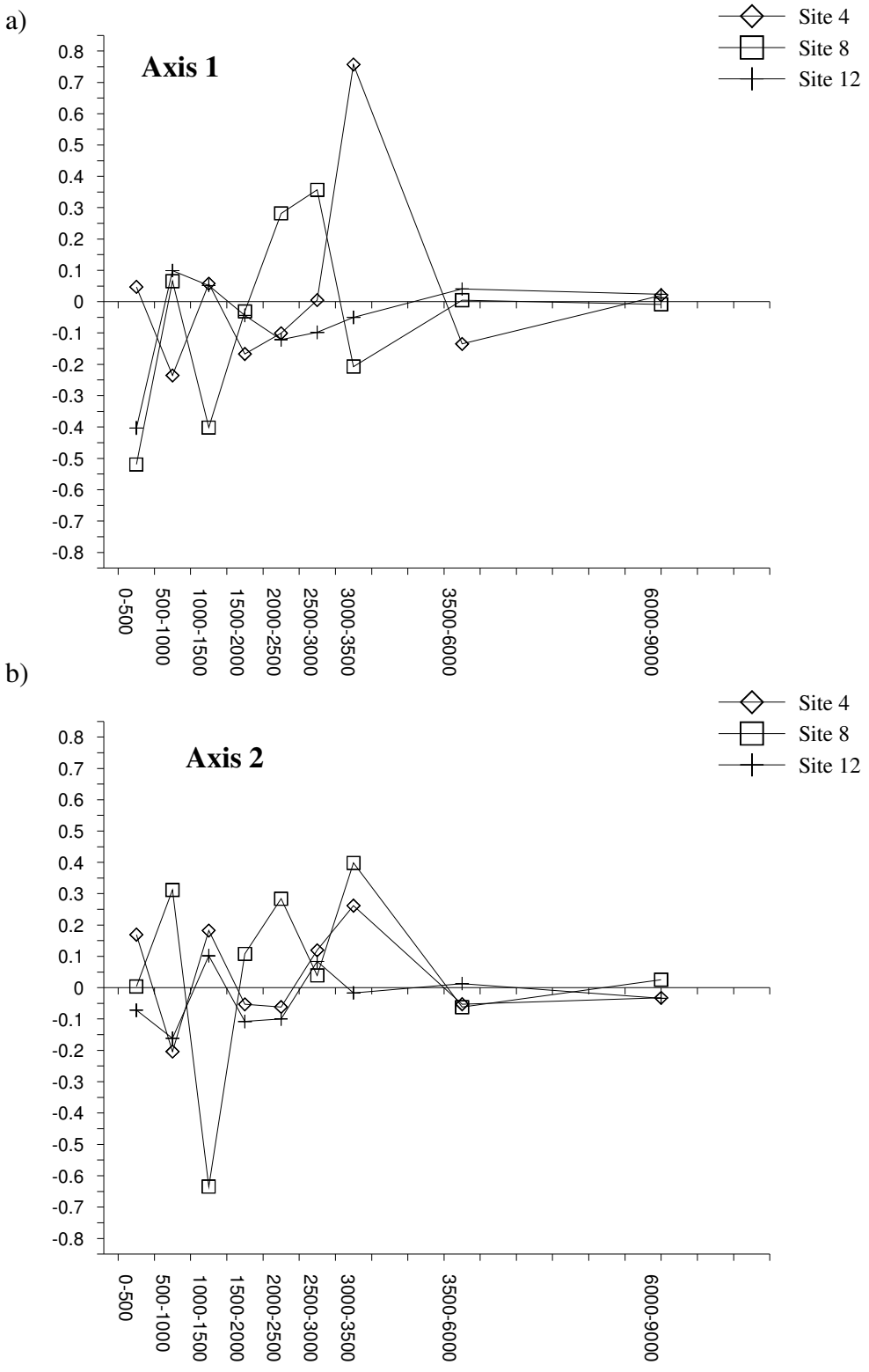

Figure E. Velocity of community composition change for the paleopollen sites belonging to ordination Group 5, the South Central Rockies sites, from the present to 9000 ybp on a) ordination axis 1 and on b) ordination axis 2.

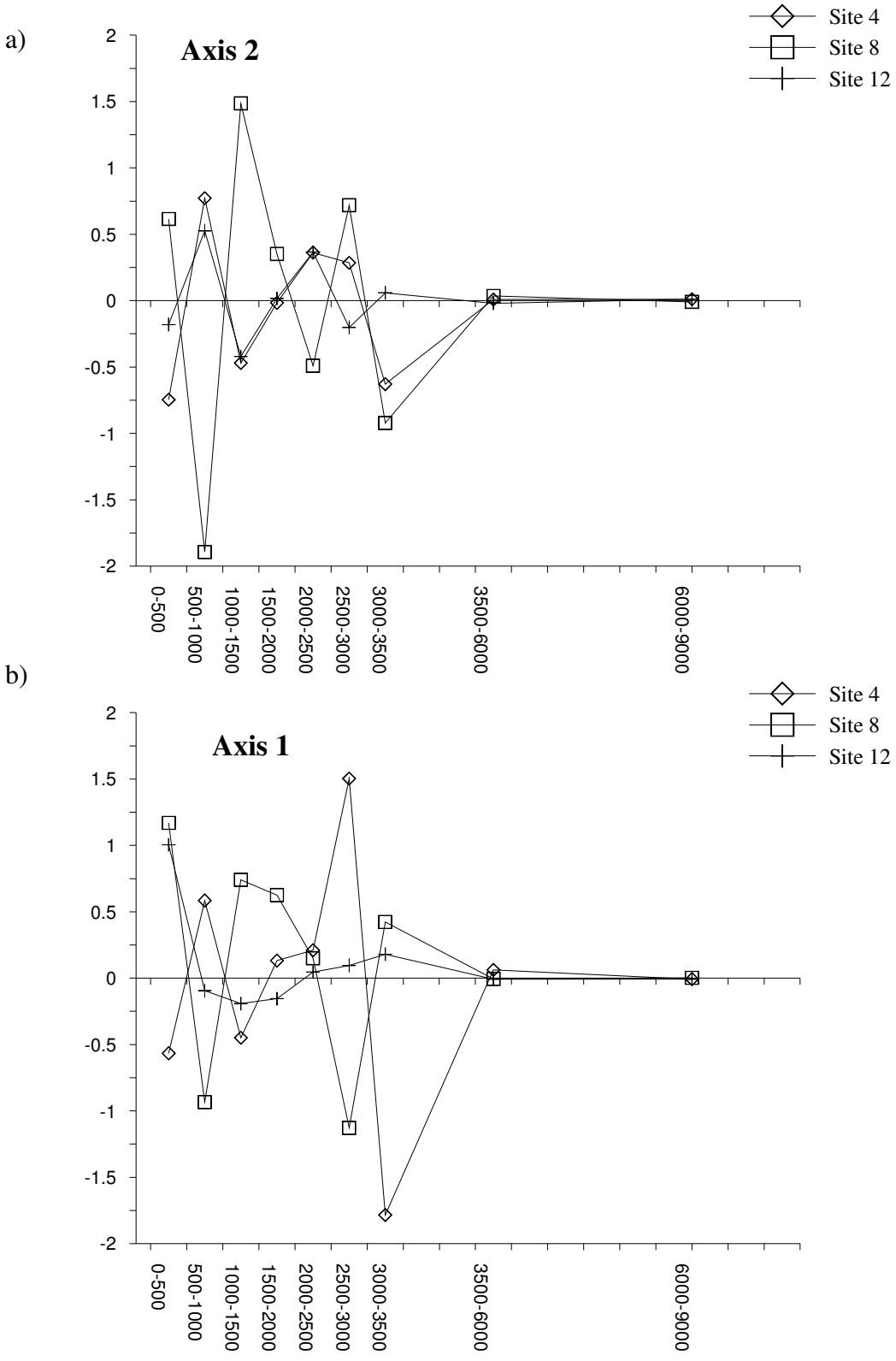

Figure F. Acceleration of community composition change for the paleopollen sites belonging to ordination Group 5, the South Central Rockies sites, from the present to 9000 ybp on a) ordination axis 1 and on b) ordination axis 2.

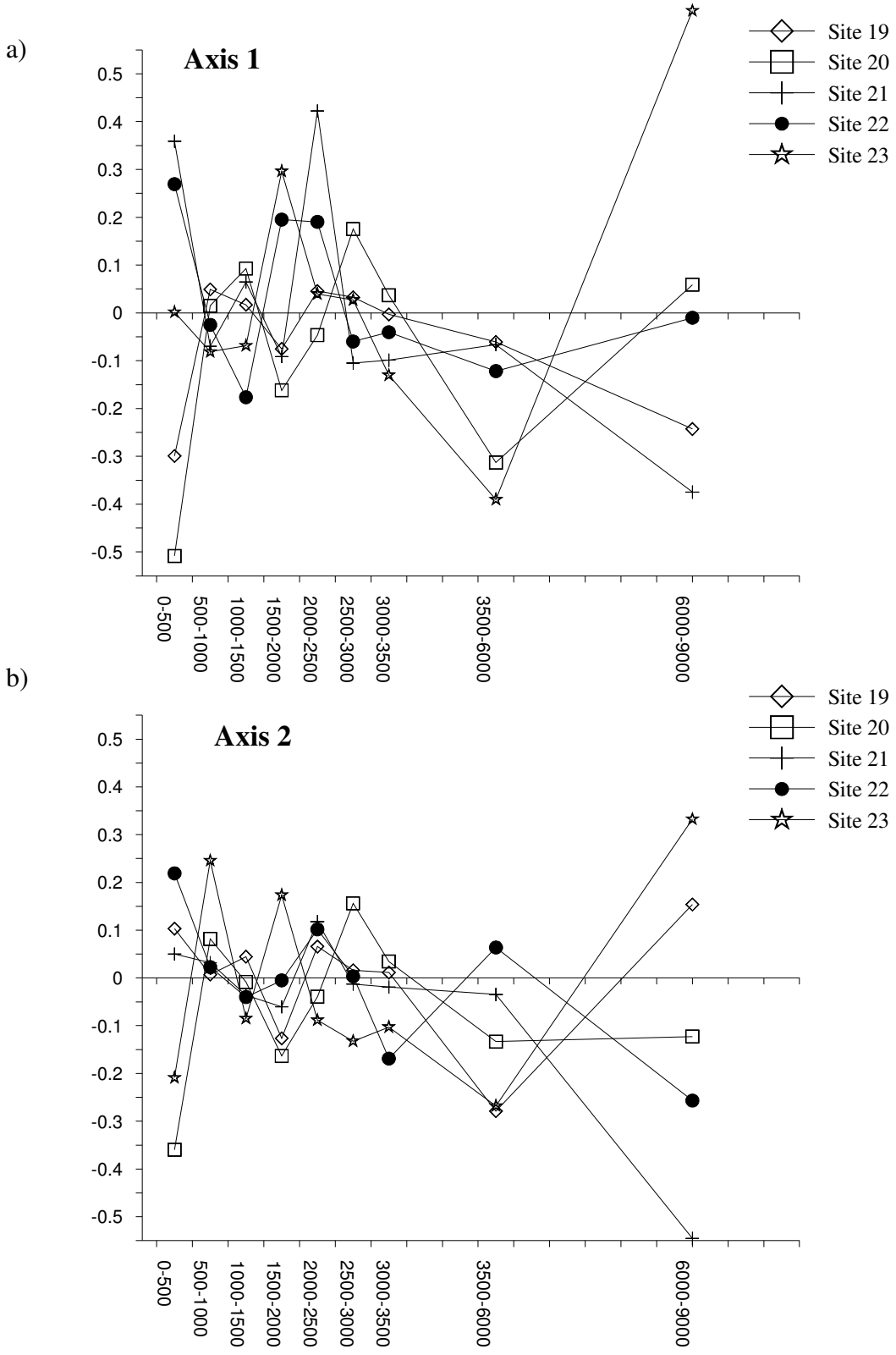

Figure G. Displacement of community composition change for the paleopollen sites belonging to ordination Group 7, the Northern Rockies sites, from the present to 9000 ybp on a) ordination axis 1 and on b) ordination axis 2.

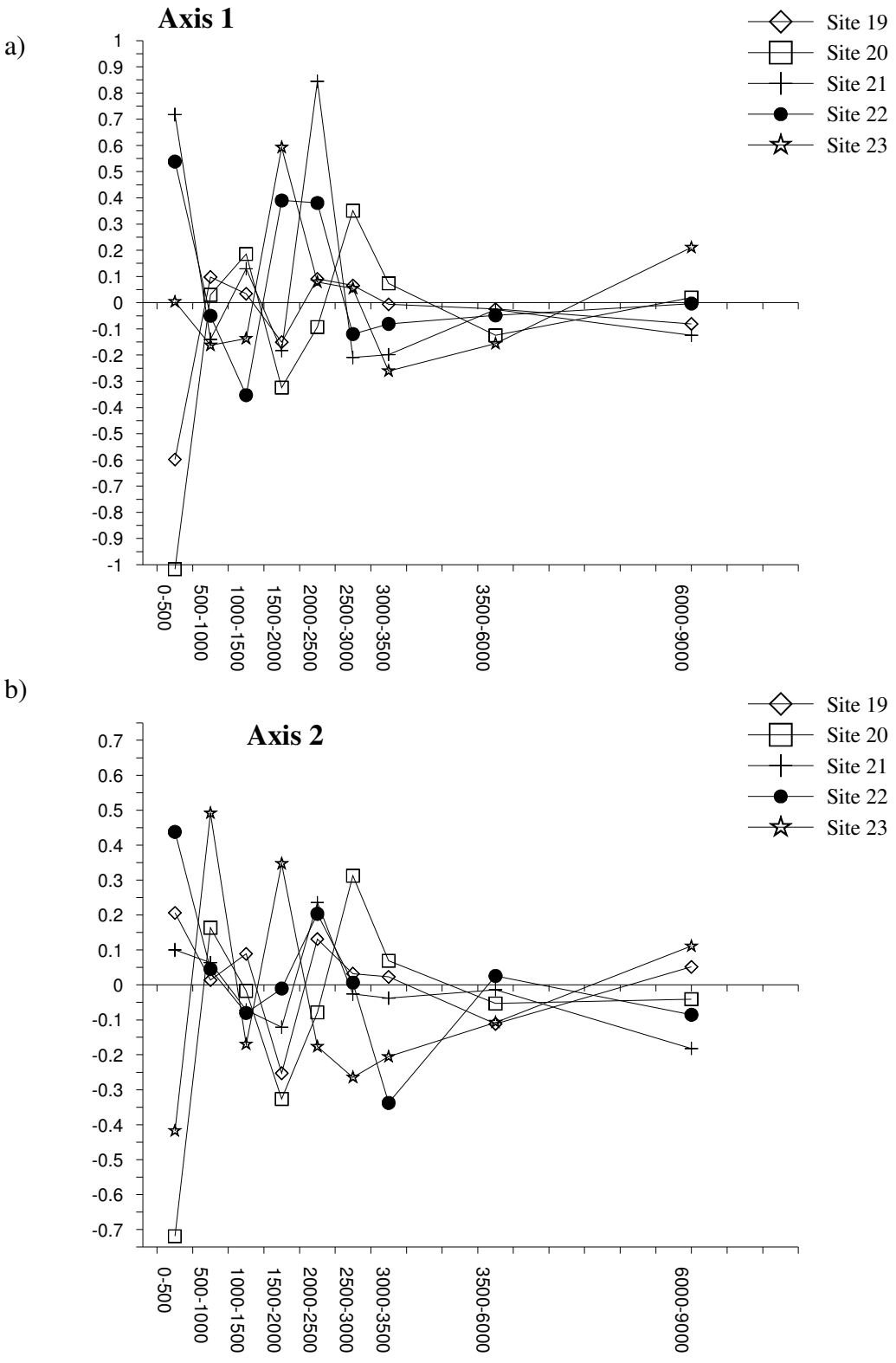

Figure H. Velocity of community composition change for the paleopollen sites belonging to ordination Group 7, the Northern Rockies sites, from the present to 9000 ybp on a) ordination axis 1 and on b) ordination axis 2.

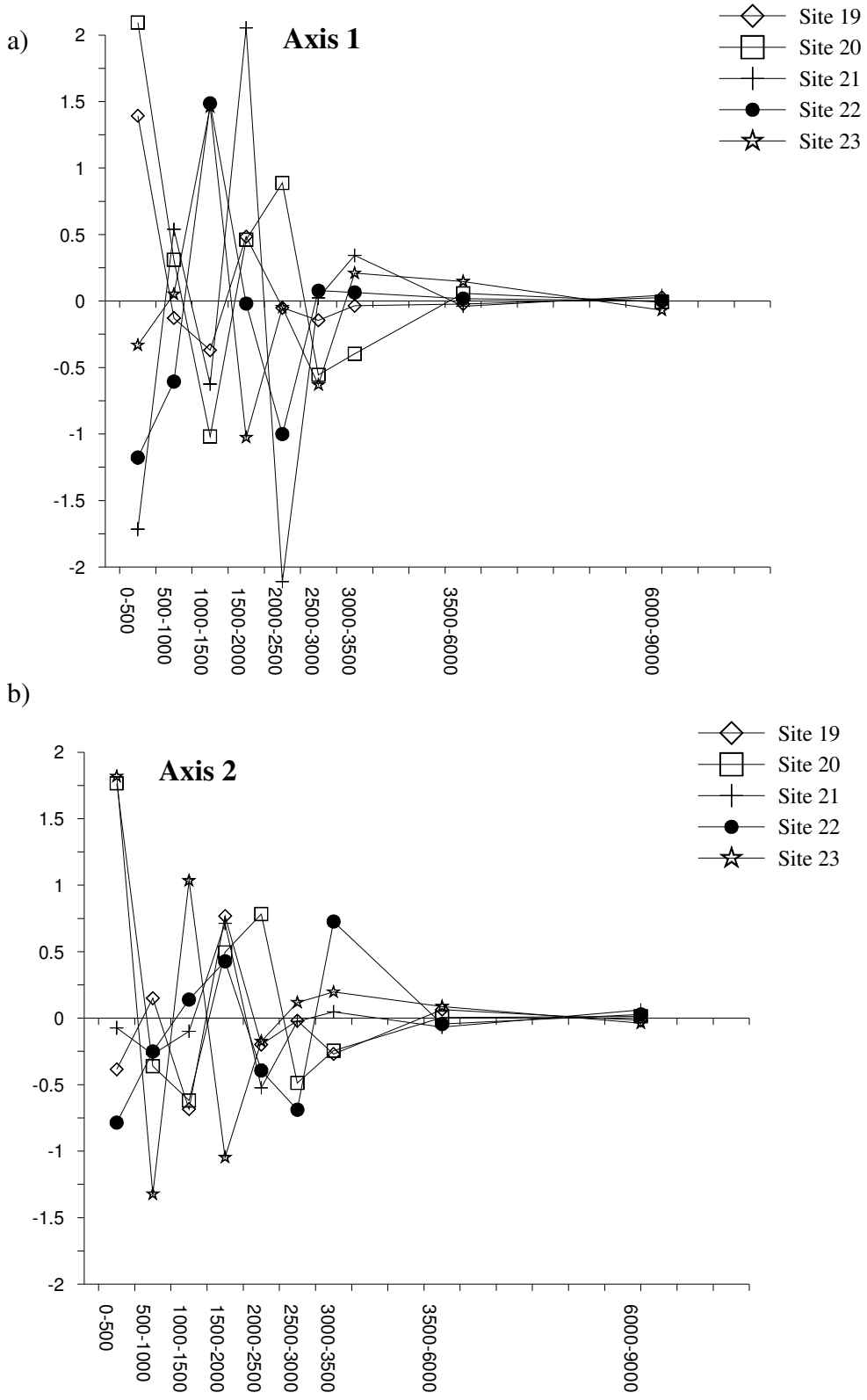

Figure I. Acceleration of community composition change for the paleopollen sites belonging to ordination Group 7, the Northern Rockies sites, from the present to 9000 ybp on a) ordination axis 1 and on b) ordination axis 2.

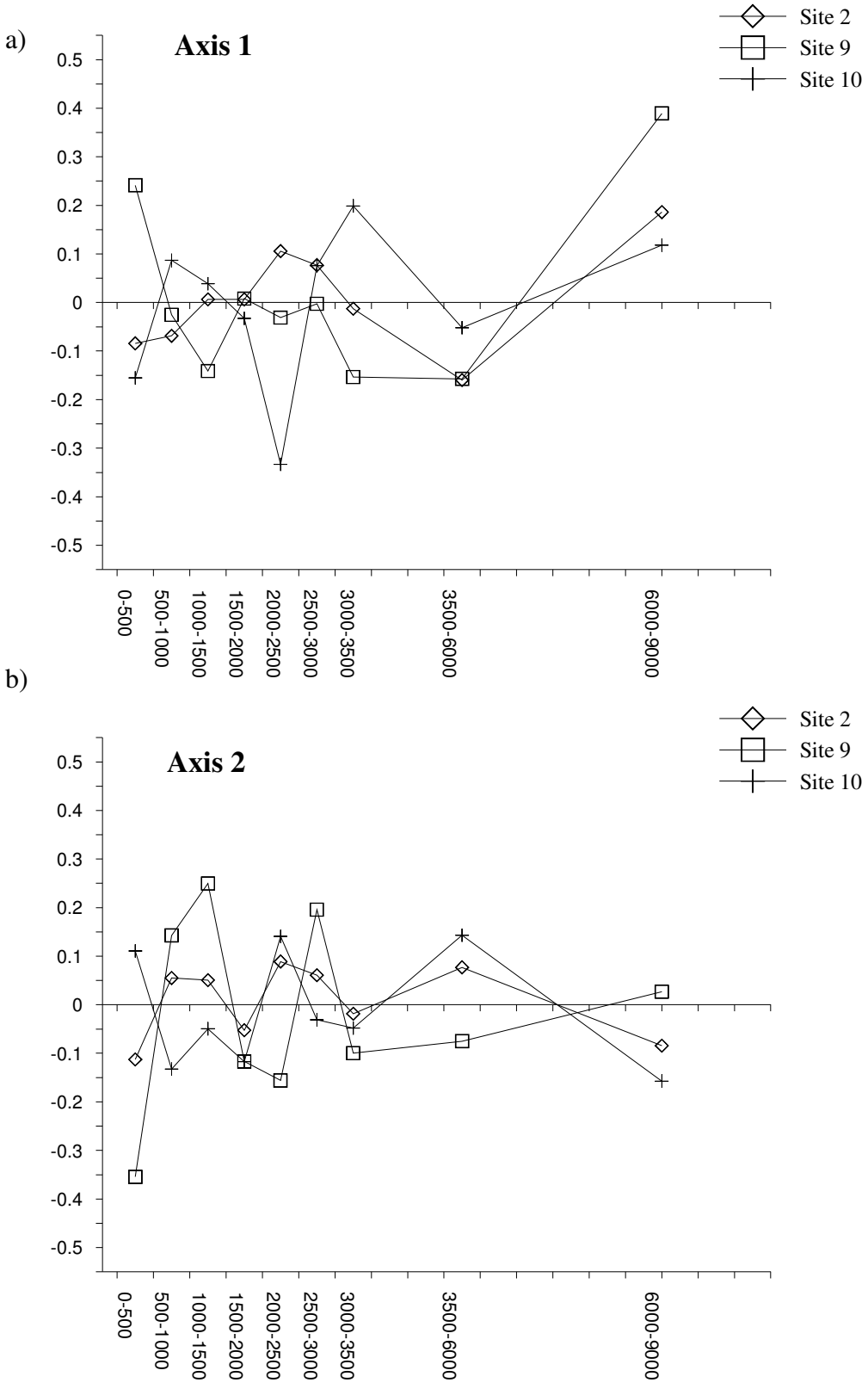

Figure J. Displacement of community composition change for the paleopollen sites belonging to ordination Group 8, the High Elevation Rockies sites, from the present to 9000 ybp on a) ordination axis 1 and on b) ordination axis 2.

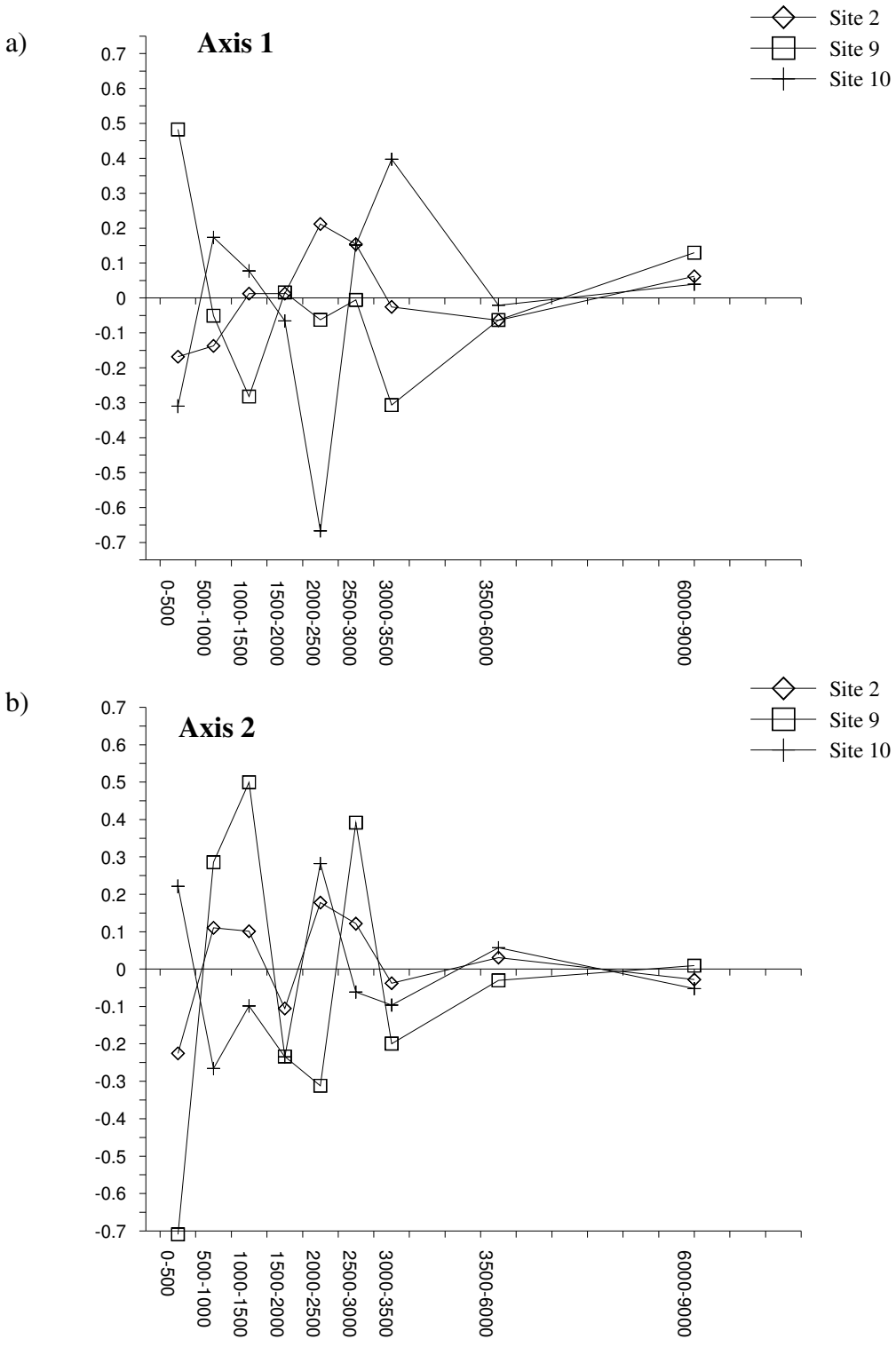

Figure K. Velocity of community composition change for the paleopollen sites belonging to ordination Group 8, the High Elevation Rockies sites, from the present to 9000 ybp on a) ordination axis 1 and on b) ordination axis 2.

a)

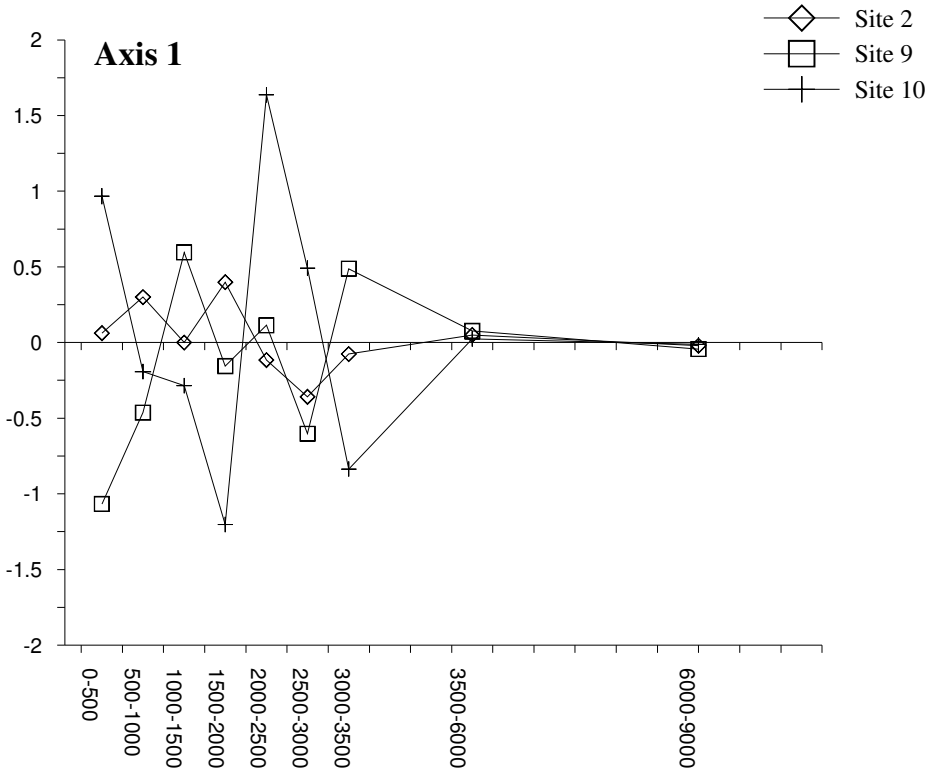

b)

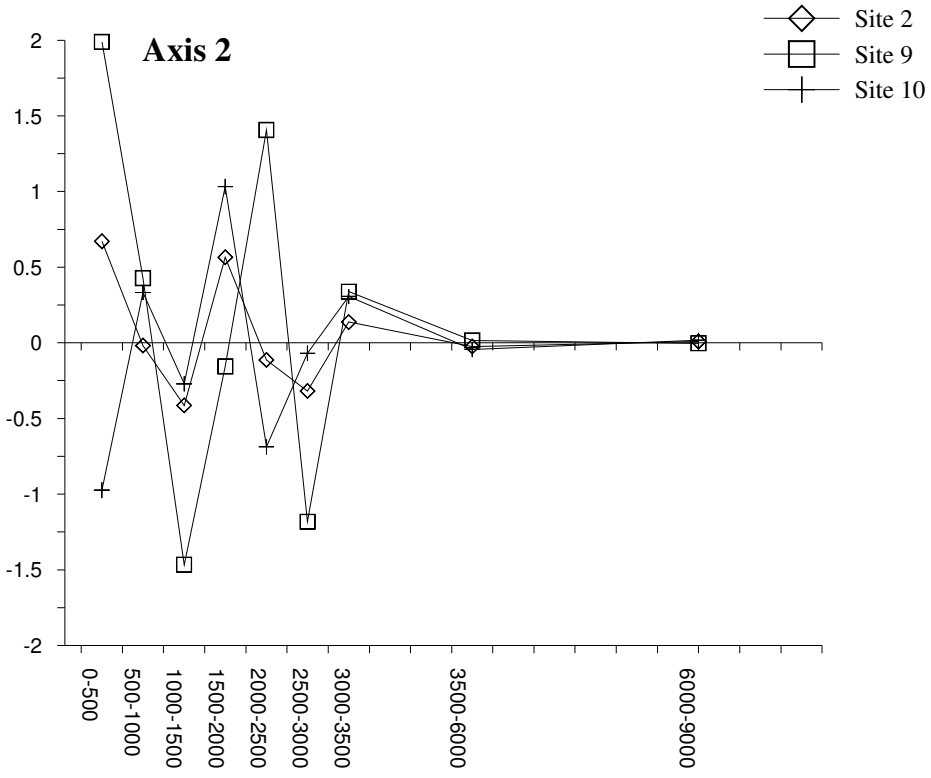

Figure L. Acceleration of community composition change for the paleopollen sites belonging to ordination Group 8, the High Elevation Rockies sites, from the present to 9000 ybp on a) ordination axis 1 and on b) ordination axis 2.